

Contents lists available at ScienceDirect

Journal of Environmental Chemical Engineering

journal homepage: www.elsevier.com/locate/jece





Synthesis, properties, and applications of polyaniline–graphene quantum dot nanocomposites: Comprehensive review

Mahnoush Beygisangchin a,*, Siti Kartom Kamarudin b, Suraya Abdul Rashid C

- ^a Fuel Cell Institute, Universiti Kebangsaan Malaysia, Bangi, Selangor 43600, Malaysia
- b Department of Chemical Engineering, Faculty of Engineering and Built Environment, Universiti Kebangsaan Malaysia, Bangi, Selangor 43600, Malaysia
- c Nanomaterials Processing and Technology Laboratory, Institute of Nanoscience and Nanotechnology, Universiti Putra Malaysia, Serdang 43400, Malaysia

ARTICLE INFO

Keywords: Polyaniline Graphene quantum dot Nanocomposite Properties Sensors Applications

ABSTRACT

Polyaniline (PANI), graphene quantum dots (GQD), and their combination have attracted considerable interest within the nanotechnology field for a multitude of uses, such as in sensors, biosensors, solar cells, supercapacitors, optoelectronic and photonic devices, and coating. However, a substantial gap exists in the research of PANI–GQD nanocomposites for several applications. PANI is a polymeric material with a chain backbone featuring high π -conjugation, which is associated with magnetic, optical, metallic, and electronic properties. GQD is a 0D quantum dot (QD) material that appears as tiny graphene pieces (2–5 nm) with unique optical, luminescent, electronic, semiconducting, biocompatible, and exceptional photostable properties, which can counteract photobleaching and blinking. It also has low toxicity due to edge effects and quantum confinement. A functional QD can exhibit van der Waals and π - π * association interactions with the conjugated polymer backbone and electrostatic properties. The uniform diffusion of GQD in PANI can result in a distinctive morphological structure, providing high sensitivity, selectivity, flexibility, specific surface area, capacitance, electrochemical catalytic activity, photovoltaic properties, and optical and electrical properties. For the first time, this review presents the comprehensive developments in the preparation, properties, and characterization of PANI–GQD nanocomposites for various applications, which are tabulated separately.

1. Introduction

Nanocomposites have gained substantial interest owing to their unique properties and wide-ranging applications. Identified as intrinsically conductive polymers (ICPs) or synthetic metals, conducting polymers (CPs) are a group of organic components that exhibit the electrical and mechanical properties of modern polymers and are integrated with electrical conductivity similar to metals [1–3]. Studies on CPs traced their origins to the 1960s when Shirakawa et al. [4] initially synthesized and examined semiconductor polymers. Since then, CPs have become

crucial in diverse applications because of their fascinating characteristics and their adaptability for use in a broad array of electronic devices [5,6].

Initially investigated roughly 150 years ago, polyaniline (PANI) is an excellent ICP with a partially flexible rod-like structure [7–11] and has garnered remarkably interest owing to its simple preparation, high selectivity and sensitivity, adjustable redox behavior, unusual thermal stability, affordability, and distinctive anticorrosion features. However, PANI in its pure form does not exhibit these characteristics and must be integrated with other suitable materials to unlock these remarkable

Abbreviations: APS, Ammonium persulfate; BP, Buckypaper; CEA, Carcinoembryonic antigen; CS, Chitosan; CPs, Conducting polymers; CSA, Camphorsulfonic acid; CNTs, Carbon nanotubes; CRI, Color rendering index; DFT, Density functional theory; DSSC, Dye-sensitized solar cells; EB, Emeraldine base; ES, Emeraldine salt; ETL, Electron transport layer; G, Graphene; GO, Graphene oxide; GQD, Graphene quantum dot; HCl, Hydrochloric acid; ICPs, Intrinsically conductive polymers; ITO, Indium tin oxide; LBL, Layer-by-layer; LEDs, Light-emitting diodes; LOD, Limit of detection; MGQDs, Magnetic GQDs; MTX, Methotrexate; NH₃, Ammonia; NMP, N-Methyl-2-pyrrolidone; OCV, Open circuit voltage; OG, Orange G; ORR, Oxygen reduction reaction; PANI, Polyaniline; PC, PANI-cellulose; PC-TENG, PANI/cellulosic hierarchical structure; PEMs, Proton exchange membranes; PTSA, P-toluenesulfonic acid; PL, Photoluminescence; QC, Quercetin; QDs, Quantum dots; RGO, Reduced graphene oxide; ROS, Reactive oxygen species; WLEDs, White LEDs.

https://doi.org/10.1016/j.jece.2024.113460

^{*} Corresponding author.

^{**} Corresponding author at: Fuel Cell Institute, Universiti Kebangsaan Malaysia, Bangi, Selangor 43600, Malaysia. E-mail addresses: m.beygi2300@gmail.com (M. Beygisangchin), ctie@ukm.edu.my (S.K. Kamarudin).

properties. The synthesis strategies for PANI are pivotal in achieving optimal characteristics for specific applications. Therefore, PANI is suitable for various applications, including in sensors [8,9,12], solar cells [13], biosensors [14,15], supercapacitors [16,17], electrochromic glasses [18], electroluminescence machines [19], photovoltaic cells [20], gas separation membranes [21], anticorrosion [22], and biomedical [23] field.

The exploration of carbon nanomaterials has started in the 1970s with the study of fullerenes and associated materials. Carbon nanomaterials encompass a broad group of components predominantly made up of carbon particles organized into diverse nanoscale designs. These components exhibit unique properties and have extensive technological applications.

Some of the well-established carbon nanomaterials are fullerenes, carbon nanotubes (CNTs), and graphene (G) and its derivatives, including graphene oxide (GO) and reduced graphene oxide (rGO) [24–29]. When combined with PANI, these carbon nanomaterials form ideal nanocomposites for various applications, such as sensing, opto-electronics, and energy-related applications, including supercapacitors and solar cells [30–34]. However, achieving an extraordinary performance for PANI combined with these carbon nanomaterials poses challenges related to nanocomposite functionalization, synthesis strategies, matrix–nanofiller compatibility, and optimized processing parameters. Therefore, the quest for eco-friendly nanomaterials and novel synthesis methods is vital and urgent.

Graphene quantum dots (GQDs) have recently gained prominence as a well-known 0D material [35,36]. They are derived from small G fragments and exhibit distinctive phenomena attributed to edge effects and quantum confinement [36–38]. GQDs are recognized for their unique optical, electrical, and chemical features coupled with eco-friendliness, biocompatibility, and superior photostability that prevents issues such as photobleaching and flashing. Their photoluminescence (PL) properties stand out as a key characteristic of GQDs [35,39]. Owing to these specific properties, GQDs are the best candidate for use in several applications including in sensors [36,38], optoelectrical detectors [40], biological imaging [41], solar cells [42,43], fluorescent probes [44,45], light-emitting diodes (LEDs) [46]263, photocatalysis [47], drug carriers [48], lithium-ion batteries [49], and fuel cells [50–52].

Combining PANI's remarkable electrical conductivity and redox properties with GQD's distinctive quantum confinement effects and high surface area, the comprehensive properties of PANI–GQD nanocomposites offer significant advantages for applications across various fields. PANI–GQD has demonstrated considerable potential in diverse areas, including in sensors [53–63], biosensors [64–68], supercapacitors [69–78], solar cells [70,79,80], optoelectronics [81–85], and coating [86]. These applications hold promise for influencing our standard of living and drawing significant commercial attention.

This review offers comprehensive findings on PANI–GQD nano-composite synthesis and properties across various applications. The preparation strategies for PANI–GQD nanocomposites are stated, including a discussion and tabulation of synthesis factors that directly effect the morphological structure of these nanocomposites. Future research directions for PANI–GQD nanocomposites are also outlined, and suggestions for compositing PANI with GQD for various applications are provided.

2. PANI

As a type of CPs, PANI has garnered considerable attention in nanotechnology and materials science. This unique component exhibits intriguing electrical conductivity, reversible redox properties (oxidation/reduction), environmental stability, and anticorrosion characteristics, making it a versatile candidate for various applications, spanning electronics [18,87–94], energy storage such as photocatalysis [95–99], supercapacitors [100–103], batteries [104,105], fuel cells [106–112],

medicine [113–115], and anticorrosion [22,116]. Despite its several unique advantages, PANI suffers from the following challenges to its utilization:

- 1) Mechanical properties: Despite its flexibility, the mechanical limitations of PANI impact device reliability. Thus, research must focus on enhancing its durability. To overcome this issue, several strategies can be applied. PANI can be combined with other materials such as CNTs, graphene, and aerogel buckypaper (BP) to improve its mechanical properties. Aerogel BP exhibits high tensile strength and flexibility, even after repeated folding and rubbing. Cai et al. [117] fabricated a novel PANI-CNT aerogel BP that demonstrates impressive durability, with a tensile strength of 25 MPa and a strain of 11.4 %. It retains 84.0 % and 59.3 % of its capacitance after 2000 and 10,000 cycles, respectively, maintaining 1.224 F/cm², and outperforming similar materials in terms of long-term stability. This work paves the way for the development of robust and durable supercapacitor electrodes with superior performance and potential for real-world applications.
- 2) Nanostructuring PANI into forms such as nanofibers, improves structural integrity and mechanical features. Mohammadi et al. [118] prepared a nano-Al/PANI composite via a solid-state milling approach, which exhibits distinct morphologies, with wire drawing producing 30–60 nm spherical particles. While the conductivity of the composite $(1.02 \times 10^{-3} \text{ S/cm})$ is lower than that of pure PANI $(1.2 \times 10^{-2} \text{ S/cm})$, the enhanced thermal stability with a total weight loss of 38.67 % compared to 46.28 % for pure PANI suggests potential applications in areas requiring both electrical conductivity and heat resistance.
- 3) Processing control: PANI properties are highly dependent on synthesis conditions, requiring precise control for desired outcomes and scalability. To overcome these issues, several strategies can be employed, including optimizing synthesis parameters, utilizing advanced polymerization techniques, improving doping methods, selecting controlled solvents and additives, implementing scalable manufacturing processes, applying post-processing treatments, and using composite materials. Shah et al. [119] established a promising approach for the affordable synthesis of electroactive PANI using diesel as a novel dispersion medium. Through optimization of reaction parameters such as the amount of monomer, oxidant, dopant, and solvents, the optimized PANI salt exhibits a highly porous morphology and thermal stability up to 417 °C. The PANI salt demonstrates good solubility in various solvents such as chloroform, N-Methyl-2-pyrrolidone (NMP), dimethyl sulphoxide, and in a 1:3 mixture by volume of 2-propanol and toluene, facilitating its application versatility. Notably, it shows significant corrosion protection potential, reducing the corrosion rate of stainless steel in marine water by 67.9 %. This work offers a cost-effective and scalable method for producing PANI with valuable properties for applications in corrosion protection and other areas.
- Conductivity: Although PANI exhibits good conductivity among polymers, improvements are necessary for its application in highspeed electronics. To overcome this problem, researchers employed a novel synthesis strategy with unique nanostructure and morphology, optimizing dopants with effective protonic acids to enhance PANI's conductivity. Beygisangchin et al. [8] synthesized PANI using p-toluenesulfonic acid (PTSA), camphorsulfonic acid (CSA), acetic acid, and hydrochloric acid (HCl) dopants, revealing optical band gaps of 3.1-3.9 eV and varied conductivity. PANI-PTSA exhibited the highest conductivity at $3.84 \times 10^{1} \, \text{S} \cdot \text{cm}^{-1}$, superior PL, and a 0.26 nM fluorene detection limit, making it ideal for sensor applications. Lan et al. [120] prepared MS@PANI as lightweight and highly efficient conductive absorbent materials by utilizing the ultra-low density and air-impedance-matching properties of existing polyimide nano-sponges. By controlling PANI's crystallinity and aggregation characteristics, the research achieved tunable electrical

- conductivity and electromagnetic parameters, thus influencing absorption properties. The resulting PANI sponge absorbers demonstrated effective absorption across the X-band, highlighting the importance of microstructural control in enhancing absorber performance and offering valuable insights for the future development and application of polymer absorbers in electromagnetic wave absorption.
- 5) Stability: Doping for enhanced conductivity raises concerns regarding stability over time, especially under changing environmental conditions. To overcome this challenge, scientists introduce crosslinking agents to enhance chemical and mechanical stability, use stable dopants to prevent degradation, and form composites with stable materials. Ali et al. [121] fabricated a highly stable CO gas sensor based on PANI/Ag₂O via an in-situ polymerization method. The results exhibited excellent performance, including a high response rate (97 %), fast response and recovery times (37 s/41 s), remarkable stability, and a limit of detection (LOD) (2 ppm). The straightforward and inexpensive in-situ polymerization technique makes it a viable option for practical applications. Further investigation into the specific mechanisms of Ag₂O doping and its interaction with PANI to enhance CO sensitivity would provide deeper insights for further optimization and potential sensor development for real-time CO detection. Xu et al. [122] established a novel and effective strategy for enhancing the durability of proton exchange membranes (PEMs) in fuel cells. The in situ growth of a porous PANI film encapsulating CeO_x nanoparticles significantly prevents the free radical attack on the PEM, as demonstrated by ex situ and in situ tests. The modified PEMFC exhibits a promising peak power density of 988 mW cm⁻² at 80 °C with 100 % RH and at least 400 hours of open circuit voltage (OCV) durability, showcasing the effectiveness of this approach in preserving the fuel cell performance. This strategy holds significant potential for improving the long-term stability and reliability of PEM fuel cells.
- 6) Sensitivity: The sensitivity of PANI to environmental issues affects the device stability and performance, especially under severe conditions. To overcome this issue, researchers employed several strategies such as optimizing doping, surface modification, composite formation, and nanostructuring to improve sensitivity. Yang et al. [123] established a new highly sensitive sensor based on a PAN-I/cellulosic hierarchical structure (PC-TENG). The combination of PANI and cellulose provides tremendous gas permeability (up to 500 ppm detection range) and abundant adsorption sites (minimum LOD of 100 ppb), leading to enhanced sensitivity. The PC-TENG sensor exhibits remarkable sensitivity, particularly for trace NH₃ concentrations (0.1-50 ppm), achieving the highest reported value of 45.41 % per ppm in this range. This work represents a significant advancement in self-powered NH3 gas sensors, offering high sensitivity, a broad detection range, and practical advantages for real-world use. Sun et al. [124] introduced a promising electrochemical sensor based on the self-supported NiC₂O₄/PANI nanocomposite electrode for dissolved ammonia (NH3) detection in smart aquaculture. The results exhibited remarkable sensitivity (41 mA $\mu M^{-1}~cm^{-2})$ and a low LOD (0.83 $\mu M),$ making it suitable for the early detection of NH₃ in water. The 3D PANI structure facilitates fast electron transport, and the specific reaction of Ni oxalate with NH₃ contributes to the sensor's high performance. Additionally, the sensor demonstrates good anti-interference ability, reusability, and long-term stability, making it a valuable tool for monitoring and managing water quality in aquaculture systems.
- 7) Film homogenous morphology: Attaining homogenous PANI films is crucial for device fabrication, but controlling its morphology poses challenges. To overcome this problem, researchers employed various strategies including optimizing solvent selection, controlled polymerization techniques, treating the substrate surfaces, and selecting proper coating methods such as spin coating. Garrudo et al. [125] studied a safer and more effective solvent system for processing

- PANI, a key material for bioelectronic devices. Using a mixture of trifluoroethanol and hexafluoropropanol as the solvent, researchers achieved significantly improved electrical conductivity (up to 70 S·cm⁻¹) and better structural ordering compared to traditional solvents like m-cresol. This new solvent system is also easier to remove, making it a promising approach for developing next-generation bioelectronic devices with enhanced performance and biocompatibility. Wang et al. [126] developed a novel strategy for homogeneous blended systems of PANI-cellulose (PC) composite using a low-temperature two-step concentrated H₂SO₄ method and a wet spinning method. With increasing PANI content, the conductivity and toughness of the composite fibers initially increased and then decreased. PC15 (15 wt% PANI) achieved a conductivity of 21.50 mS·cm⁻¹, 2.49 %/ppm NH₃ sensitivity, and a 0.6 ppm detection limit. This work paves the way for the development of next-generation e-textiles that are both functional and environmentally friendly, offering significant potential for various smart textile applications.
- Scaling and expenses: The commercial production of PANI faces challenges in scalability and cost-effectiveness. To overcome this issue, researchers use cost-effective synthesis, scale up production, optimize processes, automate manufacturing, and blend with cheaper materials such as natural materials and biowastes [127]. Khattari et al. [128] fabricated a PANI-clay composite as a cost-effective and efficient absorbent for removing Orange G (OG) dye from water. The results show a significantly higher equilibrium adsorption capacity (67.35 mg/g) compared to raw clay (47.62 mg/g), demonstrating its effectiveness in dye removal. The adsorption process follows both pseudo-second-order kinetics and the Langmuir isotherm model, indicating a chemisorption mechanism and monolayer adsorption. The negative Gibbs free energy values suggest a spontaneous adsorption process, while the increasing values with temperature indicate an endothermic nature. Computational optimization of the OG dye structure provides valuable insights into the potential adsorption mechanism.
- 9) Application-specific challenges: Each application presents unique hurdles, such as addressing charge storage capacity or sensitivity in sensors. To address this challenge, customize the synthesis, optimize processing, and functionalize materials according to specific requirements. Integrate PANI into tailored composites, incorporate it into devices with appropriate engineering, rigorously test performance, and iteratively refine based on application feedback for continuous optimization. Our previous work elaborates on these strategies in detail [129].

Therefore, explore innovative materials and synthesis techniques are crucial to enhance PANI's effectiveness and efficiency across a range of applications, particularly those demanding extensive energy and high-speed electronic usage. PANI can be synthesized via chemical or electrochemical methods, which will be presented in detail in the next section, tailoring its properties for proper application. Fig. 1 presents a summary of PANI's properties and applications.

2.1. PANI synthesis strategies

MacDiarmid [130] was the primary researcher to categorize PANI into several types: (a) leucoemeraldine colorless (completely reduced), (b) emeraldine salt (ES) in green, (c) emeraldine base (EB) in blue (semi-oxidized), and (d) pernigraniline (fully oxidized) with a violet color as shown in Fig. 2.

PANI is typically synthesized through chemical and electrochemical oxidative polymerization methods [129,131]. In these procedures, doping and polymerization occur simultaneously. Therefore, selecting the most appropriate among the available dopants, such as PTSA, HCl, and CSA, is vital to enhance PANI's electrical conductivity and in turn affect its bandgap and crystallite size [132–134].

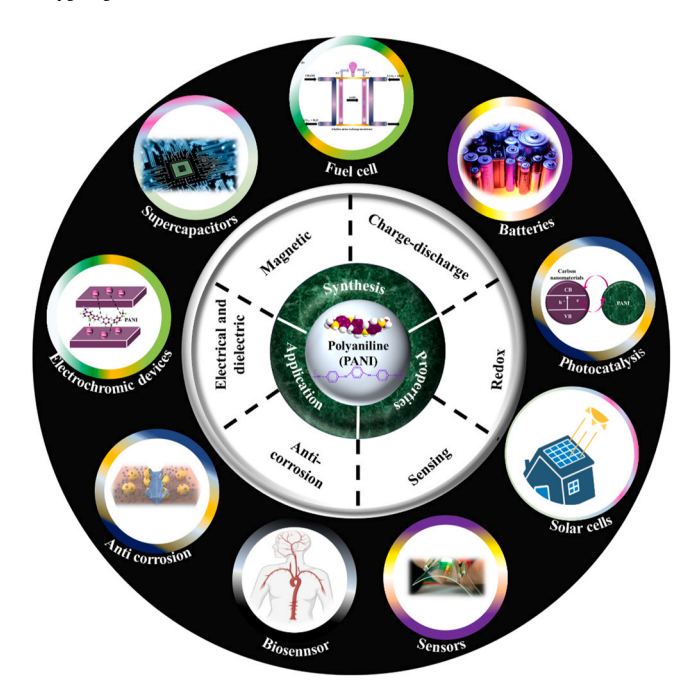


Fig. 1. Unique features and application of PANI.

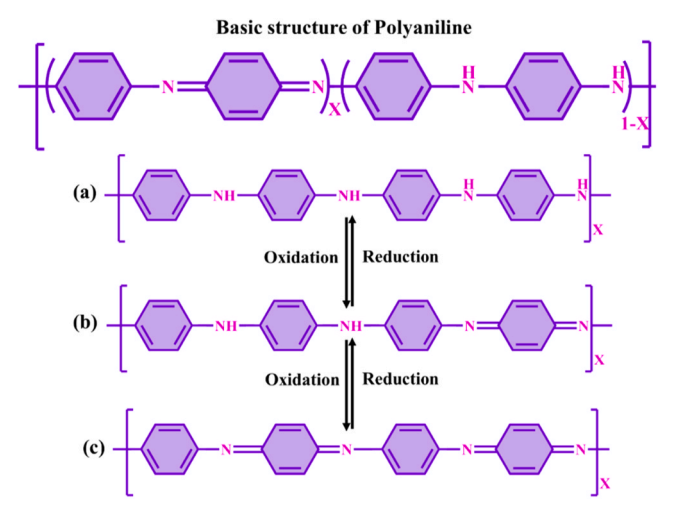


Fig. 2. Basic molecular structure of several forms of PANI: (a) leucoemeraldine, (b) ES/EB, and (c) pernigraniline [136].

The primary contrast between these methods is that the chemical approach yields better results than the electrochemical approach [135]. Nonetheless, the electrochemical method offers various advantages over the chemical technique: (1) it is cost-effective and simple; (2) it enables the solution doping of PANI with the desired ion, facilitating doping nature; (3) a catalyst is not needed in the electrochemical processes; (4) CPs appear uniform and untainted when coated onto the electrode surface; and (5) the electrochemical preparation occurs within a slot cell, comprising a counter electrode, a working electrode, and a reference electrode.

2.2. PANI properties

PANI has garnered significant attention in the field of electronics and materials science owing to its unique and versatile features, including magnetic, anticorrosive, redox, sensing, charge—discharge, electric—dielectric features, affordable, easily synthesizable, high surface area, and environmental stability characteristics. Owing to these remarkable

properties, PANI proves to be a suitable CP for various applications, such as electronics, medicine, and supercapacitors, which will be discussed in the next section. These attributes have been extensively elucidated in prior studies with detailed explanations [7]. Here, each feature of PANI is described as follows:

- Magnetic properties: PANI's magnetic properties, particularly its high spin density, have attracted significant interest [137]. Doping can modify PANI's magnetic characteristics; a previous research exploring PANI–Fe₃O₄ composites revealed their superparamagnetic behavior [138]. Researchers also observed the ferroelectric response and magnetic behavior of PANI nanotubes, especially in their applications in methanol [139].
- 2) Electrical and dielectric properties: The electrical and dielectric features of PANI make it attractive for use in polymers [140]. Doping improves conductivity, and various models were established to clarify the charge transport mechanisms in PANI nanocomposites, accounting for factors such as disorder, crystallinity, and defects [141]. Wessling projected a nonequilibrium model to explain interfacial interactions within CP nanocomposites [142].
- 3) Redox properties: The redox properties of PANI are pivotal because it can transition between various reversible forms depending on electron acceptance or removal [143]. Research has delved into PANI's electrochemical activity and reduction across different environments, unveiling its potential applications in redox-active and nanojunction components [143,144].
- 4) Anticorrosion properties: Researchers have explored the antioxidant properties of PANI, showcasing its ability to scavenge radicals as influenced by its oxidation states [145]. PANI has garnered attention for its anticorrosion capabilities, particularly in coatings for stainless steel and other substrates [146]. PANI coatings can suppress corrosion and improve the resilience of alloys against a range of environmental conditions [145,146].
- 5) Charge–discharge properties: PANI's outstanding charge–discharge properties make it suitable for utilization in Li-ion batteries [147]. The capacitive characteristics of PANI-based materials have been investigated for applications in supercapacitors, and PANI composites have shown improved performance compared with pure PANI [148]
- 6) Sensing properties: PANI and PANI-based composites possess valuable sensing properties, making them useful materials for sensors detecting various gases and ions [149]. Utilized as sensing materials, PANI thin films have been deployed for detecting polycyclic aromatic hydrocarbons and showcased remarkable stability, selectivity, and sensitivity [8,9].

2.3. PANI applications

PANI, a CP within the family of organic polymers, possesses unique conductivity, flexibility, cost-effectiveness, and ease of synthesis properties. It has gained significant attention across various fields, including electronics, medicine, and anticorrosion. In electronics, PANI serves as a conductive coating and a component in electrochromic devices [18], sensors [87-93], and solar cells [94]. Its ability to undergo reversible changes in oxidation state has paved the way for its utilization in energy storage devices, such as photocatalysis [95-99], supercapacitors [100–103], batteries [104,105], and fuel cells [106–112,150]. In the biomedical field, PANI's biocompatibility and conductivity render it a promising candidate for applications in biosensors and drug delivery systems [113-115]. Its use in anticorrosion coatings is remarkable; it forms a protective layer on metallic surfaces that prevents corrosion and enhances material durability [22,116]. Overall, the multifaceted nature of PANI continues to propel research and innovation across diverse scientific disciplines, underscoring its significance in contemporary materials science and technology.

Fenniche et al. [151] coated PANI on an indium tin oxide (ITO)

substrate using the electrodeposition method from H₂SO₄. SEM characterization shows that the morphology of PANI is uniform, with a high surface-to-volume ratio and efficient ion channels, which enhance electrochromic coloring efficiency and confirm flexibility. The PANI films significantly influenced light absorption, as demonstrated by UV spectra studies. These films exhibited outstanding mechanical flexibility during repeated compressive bending cycles, remarkable electrochromic performance, considerable optical modulation, and high staining efficiency. Hatem et al. [152] synthesized PANI with an anionic surfactant in 1D and demonstrated the promising potential of PANI fibers for hydrogen storage. The ice bath preparation method yielded semi-crystalline fibers with high conductivity and rapid hydrogen adsorption (86 % in 9 minutes). However, further research is needed to optimize the desorption process and assess the long-term stability of these fibers under practical conditions. Additionally, the specific hydrogen storage capacity (wt%) should be compared to other established hydrogen storage materials for a more comprehensive evaluation.

Zainab et al. [153] successfully prepared PANI nanofibers using a hydrothermal technique for H₂S gas sensing. The spin-coating method allowed for the deposition of the nanofibers in different solvents, with water leading to smaller energy gaps and higher H₂S sensitivity at 150°C. However, further investigation is needed to optimize the sensitivity and response/recovery times across all solvents and operating temperatures. Additionally, exploring the selectivity of the nanofibers towards H₂S compared to other potential interfering gases would provide a more complete understanding of their practical applicability.

Miraqyan et al. [154] established a novel approach for synthesizing PANI from o/m-anisidines and o-toluidine using ammonium persulfate (APS) in organic media. The formation of dihydrobenzoxazole units was shown for poly(m-anisidine), which lowers the amount of both quinonediimine and methoxy groups in PANI. While the PANI exhibits promising features like improved solubility, high thermal stability, and moderate conductivity, further investigation is crucial. Understanding the impact of dihydrobenzoxazole unit formation in poly(m-anisidine) on its properties and optimizing the doping process for enhanced conductivity are essential for realizing the full potential of these materials in various applications. Beygisangchin et al. [10] fabricated PANI films with varying NMP concentrations and introduced PANI-6 (1 % PTSA and 3 % NMP) as an optimized candidate for sensing and supercapacitor applications. The optimized film exhibits desirable properties like a low bandgap, high PL intensity, and stable conductivity. However, further investigation is needed to understand the specific role of NMP in influencing these properties and to optimize the NMP concentration for specific applications. Additionally, comparing the performance of PANI-6 to existing materials in sensing and supercapacitor devices would provide a more conclusive assessment of its potential. Table 1 presents recently reported PANI-based composites for various applications, including the preparation methods, advantages, disadvantages, and significant findings for each reference.

3. GQDs

GQD is a 0D component [35] appearing as tiny G pieces and exhibiting edge effects and quantum confinement [38]. GQD has remarkable features, including biocompatibility, unique PL, extraordinary photostability in contrast to photobleaching and blinking, and low toxicity [35,155]. GQD emits various colors such as blue, green, yellow, orange, and red, and this ability is influenced by the size, bandgap changes, and defects. With a tunable bandgap, GQD's luminescence is determined by particle size, surface chemistry, and absorption spectrum ranging from 230 nm to 350 nm [156]. The functional groups on GQD impact the absorption properties and PL outcomes, making them versatile in optoelectronic applications.

As shown in Fig. 3 [35], GQD is a significant candidate for applications such as in optoelectrical devices [157], biological imaging [41], solar cells [42], fluorescent agents [44,158,159], LEDs [160],

lithium-ion batteries [161], photocatalysis [47], and drug carriers [162]. Despite its unique advantages, GQD suffers from the following challenges in its utilization:

- 1) Limited scalability: The mass production of GQDs faces challenges due to limitations in scalability. Existing synthesis methods often struggle to produce GODs in large quantities with consistent quality, hindering their widespread application. Additionally, it is crucial to optimize synthesis methods, such as chemical and green synthesis, to improve yield. Developing advanced and scalable purification processes to ensure high purity and standardizing protocols for consistent quality are also essential steps. Shen et al. [163] prepared N,S-GQDs as probes via a scalable one-step hydrothermal synthesis for detecting Fe³⁺, Cu²⁺, and Ag⁺. The results exhibit a high yield (87.8 %), bright blue fluorescence, high quantum yield (23.2 %), and LOD (8 nM for Fe³⁺, 250 nM for Cu²⁺, 50 nM for Ag⁺). This work highlights the potential of N,S-GQDs as a powerful tool for sensitive and selective metal ion detection in various real-world applications. Survawanshi et al. [164] prepared efficient GODs with boron and nitrogen via a new approach, confirming the functionalization using FTIR and TEM. Particularly, the quantum yields were significantly enhanced for B-GQDs, N-GQDs, and B,N-GQDs compared to undoped GQDs. Enhanced quantum yields and stability were observed for B-GQDs, N-GQDs, and B,N-GQDs. B, N-GQDs demonstrated effective paraoxon detection in water with a low detection limit $(1.0 \times 10^{-4} \text{ M})$ and good repeatability (RSD 2.99 %).
- 2) Surface functionalization complexity: GQDs need surface functionalization for tailored properties, but precise control is costly. Variability hampers standardization and performance consistency. Additionally, surface functionalization of GQDs with amino, carboxy, and hydroxy groups, achieved through both covalent and noncovalent methods, significantly impacts their properties and functionalities. To enhance these properties, researchers employed an innovative and automated approach using versatile functionalization agents [165,166]. Geng et al. [167] present the impact of surface charge on stem cell fate, focusing on osteogenic differentiation. Negatively charged GQDs (GQD-) significantly enhance osteogenic differentiation in hMSCs via the BMP/Smad pathway, while positively charged GQDs (GQD⁺) show no effect. Incorporating GQD into a 3D hydrogel scaffold demonstrates potential for bone regeneration, underscoring the importance of surface charge in biomaterial design for tissue engineering. Yang et al. [168] prepared a novel fluorescent probe based on Se-GQDs for the detection of oxidative OH and GSH. Se-GQDs, with 1-3 at. layers and a lateral size of 1-5 nm, exhibited high selectivity and stability (quantum yield: 0.29, PL lifetime: 3.44 ns). The fluorescence of Se-GQDs was reversibly quenched and recovered by •OH and GSH due to reversible oxidation of C-Se groups and reduction of Se-Se groups. This switch showed a rapid response and a low detection limit (0.3 nM for •OH), outperforming switches made from organic dyes, when tested in aqueous solutions and living HeLa cells.
- 3) Photobleaching and photoblinking: GQDs suffer from photobleaching and photoblinking, decreasing their stability in optoelectronic devices and impacting the lifespan and reliability for sustained performance. To overcome this problem, scientists are looking for new strategies to optimize synthesis, protective coatings, and integration with stable materials. Gao et al. [169] established a new strategy to prepare GQDs with precise control over their oxidation degree via a bottom-up approach. The distinct properties of two water-soluble GQDs were comprehensively characterized, linking the oxidation degree to optical properties, functional groups, and molecular weight. This led to the development of robust temperature probes with a wide

 Table 1

 Recent PANI-based composites in various applications

PANI based composites	Synthesis method	Advantages	Disadvantages	Application	Findings	Reference
WO3-G-PANI	Electro- chemical	Enhanced energy storage, electrochromic ability, increased capacitance, chemical compatibility, and surface roughness	Complex fabrication procedure, potential stability issues, potential cost, and optimization challenges	Electro-chromic glasses	Good coloration efficiency with a value of 67.47 due to the introduction of nanofillers	[18]
PANI-GO	Chemical	improvements Affordable, sensitive with low LOD, rapid recovery, linear range, repeatability, stability, and superior selectivity	Complex synthesis, potential environmental or health concerns	Sensors	9.6 % response at 70 ppm, 23-second recovery, and low LOD (30–230 ppm) for NH_3	[87]
PANI-CNT	Chemical	Improved performance, real- time monitoring, robustness, conductivity, stability, gauge factor, strain sensitivity, and low hysteresis	Complex synthesis, production scalability, and possible challenges for optimization	Sensors	High gauge factor with a value of 167.94 for PANI–CNT–silicone rubber	[88]
GO/Fe ₃ O ₄ / PANI	Chemical	Simultaneous detection, dopant synergy, square wave anodic stripping voltammetry, sensitivity, reproducibility, and stability synergies	Validation in various environments and assessment of interference from complex samples	Sensor	Low LOD and oxidative peak for Pb^{2+} detection with values of 5.15 nM and -0.4899 , respectively	[89]
PANI-Au	Interfacial chemical	Novel fabrication, improved humidity sensing, mechanistic insight, high sensitivity, and scalability highlight advancements	Elevated ambient temperature resistivity, fabrication constraints, and restricted Au loading	Sensor	For PANI-Au nanocomposite: resistivity 1.3 Ω m, responsivity 79 %, response time 7.8 s, and RH range 11–85 $\%$	[90]
PANI-Ag	Chemical	Novel synthesis method, highly sensitive detection, uniform distribution of Ag nanoparticles, quick response/ recovery, reusability, and enduring stability	Validation of sensor performance needed across diverse environments, potential interference from other gases	Sensor	PANI–Ag efficiently detects NH ₃ across a broad range, with response/recovery times of 30–120 s, optimal 57 % response at 100 ppm NH ₃	[91]
PANI–Ag–Pd	Sol-gel	Versatile fabrication method, high sensitivity	Synthesis parameters need refining for consistent performance, scalability challenges must be addressed for large-scale production	Sensor	High sensitivity and low surface roughness, particularly with increasing Pd concentrations	[92]
PANI-G	Chemical	Facile fabrication, highly sensitive and responsive, remarkable flexibility, and rapid photovoltage response	Warrants further validation of sensor performance in diverse environments and addressing scalability challenges for large- scale production	Sensor	Shows potential in nondestructive health monitoring, with a peak detectivity of 6.8 \times 10°7 cm Hz^1/2 W^{-1}, responsivity of 2.5 V W^{-1}, and photovoltage response of 10 μV	[93]
Γi ₃ C ₂ T _x MXene/GO/ PANI	Chemical	Reshapable and patternable surfaces, reusability, and excellent solar thermal energy conversion	Validation of MXene/GO/PANI (MGP) evaporators across diverse environments; scalability challenges must be addressed for large-scale water purification applications	Solar cell	Evaporation efficiency of 135.6 % by the flower-shaped MGP evaporator	[94]
PANI/ Fe ₃ O ₄ / ZnO	Surface imprinting	High selectivity, enhanced photocatalytic performance, magnetic separation feature, active species involvement	Optimizing photocatalyst stability, performance in various environments, and ensuring scalability and cost-effectiveness	Photocatalysis	Superior efficiency and selective photodegradation using molecularly imprinted photocatalyst.O ₂ - and h+ indicate degradation mechanisms	[95]
PANI-Au	Electro- chemical	Facile and scalable preparation, high activity and selectivity, contribution to a carbon-neutral economy	Preparation complexity underscores the necessity for electrocatalyst stability optimization during extended use; high costs pose challenges for large-scale implementation	Photocatalysis	Core-shell nanoPANI-Au boosts e- CO ₂ RR, indicating structural importance; applied current shapes PANI-Au, revealing growth insights, with efficient CO ₂ utilization	[96]
CNTs/ AgFeO ₂ / PANI	Hydrothermal	Novel ternary nanocomposite, magnetic property, superior degradation ability, stability and reusability	Optimization of reaction conditions needed for maximum degradation efficiency and understanding of dye removal mechanisms	Photocatalysis	Shows stability and reusability over multiple cycles, promising practical use in wastewater treatment	[97]
Fe ₃ O ₄ @PANI	Chemical	Good formation and stability of aerobic granular sludge (AGS), and enhanced pollutant removal performance	Optimizing Fe ₃ O ₄ @PANI dosage, synthesis conditions for efficiency, and scalability challenges for large-scale treatment	Photocatalysis	Fe ₃ O ₄ @PANI boosts AGS stability, promotes EPS secretion, and enhances pollutant removal.	[98]
PANI-CNT	Electro- chemical	High removal rate, compatibility with coexisting pollutants, and mechanistic insights	Optimization of operating conditions, voltage parameters; scalability, and cost-	Photocatalysis	Electro-assisted NF membranes improve the removal of weakly charged micropollutants. Understanding the mechanisms	[99]

(continued on next page)

Table 1 (continued)

PANI based composites	Synthesis method	Advantages	Disadvantages	Application	Findings	Reference
PANI-MnO ₂ - CNTs	Hydrothermal	Ultracapacitance electrode component, specific capacity improvement, and cyclic stability	effectiveness challenges for large-scale implementation Optimization of synthesis parameters, composite selection for efficiency, scalability, and cost-effectiveness	Supercapacitor	aids in the design of efficient removal strategy. Improved electrochemical performance, suggesting synergy for energy storage. Long-term stability implies potential for practical, durable energy storage	[16]
RGO/RuO ₂ / PANI	Interfacial polymerization	Enhanced performance for wearable electronics, high areal capacitance, high energy density, high power density, cyclic stability, and durability	Optimization of composite composition for efficiency and addressing scalability and cost- effectiveness for large-scale production	Supercapacitor	devices. Areal capacitance: $1.66~\mathrm{F\cdot cm^{-2}}$; specific capacitance: $677~\mathrm{mF\cdot cm^{-2}}$; charge transport: $\mathrm{Rct} = 5.5~\Omega$; energy density: $60.18~\mu\mathrm{W\cdot h\cdot cm^{-2}}$; LED powered for $180~\mathrm{s}$ by $3~\mathrm{FSSSDs}$ in series	[101]
PANI/ fMWCNTs	Chemical	Improved cycling performance, electrochemical properties, specific capacitance, and stability, yielding enhanced energy density	Exploring long-term stability and scalability of synthesized composites for practical applications, warranting further investigation	Supercapacitor	Specific capacitance: 867 F g ⁻¹ ; energy density: ~77.0 Whkg ⁻¹ ; power density: ~801 Wkg ⁻¹ ; coulombic efficiency: 97 %; retention: 98.5 % after 10,000 cycles	[102]
Fe ₃ O ₄ -NH- PANI	Chemical	High-specific capacitance and high-performance energy storage	Exploring high stability, sensitivity, scalability, and cost- effectiveness for practical	Supercapacitor	Specific capacitance of 336.4 F g ⁻¹ at 10 mVs ⁻¹ scan rate, with specific energy of 11.81 Wh Kg ⁻¹ and	[103]
Nafion/RGO/ PANI	Chemical	Enhanced rate performance, increased discharge capacity, improved reaction kinetics, conductivity, and intricate porous structure	applications Costly and complex fabrication procedures, optimization of synthesis parameters to investigate high scalability, cycling performance, and suitability for practical applications	Lead-acid batteries	specific power of 1258.3 W Kg ⁻¹ HNGP composites improve lead- acid battery discharge capacity and rate performance by boosting conductivity and creating a porous structure, aiding electron migration and ion diffusion.	[104]
PANI-G	Chemical	Advanced functionality, enhanced performance, long cyclability, minimal overpotential, outstanding volumetric capacity, and	Complexity of preparation for 2D mesoporous materials, manufacturing challenges requiring specialized techniques, and limited practical	Micro battery and gas sensor	2D mesoporous nanosheets enable high-performance microsystems with dendrite-free zinc anodes and sensitive gas sensors.	[105]
ANI-Pd	Chemical	ultrastable sensitivity Controlled structure and morphology, tailored charge transfer properties, enhanced catalytic activity, and remarkable theoretical insights	application data Protocol complexity hinders scalability, synthesis, characterization. MnO ₂ variation challenges material selection. Research focuses on specific catalytic reaction, limiting generalizability.	Fuel cells	Controlled synthesis of Pd/PANI catalysts using $\rm MnO_2$ templates enhances TOF in furfural coupling.	[106]
PANI-Pd	Chemical	Green synthesis, strong interaction, excellent catalytic activity	Exploration constrained to specific reactions, base choice influences catalytic activity. One-pot synthesis challenges	Fuel cells	Pd-PANI nanocomposite synthesized in water exhibits efficient Suzuki-Miyaura coupling catalysis in diverse media.	[107]
PANI-Fe	Chemical	High selectivity, enhanced dispersion and reduction, supported hydrogenation	industrial scaling. Exploration of catalyst's potential with different reactions/reactants. Lack of understanding of PANI's performance in this application	Fuel cells	PANI-supported Fe catalysts boost lower olefin selectivity in synthesis gas conversion, enhancing propylene yield.	[108]
PANI-G	Electro- chemical	High conductivity, and large electrochemically active surface area, and enhanced bacterial biofilm loading	Exploration in diverse applications or electrode configurations. TSGP surpasses carbon cloth; lacks comparison with other materials	Microbial fuel cell	TSGP-modified MFC anode enhances voltage and power density, outperforming carbon cloth controls.	[109]
GO–PANI–Ag	Chemical	High removal rate, enhanced performance, and high energy generation	GO-PANI-Ag outperformed GO, but full comparison is lacking. MFC challenges persist despite material advancements,	Microbial fuel cells	GO–PANI–Ag outperformed GO in MFCs with a peak power density of $2.09~\mathrm{mW/m}^2$.	[110]
PANI/c- MWCNT/CF	Chemical	Improved performance, high stability, durability, and environmental compatibility	warranting further attention. Composite analysis limits understanding. Scale-up challenges hinder practicality. Gas production effective but unexplored application	Fuel cell	The prepared composite enhances gas production by 59 %, showing potential for underwater energy harvesters.	[111]
Pt@Fe ₃ O ₄ / MWCNT/ PANI	Chemical	Enhanced electrocatalytic activity, facile synthesis, support for immobilization, and maximum current density	Lacks details for the nanocomposite, hindering electrocatalytic insight. Glucose cell focus restricts exploration.	Biofuel cell	The prepared nanocomposite achieves 7.3 mA cm^{-2} current density and 0.6 V OCV.	[112]
PANI-Ag	Solution	Enhanced antibacterial properties, versatile sensing	Lacks details on the Ag/PANI nanostructure, hampering	Biosensor	Ag/PANI nanostructures exhibit strong antibacterial properties,	[113]

Table 1 (continued)

PANI based composites	Synthesis method	Advantages	Disadvantages	Application	Findings	References
		capabilities, low toxicity, simple synthesis method, high reproducibility, and efficiency	further insights; focus on antibacterial/sensing; sensitivity affects applicability		inhibiting <i>E. coli</i> growth and are effective for melamine detection in milk.	
Pd-Fe/PANI	Sol-gel	Efficient <i>Leptospira</i> detection, tailored morphology, highly sensitive	Requires sensitivity boost for lower concentrations; sol-gel spin coating complexity hinders scalability; specificity validation vital to avoid false positives	Biosensor	The prepared biosensor exhibits high sensitivity (16.9 %) for detecting <i>Leptospira</i> bacteria.	[114]
PANI/Ni-MOF	Electro- chemical	High sensitivity and specificity, label-free detection, real-time monitoring, exceptional accuracy, and cost- effectiveness	Fabrication complexity hampers scalability; biosensor promising but requires validation across sample types; tailored for HCV RNA and lacks versatility	Biosensor	The prepared label-free electrochemical biosensor achieves highly sensitive HCV RNA detection (0.75 fM).	[115]
PANI-G	Chemical	Effective corrosion protection, tunable anticorrosion performance, and novel application	Additional data and characterization needed for mechanism understanding. PANI ES concentration optimization crucial. Real-world performance evaluation vital for practicality.	Anticorrosion	Rubber-modified PBZ with PANI ES filler enhances the anticorrosion properties of carbon steel coatings.	[22]
PANI-Pr	Chemical	Eco-friendly, enhanced corrosion protection, high stability	Research needed for diverse performance assessment. Coating optimization crucial for scaling.	Anticorrosion	Silane-based coatings incorporated with Pr-PANI composite enhance anticorrosion properties and reduced magnesium degradation.	[116]

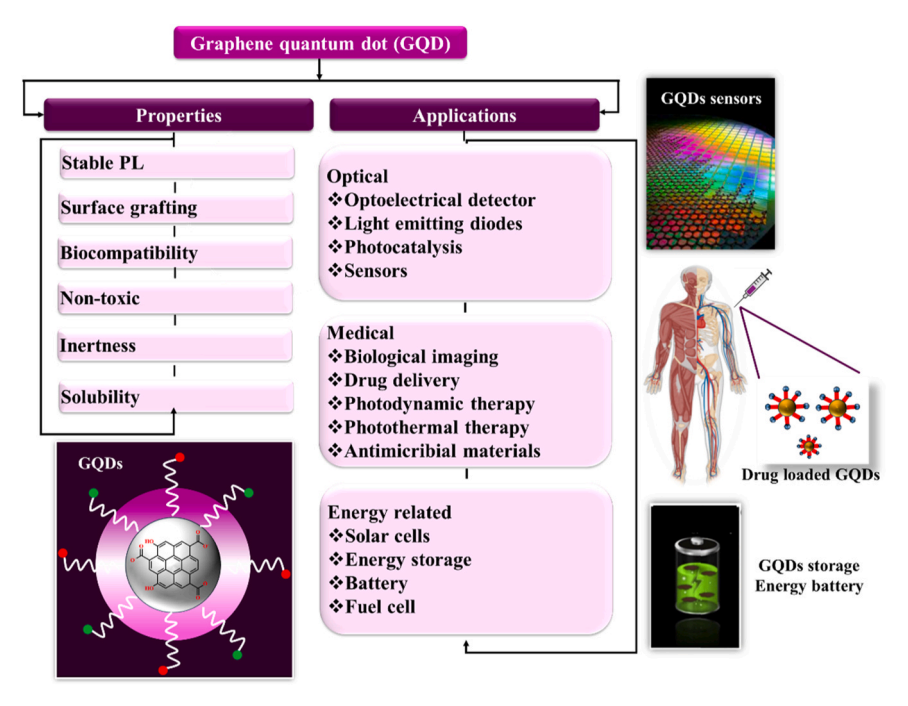


Fig. 3. Prominent properties and usage of GQD.

response range (0–60°C), successfully demonstrated in HeLa cells, indicating potential for biological and selective temperature detection applications. In another of their works, Gao et al. [170] fabricated GQDs with blue, yellow, and red emissions using polyethyleneimine coatings. The blue-emitting GQDs were monocoated, while the red-emitting GQDs were multicoated. These GQDs exhibited excellent chemical stability and low cytotoxicity, making them ideal for bioimaging. The study highlights their potential for multicolor imaging and bioanalysis. However, addressing challenges such as cost-effectiveness, controlling reactive oxygen species (ROS) generation for photodynamic therapy, and ensuring long-term biocompatibility remains crucial areas of research.

4) Environmental sensitivity: GQDs' optical and electronic properties are influenced by temperature, humidity, and pH. Ensuring stability against environmental changes for reliable performance is challenging. To overcome this issue, researchers are developing robust encapsulation techniques, enhancing surface passivation, using stable functionalization agents, and integrating protective coatings to ensure consistent performance under varying environmental conditions [171]. Anjila et al. [172] fabricated Tb-GQDs as a rapid and sensitive spectroscopic tool for detecting melamine in food via microwave and chemical methods. The results show a spherical shape around 6 nm, a high quantum yield of 52, and a LOD of 0.31 μM. This work demonstrates the potential of Tb-GQDs as a sensitive and effective platform for

- real-time melamine detection in food, particularly in milk, offering a valuable tool for the food industry. Balakrishnan et al. [173] introduced a highly sensitive luminescence gas sensor for detecting nitrobenzene, using nGQDs encapsulated in ZIF-8. The nGQD@ZIF-8 sensor detects nitrobenzene gas within 8–320 ppm, with a detection limit of 0.44 ppm. It shows high selectivity (57 %) for nitrobenzene over other VOCs, stability at room temperature, and resistance to humidity and heat. This sensor is promising for reliable environmental monitoring of nitrobenzene.
- 5) Biocompatibility concerns: GQDs show potential application in biomedical fields such as imaging and drug delivery, but concerns regarding their biocompatibility, especially in vivo, necessitate thorough investigation and mitigation strategies for safe use. Additionally, to overcome these issues, employing non-toxic and eco-friendly synthesis methods is required. Abbas et al. [174] present an eco-friendly, acid-free method for synthesizing GQDs from cost-efficient biomass waste, avoiding contamination and high costs. The GODs, averaging ~3 nm in size, are effective fluorescence probes for detecting ferric ions, with a LOD of 0.29 µM. This green synthesis method holds promise for applications in photocatalysis, bioimaging, and sensing. Halder et al. [175] established a novel, one-pot, green synthesis method for GQDs using GO and H₂O₂, completed in 2 hours without harsh reagents or post-purification. The resulting GQDs exhibit high photostability and biocompatibility in macrophages, endothelial cells, and cancer cells, and are internalized primarily via caveolae-mediated endocytosis. These GQDs are effective fluorescent nanoprobes with potential applications in bioimaging, diagnostics, and drug delivery.
- Cost of production: High-quality GQD production involves costly techniques and materials, hindering their widespread applications, especially in cost-sensitive processes. Therefore, researchers should focus on utilizing cheaper, abundant raw materials like waste biomass, and developing eco-friendly, energy-efficient synthesis methods. Optimizing scalable production techniques such as chemical vapor deposition and hydrothermal methods is crucial, alongside implementing continuous flow processes for greater efficiency. Abbas et al. [176] prepared GQDs using sustainable biomass and microwave methods to detect Fe³⁺. This surpasses previous biomass methods and offers highly luminescent GQDs. Further modification boosts the quantum yield to 23 %. The results present a LOD with a value of 2.5×10^{-6} M, paving the way for cost-effective, scalable GQDs for practical sensing applications. In another of their works, Abbas et al. [177] synthesized eco-friendly GQDs for commercialization using cheap biomass and minimal environmental impact solvents like ethanol by proposing a one-step process to detect Fe³⁺. This eliminates the use of harsh acids and expensive precursors. The resulting GQDs boast exceptional properties: an ideal size for many applications (0.5–4 nm), a high layer count (1-3), and excellent fluorescence (21 % quantum yield). The results demonstrate selective Fe $^{3+}$ ion detection with a LOD of 0.5 μ M. This work highlights the potential of sustainable methods for producing high-quality GQDs for diverse applications, including photocatalysis, bioimaging, and practical sensors.
- 7) Integration challenges: Integrating GQDs into existing technologies poses challenges due to compatibility differences. Seamless integration demands thorough research and development to maintain performance and stability. Additionally, researchers aim to overcome this issue by exploring GQD interactions at the atomic level, tackling GQD agglomeration through surface modification, and developing scalable synthesis methods. Lakshmi Narayana et al. [178] address limitations of stability in supercapacitor materials by introducing high-performing NCO/GQDs. Chemical tuning achieves a specific capacitance of

- 3940 Fg⁻¹ at 0.5 Ag⁻¹, exceeding prior materials. Notably, the NCO/GQD-10 % electrode retains nearly 98 % capacitance after 5,000 cycles, demonstrating exceptional stability. These NCO/GQDs further translate to asymmetric and symmetric supercapacitors with impressive energy and power densities, paving the way for next-generation, sustainable energy storage devices. Zhang et al. [179] present a novel fluorescent film based on N-GQDs@HNTs for detecting fish spoilage. The results exhibit strong fluorescence that is quenched by NH₃, a byproduct of fish spoilage, in the linear range of 20–500 ppm, with a LOD of 0.63 ppm. Furthermore, the film successfully monitored the freshness of fish stored at different temperatures, demonstrating its potential for real-world applications in non-destructively monitoring fish spoilage.
- 8) Quantum vield variability: GODs display variable quantum yields, impacting their efficacy in light emission and sensing. Ensuring consistent, high yields poses a challenge for device reproducibility and reliability. Researchers are looking to refine synthesis methods and explore surface passivation to reduce defects and improve light-emitting properties. Carbajal Valdez et al. [180] synthesized GOODs from electrospun PAN fibers and explored their optical properties. The GOQDs exhibit strong light (200-350 nm) and well-defined (550-552 nm). Notably, centrifugation significantly improves quantum efficiency (0.954-0.997), suggesting a route to optimize GOQDs for optoelectronic and biomedical applications, particularly those requiring high light emission. Jin et al. [181] prepared long-wavelength emission (red) and high-efficiency GQDs using 2,7-DHN and PA through a simple one-pot method. The results exhibit dual emission (green and red), with the red emission reaching a remarkable absolute quantum efficiency of 54.9 % in ethanol, among the highest reported for GQDs. Additionally, the GQDs boast good water solubility, low cytotoxicity, and resistance to photobleaching. These properties culminated in successful in vitro labeling of HeLa cells, making them a promising candidate for efficient fluorescent bioimaging applications.
- Device fabrication complexity: Creating GQD-based devices requires complex processes and equipment, thus raising fabrication costs. Simplifying techniques while preserving performance and scalability is a persistent challenge in GQD research. To tackle this issue, researchers explore novel nanomaterials and methods like bottom-up assembly and transfer techniques for precise positioning of GODs. Bajwa et al. [182] address the challenge of uneven CNC dispersion in hydrophobic polymers like HDPE by introducing a CNC/GQD hybrid system. Analyses confirmed successful interaction between CNC and GQD, leading to a uniform, honeycomb-like structure in the final composite. Remarkably, the GQD incorporation improved thermal stability, increased elastic modulus, and resulted in purely capacitive behavior in the electrical response. This signifies significantly better CNC dispersion compared to traditional methods, paving the way for stronger and more functional HDPE composites. Das et al. [183] established a label-free E. coli sensor based on AuPt@GQDs for food contamination detection with impressive performance. The AuPt@GQDs at 0.05 % loading achieved a very low LOD of 1.5×10^2 cells/mL, demonstrating high sensitivity (171,281.40 μF⁻¹ mL cells⁻¹ cm⁻²). Furthermore, the sensor boasts extended reusability (48 weeks) and excellent reproducibility, making it a promising candidate for real-world applications in food safety monitoring.
- 10) Limited understanding of fundamental properties: Despite extensive research efforts, the limited understanding of GQD properties hampers optimization and may cause unexpected performance issues in practical applications. Researchers address this problem by combining advanced characterization techniques with theoretical modeling. This approach aims to bridge the

knowledge gap and predict GQD behavior for better control and future advancements [184]. Ullah et al. [185] present a theory and experiment on TiO2-GQDs to improve solar-powered hydrogen production. Using density functional theory (DFT) and various microscopy techniques, the researchers confirmed that GODs enhance light absorption and promote electron transfer from GQDs to TiO2. This reduces the recombination of electrons and holes, leading to a significantly higher hydrogen production rate (31,063 µmol g⁻¹ h⁻¹) nearly five times more efficient than unmodified TiO2. The study proposes a mechanism for this improved efficiency, paving the way for better photoelectrochemical cell design for clean hydrogen production. Sharma et al. [186] explore oxygen and boron functionalization of GQDs for hydrogen production using DFT. All three functionalized GQDs (O-GQD, BC2O-GQD, BCO2-GQD) achieved near-ideal hydrogen adsorption energy (ΔG close to 0 eV), suggesting their potential as HER catalysts. This in silico approach provides valuable insights and guides future experiments towards developing low-cost, multifunctional GQD-based catalysts for clean hydrogen energy (around -0.03 to -0.06 eV hydrogen adsorption energy).

Therefore, investigating novel materials to combine with GQD and developing new composite and synthesis methods are vital for enhancing GQD's performance and efficiency across various applications.

3.1. GQD synthesis strategies

The synthesis methods of GQD are classified into two major categories: bottom-up and top-down. Bottom-up methods involve assembling basic structures from a carbon source into a considerable molecular carbon structure. Examples include using benzene products as initial materials through step-by-step soluble chemistry approaches [187], carbonization of initial components using a microwave-assisted hydrothermal process [188], fullerenes as initial components using ruthenium-catalyzed cage-opening [189], molecular carbonization [190], and electron beam irradiation methods [35] to successfully prepare GQD as illustrated in Fig. 4(a).

The size of GQD typically ranges from 3 nm to 20 nm [35], and most GQD forms are either elliptical or circular. However, some studies reported variations, stating that GQD can also take the form of square, triangular, and hexagonal dots [191] as depicted in Fig. 4(b). In the top-down method, large G sheets, CNT, carbon fibers, or graphite are cut into small parts of G sheets. By contrast, GQD is produced from small molecules in the bottom-up method.

Nanolithography [192], acidic oxidation [193], photo Fenton reaction [194], selective plasma oxidation [195], chemical oxidation method [196,197], chemical exfoliation [198], hydrothermal method [199], ultrasonic-assisted methods [200], electrochemical oxidation methods [201], chemical vapor deposition [202], and pulsed laser ablation [203] or a combination of these approaches [204] are among the most well-known methods in the top-down category for preparing GQD. The bottom-up synthesis of GQDs offers precise size control and high purity but is complex and costly. Top-down methods provide

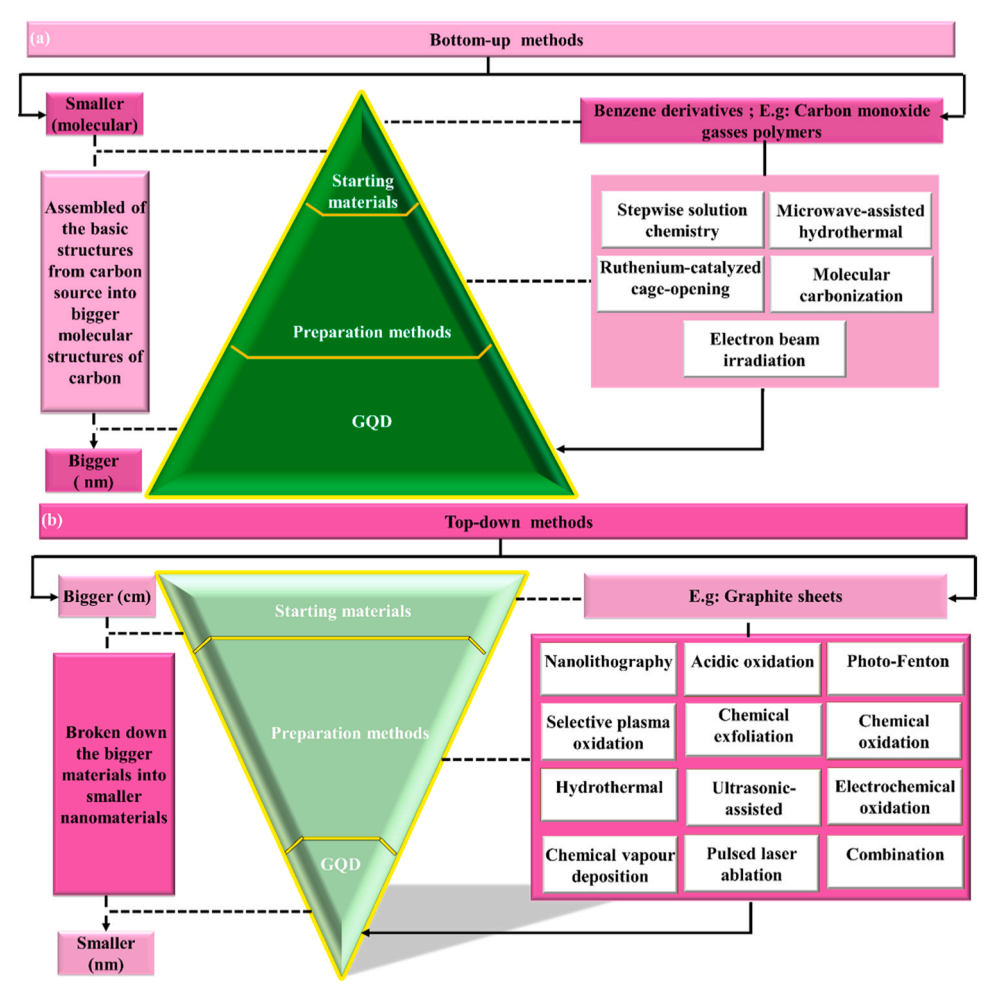


Fig. 4. (a) Bottom-up and (b) top-down methods for GQD preparation.

scalability and versatility but may yield heterogeneous products. Balancing these advantages and disadvantages is crucial for optimizing GQD synthesis strategies to effectively meet specific application requirements.

3.2. GQD properties

GQDs are nanoscale G fragments that exhibit unique structural, electronic, optical, biocompatibility, and cytotoxicity properties [205–208]. These properties make them suitable for several applications, such as optical, medical, and energy-related fields. The following are some of the key properties of GQDs:

- Structural properties: GQDs, OD materials with dimensions below 30 nm, exhibit high crystallinity in a honeycomb lattice. Their structure is influenced by factors such as functional groups and heteroatom dopants, including sodium, chlorine, and nitrogen [209, 210]. Diverse GQDs with functional groups such as amide and epoxy have been synthesized, resulting in complex structures [211]. Although high crystallinity remains a common feature, the synthesis techniques, dopant composition, and defect concentrations must also be considered in determining specific GQD forms.
- 2) Optical properties: GQDs possess unique optical properties, including tunable fluorescence, size-dependent quantum confinement effects, and versatile absorption spectra, rendering them ideal for applications in bioimaging, optical sensing, and advanced opto-electronic devices [212,213].
- 3) Electronic properties: The metallic conductivity of G results from a zero bandgap between conduction and valence bands. Different from G, GQDs exhibit semiconductor properties with tunable bandgaps influenced by size, edge states, functional groups, and defects, highlighting the dominance of quantum confinement in small sizes [214,215]. Zigzag and armchair configurations impact GQD electrical characteristics, with phosphorus doping providing tunability.
- 4) Biocompatibility and cytotoxicity: GQDs show reduced cytotoxicity due to water stability and their carbon-based structure [216]. In vivo studies demonstrated their nonaggregation, rapid kidney elimination, and reduced cytotoxicity, making them valuable for therapeutic delivery and intracellular imaging. GQDs in a polyethylene glycol matrix demonstrate reduced cytotoxicity, which is valuable for therapeutic delivery and intracellular imaging [39,217]. Heteroatom-doped GQDs exhibit biocompatibility, but further research is needed to understand their specific mechanisms and in vivo toxicity.

3.3. GQD applications

The extensive features of GQDs would advance their numerous applications in various areas, including the medical fields of biological imaging [218-220], drug delivery [221-224], photodynamic therapy [225-229], photothermal therapy [230-233], and antimicrobial materials [234-236]. In optical domains, GQDs show promise in optoelectrical detectors [237-239], LEDs [240-242], and photocatalysis [243-247]. They also exhibit potential in energy-related areas such as solar cells [248-251], energy storage batteries [252,253], and fuel cells [254], which can significantly influence our superiority of life and attract substantial commercial interest. Su et al. [255] present a simple hydrothermal method for synthesizing N-GQDs with high quantum yield (0.46). These N-GQDs, averaging 1.84 nm in size, outperform other top-down methods in terms of fluorescence efficiency. Furthermore, cytotoxicity assays indicate good biocompatibility, and confocal microscopy confirms cellular uptake via endocytosis. Overall, the research demonstrates a promising one-step approach for producing efficient N-GQDs with potential applications in biological imaging. Mohamed et al. [256] synthesized GQDs from sugarcane bagasse and pith using a green method. The GQDs exhibit excellent optical properties, water

solubility, and low cytotoxicity. HR-TEM confirms their size and structure. They demonstrate significant antioxidant and anti-inflammatory activities, highlighting their potential for sustainable, cost-effective bioapplications.

Poursadegh et al. [257] explore chitosan (CS)-based hydrogels with varying amounts of magnetic GQDs (MGQDs) for pH-sensitive drug delivery of Methotrexate (MTX). The hydrogels successfully encapsulated MTX (with loading percentages ranging from 84 % to 64 %) and exhibited pH-dependent swelling and drug release. Higher MGQD content (CS-MGQD 15 %) led to better stability and controlled release in acidic environments. The Weibull kinetic model accurately described the MTX release behavior. These findings suggest promising potential for these hydrogels as implantable drug delivery systems for targeted cancer treatment, exploiting the acidic tumor microenvironment for controlled drug release. Najafi et al. [258] propose a pH-responsive hydrogel based on α-Fe₂O₃@Aga/GQD for controlled release of the anti-cancer drug Quercetin (QC). The results show improved QC loading (47 % vs 35 %) and encapsulation efficiency (86.25 % vs 67 %). The 279 nm sized nanocarriers exhibit a positive surface charge and show enhanced anti-cancer activity in vitro. This approach holds promise for targeted drug delivery with potential benefits for cancer treatment.

Mojgan et al. [259] designed a promising photosensitizer for photodynamic therapy based on N-GQDs/TiO2 nanoparticles. The 21 nm N-GQDs/TiO2 nanocomposite significantly outperformed individual components in generating singlet oxygen (with a 94 % reduction) and hydroxyl radicals (with a 93 % reduction) under UVA light. This enhanced production of ROS is attributed to efficient energy transfer and reduced recombination within the composite. Moreover, the biocompatible nanocomposite shows no dark toxicity, indicating good biocompatibility. Overall, this work paves the way for a next-generation PDT approach with a potent nanocomposite for targeted cancer treatment. Dash et al. [260] designed a multifunctional nanocomposite, rGOQD/IR820/MnO₂/Q/CPP, for treating glioblastoma by combining photothermal therapy and photodynamic therapy. This nanocomposite achieved dual action with high photothermal conversion efficiency and ROS generation under near-infrared light. The inclusion of MnO₂ (with a 7.4 % weight loading, not specified here) effectively countered tumor hypoxia, while QC inhibited HSP70, sensitizing cancer cells to treatment. In vivo studies demonstrated tumor shrinkage and prolonged survival, indicating a promising strategy for targeted and improved glioblastoma therapy. Kazeminava et al. [261] present a promising antibacterial wound dressing material based on the CS/Ag@S-GQD nanocomposite hydrogel film. The resulting films exhibited good biocompatibility, with over 90 % cell viability after 48 hours, and demonstrated antibacterial activity against various bacteria, with inhibition zones ranging from 0.2 to 0.8 cm. These combined properties make CS/Ag@S-GQD films a promising candidate for further development as wound dressings.

Mondal et al. [262] introduce a core-shell SiNW/N-GQD photodetector with significantly improved performance. KOH etching of SiNWs increases the surface area, leading to a higher photocurrent to dark current ratio (up to 5×104) and remarkably low dark current (55 nA). The N-GQDs enhance light absorption in the UV spectrum and re-emit in the visible range, matching the absorption spectrum of SiNWs. This contribution results in an external quantum efficiency exceeding 150 % in the near IR and 500 % at 460 nm in the visible spectrum. This design offers a promising path towards high-performance optoelectronic devices due to its combined advantages in light absorption, reduced noise, and efficient charge collection. Yin et al. [46] overcome the limited color rendering of white LEDs (WLEDs) by incorporating green and red QDs, resulting in a color rendering index (CRI) of around 70. The resulting WLEDs achieved near-white light emission with CIE coordinates of (0.3332, 0.3359) and a color temperature of 5464 K at 30 mA, indicating a broader color spectrum. This suggests that quantum dots have the potential to improve WLED color rendering by offering a wider range of colors compared to traditional phosphors. Wei et al. [46] present a

photocatalyst based on N-GQDs/Bi $_2$ Fe $_4$ O $_9$ for the simultaneous removal of toxic Cr(VI) (99.8 %) and organic pollutant BPA (99.9 %) from wastewater under visible light. N-GQDs in the photocatalyst enhance charge transfer and promote the generation (1.64 μ M min⁻¹) and activation (0.0063 min⁻¹) of H $_2$ O $_2$, leading to an increased production of hydroxyl radicals for degradation. The presence of Fe(II) sites and the photo-Fenton reaction further contribute to Cr(VI) reduction. This N-GQDs/Bi $_2$ Fe $_4$ O $_9$ photocatalyst offers a promising single-step approach for efficient wastewater treatment using solar energy.

Li et al. [263] significantly improved perovskite solar cell performance by incorporating GQDs into the SnO2 electron transport layer (ETL). The GQD-modified ETL resulted in a gradient energy band structure, leading to an enhanced efficiency of 22.3 % compared to a standard SnO₂ ETL efficiency of 19.8 %. Moreover, unencapsulated devices exhibited remarkable stability, retaining 86 % efficiency after 1000 hours under simulated sunlight. GQDs not only promoted better charge transport but also passivated defects in SnO₂, thereby reducing recombination and boosting overall efficiency and stability. This approach holds potential for broader applications in optoelectronic devices beyond perovskite solar cells. Perveen et al. [264] explore a GQDs@PEG@Mg-ZnFe₂O₄ nanocomposite with exciting possibilities for energy applications. It exhibits a high permittivity of 104, making it suitable for potential use in low-frequency electronics. Furthermore, the nanocomposite demonstrates excellent energy storage properties with a capacitance of 100 F g-1 and good stability, retaining 99 % of its capacitance over 1000 cycles. Notably, the material shows promise for water splitting due to its electrocatalytic activity towards both hydrogen (with a Tafel slope of 90 mV dec⁻¹) and oxygen (with a Tafel slope of 110 mV dec⁻¹) evolution at low current densities. These results highlight the nanocomposite's potential as a multifunctional material for next-generation energy storage and conversion technologies. Liu et al. [265] GQDs and studied high-entropy GQDs (around 5 nm) as a metal-free oxygen reduction reaction (ORR) catalyst for fuel cells using a microwave method. The GQDs exhibit a high active surface area and stability, with the ORR peak occurring at -0.5 V and an onset potential of -0.1 V, indicating good activity. Doping with multiple elements enhances their catalytic performance. These findings highlight GQDs as a potentially cost-effective alternative to traditional metal catalysts for ORR in fuel cells.

Table 2 presents recently reported GQD and GQD-based nanocomposites in various applications, including the preparation methods, advantages, disadvantages, and significant findings for each reference.

4. PANI-GQD nanocomposites

PANI–GQD nanocomposites represent an advanced class of materials harnessing the tremendous features of PANI and GQDs. These materials have garnered attention across various fields due to their synergistic effects, resulting in improved electrical, optical, and electrochemical properties. The performance of PANI has been enhanced through composite nanostructures, leveraging the nanoparticle semiconductors known as QDs with unique electronic, optical, and luminescent features [266,267]. QDs have been synthesized from inorganic particles and nanosized carbon allotropes. When combined in composites, PANI and QDs form superior components with remarkable structure, sensing capabilities, capacitance, and conductivity features [268–270].

Owing to these unique properties, PANI-based QD nanocomposites have been applied in sensors, solar cells, dye removal, capacitors, and biomedical field [266,271–274]. However, their effective performance still faces challenges related to QDs' functionalization passivation, synthesis procedures, matrix–nanofiller compatibility, and enhanced processing factors. Concerns regarding environmental hazards and heavy metal toxicity have been raised for most semiconductor QDs [275, 276].

Dimensionless GQDs can potentially replace semiconductor QDs due to their advanced optoelectronic features. PANI and GQDs can be

compounded through electrical alteration, impacting the mechanical properties of the PANI matrix. This compound finds primary applications in various fields. With PANI and GQDs having individual merits, their combination in a nanocomposite form influences the synergistic effects of both components, leading to superior overall performance. PANI–GOD nanocomposites offer several advantages as follows:

- 1) Enhanced electrical conductivity: Combining PANI with GQDs enhances the electrical conductivity due to GQDs' high surface area and charge transport properties, improving the electron transfer within the nanocomposite [77,277].
- 2) Improved mechanical properties: GQDs' 2D structure and high aspect ratio bolster PANI's polymer matrix, enhancing the mechanical strength crucial for applications that demand resilience against stress, such as flexible electronics or structural materials [69,278].
- 3) Enhanced electrochemical performance: PANI–GQD nanocomposites exhibit superior electrochemical performance over pure PANI due to the increased surface area and active sites for charge storage. As a result, the specific capacitance and charge/discharge kinetics of the nanocomposite are enhanced, showing promise for supercapacitors and energy storage [279–281].
- 4) Improved chemical stability: GQDs act as protective shields, safe-guarding PANI from degradation and thus enhancing its chemical stability. This feature is crucial for applications in harsh environments or with corrosive substances [84,282,283].
- Tunable properties: PANI–GQD nanocomposites' properties can be adjusted by varying the PANI to GQD ratio and the synthesis parameters. This customization caters to specific application needs [81, 284,285].
- 6) Multifunctionality: PANI–GQD nanocomposites feature multifunctional traits stemming from PANI and GQD fusion and encompassing conductivity, electrochemical, optical, and catalytic capabilities, broadening their applications in electronics, energy storage, sensing, and environmental cleanup [72,286].
- 7) Environmental friendliness: PANI, a cost-effective CP, is synthesized using eco-friendly methods from inexpensive materials. GQD integration bolsters sustainability by enhancing the performance of in PANI–GQD nanocomposites and minimizing reliance on rare or toxic substances [287].
- 8) Compatibility with various substrates: PANI–GQD nanocomposites boast strong adhesion properties, allowing easy deposition on diverse substrates such as flexible materials, ceramics, and metals. This versatility expands their applicability across various fields [79, 284].

PANI–GQD nanocomposites offer a unique combination of electrical conductivity, mechanical strength, electrochemical activity, chemical stability, and versatility, making them highly attractive for a wide range of applications in electronics, energy storage, sensors, and beyond. Fig. 5 presents a summary of the features and applications of PANI–GQD nanocomposites. Despite their endless potential, PANI–GQD nanocomposites still suffer from the following drawbacks: complex, costly synthesis limits scalability; prone to instability and aggregation; compromised mechanical properties; processing challenges; and knowledge gaps hindering optimization. Researchers should overcome these challenges by improving dispersion and interfacial interactions. This involves strategies such as modifying GQD surfaces and optimizing synthesis processes to create well-distributed, high-performance materials [287].

Wang et al. [282] established a PANI/GQD-rGO/CFC flexible electrode for supercapacitors using a novel and simple spraying method. The GQD-rGO solution modifies the carbon fiber cloth, enhancing its interaction with PANI for improved electrode performance. The results show a capacitance of 82.9 mF cm $^{-2}$ (1036 F g $^{-1}$) and exceptional stability, retaining 97.7 % after 10,000 cycles. The capacitance remains stable even when bent, and the layer-by-layer (LBL) spraying technique offers

Table 2Recent GQD and GQD-based composites in various applications.

GQD based composites	Synthesis method	Advantages	Disadvantages	Application	Finding	Reference
NPs-GQDs-PEG	Bottom-up molecular approach	Enhanced bioimaging, prolonged blood circulation, multifunctional, highly photostable, long term, and real time	Molecular approach may impede scalability. Biocompatibility and toxicity require clinical evaluation. Optimization is crucial for precise tumor imaging.	Biological imaging	Planted GQDs in PEGylated nanocomposites enable prolonged circulation and enhanced tumor bioimaging in vivo.	[218]
Gd (DTPA)–GQDs	Chemical	High longitudinal proton relaxivity, and biocompatibility	Complex synthesis hampers scalability and practicality, elevating MRI imaging costs.	Biological imaging	Exceptionally high longitudinal proton relaxivity (r1) of $10.90 \text{ mM}^{-1} \text{ s}^{-1} (\text{R}^2 = 0.998)$	[219]
Doped GQD	Bottom-up hydrothermal reaction	Radical scavenging, diverse metals, high Pl, biocompatibility, antioxidant, and multifunctionality	Complex synthesis impedes scalability, elevating production costs with costly materials and equipment.	Biological imaging	Enhanced radical scavenging with aluminum and Tm variants, comparable with ascorbic acid	[220]
GQDs-Fe ₃ O ₄ -FA	Chemical	Superparamagnetic, smart pH- responsive magnetic, multifunctionality, biocompatibility, and controlled drug release	Complex synthesis might impede scalability. Optimizing curcumin release is crucial for targeted drug delivery efficacy.	Drug delivery	Promising as an anticancer carrier: controlled release (33 % pH 5.5, 15 % pH 7.4 over 150 hours), enhanced cytotoxicity	[221]
GOQDs-GlcN-BA	Simple solution mixing	Enhanced drug loading and release, pH-responsive drug release, superior anticancer, and cellular internalization	Complex preparation may impede scalability. BA addition improves drug properties, requiring further optimization for biomedical use.	Drug delivery	90 % DOX loading, 20 % release, pH 5.5 cytotoxicity, promising for anticancer delivery	[222]
SDNCs-Chi- NGQDs	Non-thermal microplasma	Smart, eco-friendly, biocompatibility, enhanced mechanical properties, real- time monitoring of drug release, and anticancer efficacy	Limited scalability Low NGQD content may limit functionality; further optimization is needed. Promising in vitro results require in vivo validation for safety and efficacy.	Drug delivery	The prepared composite enables pH-responsive drug delivery, enhanced toughness, and anticancer efficacy.	[223]
CS/CMC/GQDs/ ZnO@QUR	Double emulsion technique	Enhanced drug stability, bioavailability, BBB penetration, controlled release, biocompatibility, effective anticancer, and low cytotoxicity	Specialized equipment and expertise for characterization may hinder scalability. In vivo validation essential for safety and efficacy assessment	Drug delivery	Enhanced brain tumor drug delivery: 219.38 nm, –53 mV, 72-hour release, U- 87 MG effective, low cytotoxicity	[224]
Am-N-GQD	One-step Rf conjugation	Superior biocompatibility, enhanced treatment depth, specific accumulation in tumor cells, and dual functionality of Rf	Complexity may limit scalability. Promising results were obtained in vitro; in vivo validation is crucial.	Photodynamic therapy	Improved photodynamic therapy depth, increased cellular uptake, enhancing cancer treatment effectiveness	[225]
GQD NT	Self-assembly	Improved tumor accumulation, long-term retention, enhanced penetration, and release of photosensitizers (PSs)	Scalability challenge Reduced dose for minimal side effects Regulatory validation is crucial.	Photodynamic therapy	Extended tumor retention, repeated therapy, low PS dosage	[226]
Af-GQD/UCNPs	Single step hydrothermal	Excellent biocompatibility, multifunctionality, upconversion luminescence, photodynamic, and enhanced imaging performance	Scalability challenge, positive for cytotoxicity assessment; long-term effects; immunogenicity for translation; regulatory approval and validation may delay adoption	Photodynamic therapy	Promising bio-imaging, photodynamic therapy with strong X-ray attenuation, PDT effects	[227]
GQD-based materials (i.e., GQDs, N-GQDs, amino-GQDs, and amino-N- GQDs)	Modified Hummers' method	Enhanced optical properties, two photo excitation capability, superior photochemical effect and favorable intrinsic luminescence	Sorted amino-N-GQDs may limit scalability. Crucial biocompatibility, safety evaluation Regulatory approval is essential.	Photodynamic therapy	Enhanced two-photon properties, effective PDT, and favorable bioimaging contrast in NIR-II region	[228]
GQD-loaded macrophages	Vitro 3D culture model	Site-specific delivery, therapeutic efficacy, fluorescence imaging, biomimetic delivery	Limited human tumor mimicry; refining GQD therapy in macrophages requires optimization.	Photodynamic therapy	LED PDT using GQDs induces cell death, enhancing efficacy as supported by fluorescence bioimaging in mouse xenografts.	[229]
GQD-Gd/ IR820@AAG	Self-assembled	Remarkable T1-MRI, multifunctional treatment, reduced biotoxicity, near- infrared fluorescence imaging	Complex synthesis hinders scalability. Biocompatibility assessment is crucial. Regulatory validation is essential.	Photothermal therapy	Novel nanoprobes downregulated heat shock proteins, enhancing liposarcoma photothermal therapy.	[230]

(continued on next page)

Table 2 (continued)

GQD based composites	Synthesis method	Advantages	Disadvantages	Application	Finding	Reference
RGQDs	Top-down and Bottum up	High photothermal conversion efficiency, significant NIR absorption, fluorescence, biocompatibility, and cell viability inhibition	GQD synthesis complexity hinders scalability; uptake mechanisms need clarity.	Photothermal therapy	Robust photothermal and imaging capabilities. In vitro findings showed effective cancer cell eradication, indicating theragnostic potential.	[231]
AuNRs/GQDs	Electrostatic interaction	High media stability, biocompatibility, photo cytotoxicity, and passivation	GO boosts AuNRs' photothermal efficiency, but GQDs might hinder it. Exploring cytotoxicity is crucial.	Photothermal therapy	GQDs improve the colloidal and photothermal stability of AuNRs.	[232]
Rf-N,S-GQD	Electrostatic	High phototoxicity, and performance, synergistic therapy, colloidal stability, and singlet oxygen generation	Complex synthesis may hinder scalability. Biocompatibility is vital and requires in vivo studies. Stability and tissue penetration are crucial.	Photothermal therapy	The novel nanohybrid for combined two-photon TP-PDT/PTT against cancer, enhancing therapy effectiveness.	[233]
GQD-TiO₂	Hydrothermal treatment	Antibacterial properties, improved hydrophilicity, good biocompatibility, and osteogenetic potency	composite needs long-term examination for sustained antibacterial effectiveness. In vivo evaluation is crucial for clinical suitability, safety, and scalability.	Antimicrobial materials	Incorporating GQDs into ${\rm TiO_2}$ enhances the resistance of Ti implants against bacterial infections.	[234]
GOQD/ZnO	Pyrolysis and hydrothermal	Enhanced photocatalytic, antibacterial activity, synergy, low dislocation density, and large surface area	Complex synthesis impedes scalability and reproducibility. Advanced characterization poses significant challenges.	Antimicrobial materials	Superior photocatalytic activity (97.6 % degradation at 60 min) and antibacterial efficacy against <i>E. coli</i> and <i>S. aureus</i> .	[235]
GQDs/Mg (OH) ₂	Chemical	Good antimicrobial, and antioxidant	The complex synthesis requires further optimization.	Antimicrobial materials	Strong antimicrobial (MIC: 15.625 µg/mL against fungi, 62.5 µg/mL against bacteria) and moderate antioxidant (62.18 % H ₂ O ₂ scavenging) activities	[236]
GQD	Solvothermal	High PL, strong UV absorption, and large Stokes shift, scalability, and cost- effectiveness	Challenges arise from limited spectral range and integration complexity.	Optoelectrical detector	GQDs enhance Si photodiode UV detection to 300 nm, with 20 % relative enhancement.	[237]
ZnO/GQDs	Chemical	Good self-powering, increased responsivity and detectivity	Potential complexity and engineering challenges	Optoelectrical detector	Sevenfold higher on/off ratio and enhanced responsivity compared with bare ZnO	[238]
GdNPs-PEI@N- GQDs	Hydrothermal	High electrical, controlled modification, and rectification property	Study lacks broader application insights. Gd specificity limits generalizability, requiring dopant diversity exploration.	Optoelectrical detector	Doping Gd alters GQDs' electrical properties, shifting diode behavior from rectifying to ohmic.	[239]
GQD	Hydrothermal	Low-cost and sustainable synthesis, full spectrum coverage, highly crystallized, and high efficiency	Lacks additional analyses for a comprehensive understanding of properties and broad applications	Light emitting diodes	Single-layered GQDs emit red, yellow, green, and blue light, enabling LED applications.	[240]
BGQDs	Hydrothermal	Enhanced optical, mechanical, elastic properties, high CRI	Intricate boron-doped GQD synthesis hinders scalability. Comprehensive characterization is essential.	Light emitting diodes	BGQDs offer stability, enhanced by PBA0.8-co- PNMA0.2 for WLEDs.	[241]
3-GQDs, G-GQDs, and R-GQDs	Solvothermal	Multicolor tunable emission, excellent fluorescence, and photostability	R-GQDs exhibit lower QY than B- and G-GQDs. Solvothermal synthesis complexity may hinder scalability.	Light emitting diodes	The relative quantum yields (QYs) for B-, G-, and R-GQDs are 68 %, 62 %, and 27 %, respectively.	[242]
GQDs/CuWO ₄	Simple mixing and hydrothermal reaction	Visible light responsiveness, maximum efficiency, cost- effectiveness, and mechanism understanding	CuWO ₄ /GQD photocatalyst faces scalability limits; moderate phenol degradation needs optimization.	Photocatalysis	Maximum phenol photodegradation efficiency of 53.41 % with 0.5GCW sample	[243]
C/G/Z: TiO ₂ / GQD/ZIF-8	Hierarchical	Enhanced photocatalytic activity, GQD doping optimization, degradation mechanism understanding, and high efficiency	High GQD doping hampers photocatalytic activity; pollutant and scavenger influence degradation, limiting applicability.	Photocatalysis	Increasing GQD content from 0.002 g to 0.02 g enhanced photocatalytic activity, leading to the effective degradation of pollutants.	[244]
GQDs-TiO ₂ /AC	Sol–gel	Superior removal efficiencies, and fast photodegradation rate	Efficiency diminishing with increasing concentrations, relying on costly H ₂ O ₂ .	Photocatalysis	Superior MB dye removal, achieving 97.6 % efficiency in 30 minutes	[245]
OH-GQDs/NH ₂ - MIL-101(Fe) (OGNM)	Solvothermal	Enhanced photocatalytic activity, stable performance, uniform dispersion, environmentally friendly,	The composite's photocatalytic activity is discussed, but the mechanism is not explored. Complexity CO ₂ focus limits scalability.	Photocatalysis	Superior CO_2 photoreduction activity, yielding 128.68 μ mol·g ⁻¹ CO within 10 hours.	[246]

(continued on next page)

Table 2 (continued)

GQD based composites	Synthesis method	Advantages	Disadvantages	Application	Finding	References
		highly efficient, and cost- effective				
PTh/GQDs/TiO ₂	Electrospinning with chemical deposition	Excellent photocatalytic activity, visible light response, and high regeneration efficiency	Fabrication complexity hinders scalability. Degradation mechanisms are explored, but optimization and broader pollutant range warrant further research.	Photocatalysis	High photocatalytic activity, degrading MB and TC by 92.90 % and 80.58 %, respectively.	[247]
N-GQDs/PMMA LDS	Simple mixing and spin coating	High efficiency, performance, mechanical strength, chemical stability, improved photovoltaic cell performance	Limited temperature range restricts insights. Further exploration needed beyond CIGS applicability.	Solar cells	N-GQDs/PMMA layer annealed at 60 °C enhances CIGS solar cell with 16.13 % efficiency.	[248]
CCS/MWCNT/ GQD	Hydrothermal	Enhanced electrochemical activity, conductivity, power conversion efficiency, superior bifunctional electrocatalysts	Limited exploration hampers alternatives; complex synthesis hinders scalability; energy focus narrows potential.	Solar cells, and supercapacitors	Superior energy conversion (PCE: 4.15 %) and storage (specific capacity: 402 C g-1)	[249]
WM@GQDs	Ultrasonication	Excellent power conversion efficiency, high catalytic activity, improved charge transport properties, and low- cost synthesis	Solar device performance varies with GQD amount; optimization and mechanism exploration are required.	Solar cells	Power conversion efficiency (PCE: 10.38 %) superior to that of platinum in DSSC.	[250]
NaNT:NS-GQD	Simple mixing	Tremendous electron transport, enhanced electric conductivity, and promising solar cell performance	Study lacks numerical data or comparisons, hindering the comprehensive assessment of synthesized heterostructures' performance.	Solar cells	Enhanced electrical conductivity, promising for QDSSC ETL	[251]
GQD/ CNT- Fe ₃ O ₄	Chemical	Simple synthesis, high capacity, cycle life, energy, and power density	Study lacks detailed characterization discussion, hampering the understanding of nanocomposite structure.	Energy storage battery	Excellent electrochemical performance, ideal for supercapacitor applications	[252]
GQDs-PolyFc/ Fe ₃ O ₄ /PANI	Simple physical mixing	High capacity, energy density, high power density, and long term cycling stability	Limited structural discussion hampers insights into electrode electrochemical performance.	Energy storage battery	The nanocomposite shows 295 mAh/g capacity and 91.45 % retention after 5000 cycles.	[253]
BGQDs/MOF-t	Electro-deposition	Highly active, robust cathodic catalyst, improved conductivity and electrolyte interface	Details on critical reproducibility and scalability for electro-deposition are lacking	Fuel cell	The prepared cathode reaches 703.55 mW m^{-2} , surpassing Pt/C.	[254]



Fig. 5. Outline of the features and applications of PANI-GQD nanocomposites.

easy operation and versatility for producing foldable energy storage devices. This research paves the way for high-performance, flexible supercapacitors with potential applications in wearable electronics and

future energy storage solutions due to the simple and scalable fabrication process.

Lin et al. [288] developed a flexible and sensitive sensor based on an

N-GQDs/PANI nanocomposite for glucose detection. While PANI is commonly used for wearable biosensors due to its flexibility, it exhibits lower electroactivity and conductivity in a neutral electrolyte. To address these issues, N-GQDs were introduced as electron transfer agents due to their abundant N-rich functional groups. The results show improved $\rm H_2O_2$ detection sensitivity (68.1 $\mu A~mM^{-1}~cm^{-2}$) compared to PANI alone (44.06 $\mu A~mM^{-1}~cm^{-2}$) and retain 93.2 % sensitivity for glucose detection on a flexible platform after a bending test, compared to a Pt-based sensor (71.3 %). This significant improvement in mechanical stability (21.9 % higher) suggests that the N-GQDs/PANI nanocomposite is a promising material for long-lasting and reliable wearable biosensors for non-invasive sweat glucose monitoring.

4.1. Synthesis strategies for PANI-GQD nanocomposites

The synthesis of PANI-GQD nanocomposites offering enhanced electrical, optical, and mechanical properties represents a significant advancement in the field of multifunctional materials. Several methods can be employed for the synthesis of PANI-GQD nanocomposites, including chemical oxidative polymerization [53-57,59,60,64,71, 74-76,80-82,289,290], electrochemical oxidative polymerization [58, 61,65,69,70,79,84], simple solution mixing [66–68,72,85,86], LbL assembly [73,291], hydrothermal [62,63], polycondensation [77], solution-casting [78], and molecular dynamics [83]. We generally categorized these approaches into in-situ polymerization methods (chemical oxidative polymerization/electrochemical oxidative polymerization) and self-assembly approaches. In-situ polymerization offers purity and controlled morphology but faces compatibility issues and complex conditions. Self-assembly is simple and versatile but lacks precise control and scalability, depending on GQD compatibility. Further details will be discussed in the following sections.

4.1.1. In-situ polymerization methods

In-situ polymerization approaches for the fabrication of PANI–GQD nanocomposites can be primarily categorized according to their reaction mechanisms: chemical oxidative and electrochemical oxidative approaches as listed in Table 3 and Table 4, respectively. Chemical oxidative procedures for PANI preparation typically involve oxidants such as APS and ferric chlorides. These methods offer conveniences for controlling the nucleation and growing approach in the in-situ polymerization of aniline and GQD.

Chemical oxidative polymerization ensures precise control over the composition, morphology, and distribution of PANI–GQD

nanocomposites as influenced by reaction conditions. Meanwhile, chemical oxidative polymerization is efficient for commercial production. Nevertheless, achieving uniform GQD dispersion remains a challenge, potentially leading to a low surface area and hindering aniline polymerization. Breczko et al. [71] successfully synthesized s-PANI-NTs/GQDs composites through a chemical oxidative polymerization method for supercapacitor electrodes. The synthesis of GQDs (2–5 nm) with various oxygen functionalities and s-PANI-NTs/GQDs composites involved optimizing reagent concentrations (aniline, TSA, APS) and the timing of GQD introduction (4, 12, or 24 hours after APS addition). Although the process is described in detail, the lack of information on the final yield and the concentration of GQDs in the composite hinders a complete evaluation.

Electrochemical oxidative polymerization methods involve the galvanostatic or potentiostatic deposition of aniline from electrolyte on the GQD surface and the deposition of GQD on substrates such as polydimethylsiloxane or ITO [7–10]. This process immobilizes PANI on GQD electrodes, offering advantages for free electrode preparation and maintaining a uniform PANI layer. Nasr-Esfahani et al. [61] developed a new sensor for imidacloprid detection, focusing on the preparation of a composite electrode (GCE/GQDs/IL/MWCNTs) for electrochemical studies. While a specific weight ratio (2:1:1) of IL to GQDs and MWCNTs is used, the final dispersion volume (15 mL) is not specified, hindering the concentration analysis. The 5 μ L casting suggests an emphasis on forming a thin film layer for the composite.

4.1.2. Self-assembly methods

The fabrication of PANI–GQD nanocomposites involves self-assembly with electrostatic interactions, providing cost-effective control over PANI and GQD for diverse morphologies. Efficient dispersion in aqueous media is crucial for hierarchical formation, offering versatility. Water-dispersible PANI nanofibers and stable GQD dispersion are achieved through in-situ polymerization and pH control, respectively, preventing aggregations due to doped PANI acid characteristics [73,291].

Wang et al. [73] addressed dispersion issues by synthesizing stable PANI nanofiber dispersions through dialysis, facilitating self-assembly with GQD. By utilizing electrostatic and $\pi-\pi$ interactions, they alternately deposited GQD-rGO and PANI onto ITO and quartz substrates to construct GQD-rGO/PANI LbL self-assembly films. The precise substrate preparation involved cleaning, hydrolysis, and oxidative treatments for uniform hydroxyl group distribution.

A series of PANI-GQD nanocomposites with PANI nanostructures and outstanding electrochemical acts was prepared by self-assembly.

Table 3Comparison of chemical oxidative polymerization parameters for the synthesis of PANI–GQD nanocomposites.

Aniline	GQD	Water	Dopant	Polymerization condition	APS	Dehydrate condition	References
1 mL	1 mg.mL^{-1}	10 mL	HCl (30 mL)	24 h	1.2 g	Overnight; 80 °C	[53]
200 μL	20 mg	20 mL	_	1.5 h; 10 °C-12 °C	10 mL	Overnight	[54]
91.75 mL	1 mL	30 mL	HCl (2.5 mL)	2 h; Ice bath	_	_	[56]
0.03 mL	10 mL		DBSA (0.3 g)	_	0.1 g	_	[57]
_	_	_	HCl (50 mL)	3 h; 0 °C		24 H; 60 °C	[59]
0.03 mL	10 mL	_	_	_	10 mL $+$ 0.0.3 g DBSA $+$	_	[60]
					0.1 g APS		
0.1 mL	_	15 mL	HCl (10 mL)	15 min; Ice bath	0.3 KPS	_	[64]
$0.055 \; mol \; dm^-$	5 mL (20, 40, 60) mg mL ⁻¹	-	TSA (7.12 mmol dm ⁻³⁾	(4, 12, 24) h	$0.059 \text{ mol dm}^{-3}$	-	[71]
100 μL,1.1 mmol	(0, 5, 10, 15, 20) mg	-	-	1 h; 10 °C	250 mg,	24 h; Room temperature	[74]
1.0 g			HCl (30 mL)	12 h	2.28 g	24 h; 60 °C	[75]
_				10 °C	-	12 h; 60 °C	[76]
- 100 μL	(10, 20, 33.3, 50) mg	10 mL		1 h; 10 °C-12 °C	5 mL	2 d; 30 °C	[80]
_	_		HCl	30 min; 80 °C	4 °C	50 °C	[81]
4 g	0, 1, 5, 10 %	_	0.17 M CSA	1 h +1 d; 10 °C	0.085 M	24 h; 80 °C	[82]
0.1 mL	33.3 mg	10 mL		1 h; 80 °C	5 mL	2 d; 40 °C	[289]
100 μ	5, 10, 20, 40 mg	-	-	1 h+ overnight; 10 °C-12 °C	5 mL	-	[290]

Table 4Comparison of electrochemical oxidative polymerization parameters for the synthesis of PANI–GQD nanocomposites.

Aniline	GQD	Dopant	Scan rate range	Scan rate	Glass electrode	Temperature	References
10.00 mL	360 μL	H ₂ SO ₄ (4 M)	-1.3 V to 0.8 V	$50~{\rm mVs^{-1}}$	_	25 °C	[58]
7.3 mmol L^{-1}	5.0 mg	H ₂ SO ₄ (0.25 M)	-0.20 V to 0.90 V	$20~\mathrm{mVs}^{-1}$	_	25 °C	[61]
1.0 M	10 μL	HCl (2.0 M)		_	_	25 °C	[65]
0.1 M	2.5 and 5 mL	H ₂ SO ₄ (0.5 M)	–0.5 V to 1.5 V	$10~{\rm mVs^{-1}}$	_	25 °C	[69]
0.1 M	3.0 mg	H ₂ SO ₄ (0.1 M)	0.75 V	_	_	25 °C	[70]
0.1 M	5 wt%	H ₂ SO ₄ (0.5 M)	0.0-0.8 V	$10~\mathrm{mVs}^{-1}$	FTO	25 °C	[79]
_	-	Ptsa (0.2 M)	-0.20 to 0.8 V	$20~{\rm mVs^{-1}}$	ITO coated PET	25 °C	[84]

Guo et al. [291] created PANI–GQD nanocomposites through LbL assembly, achieving nanoscale ordering as shown in Fig. 6. LbL provided precise control over the internal structure, thickness, flexibility, improved chemical stability, and electrical conductivity of the GQD/3D-G/PANI nanocomposite electrodes.

4.2. PANI-GQD nanocomposite properties

PANI–GQD nanocomposites represent a fascinating class of materials with synergistically improved properties arising from the combination of PANI and GQDs. These nanocomposites exhibit enhanced electrical conductivity, mechanical strength, and tunable optical features, making them a suitable choice for a wide range of applications, which will be discussed in detail in the next section. The key properties of PANI–GQD nanocomposites are as follows:

- Optical properties: PANI–GQD nanocomposites showcase intriguing optical properties with tunable characteristics due to the quantum confinement effects of GQDs. This tunability is advantageous for optoelectronic applications such as sensors and LEDs, enhancing the optical performance and introducing multifunctionality to the material [292–294].
- 2) Electrical properties: PANI–GQD nanocomposites are of great interest due to their enhanced conductivity. The GQDs in the PANI matrix create additional charge pathways, modifying the band structure and optimizing the electrical conductivity. This property is promising for applications in flexible electronics and conductive coatings [86, 295–297].
- 3) Mechanical properties: PANI–GQD nanocomposites exhibit enhanced mechanical properties. The incorporation of GQDs strengthens the polymer matrix, leading to increased tensile strength and modulus that are crucial for ensuring the durability of electronic devices. The synergistic blend of PANI and GQDs broadens potential applications across diverse technological domains [69,72].

4.3. PANI-GQD nanocomposite applications

Owing to the combination of PANI with tremendous electrical conductivity and redox properties and GQD with unique quantum confinement effects and a high surface area, the extensive properties of PANI–GQD nanocomposites hold significant potential for various applications in diverse fields. To date, PANI–GQD has demonstrated promise in several areas such as sensors [53–63], biosensors [64–68], supercapacitors [69–78], solar cells [70,79,80], optoelectronics [81–85], and coating [86], improving our quality of life and attracting substantial commercial interest. In the future, PANI–GQD nanocomposites may be developed as common nanomaterials for cutting-edge nanotechnology. This section presents the current applications of PANI–GQD nanocomposites.

4.3.1. Sensors

The sensor applications of PANI–GQD nanocomposites span a wide range of fields, including environmental monitoring, healthcare, and industrial processes [53–65,67,68,290]. In environmental sensing, these nanocomposites have demonstrated remarkable sensitivity to various gases, pollutants, and analytes. The tunable properties of PANI and the enhanced electrical conductivity imparted by GQDs enable the detection of specific target molecules with high selectivity and sensitivity. In addition, the incorporation of GQDs enhances the stability and repeatability of PANI-based sensors, making them suitable for long-term monitoring applications.

Gavgani et al. [53] successfully developed a flexible NH₃ sensor based on S, N: GQDs/PANI via chemical oxidative polymerization. The prepared sensor exhibits high sensitivity, selectivity, flexibility, and fast response and recovery times at room temperature (Fig. 7). The underlying sensing mechanism was also determined. However, further research is vital to optimize the sensor's performance for specific applications and to explore its long-term stability and reliability. Practical considerations such as manufacturability and scalability should also be addressed for the widespread adoption of this technology. Masemola et al. [55] describe a promising gas sensor based on the NGQDs/PANI

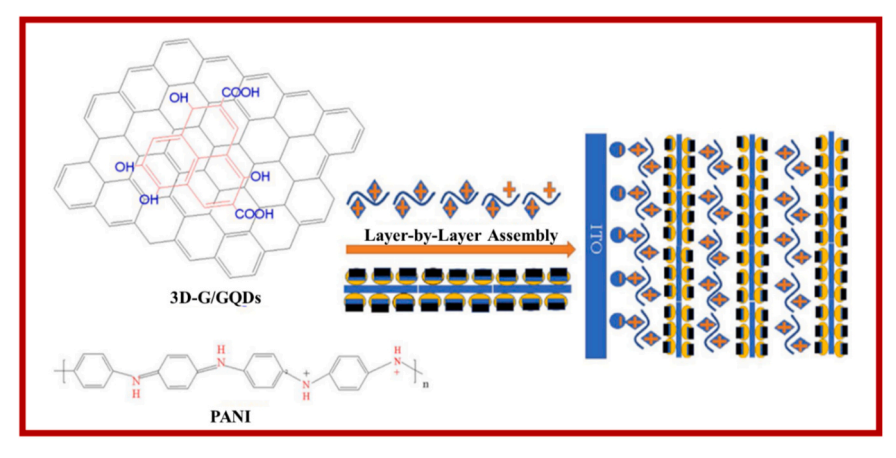


Fig. 6. Schematic of GQD/3D-G/PANI LBL self-assembled films [291].

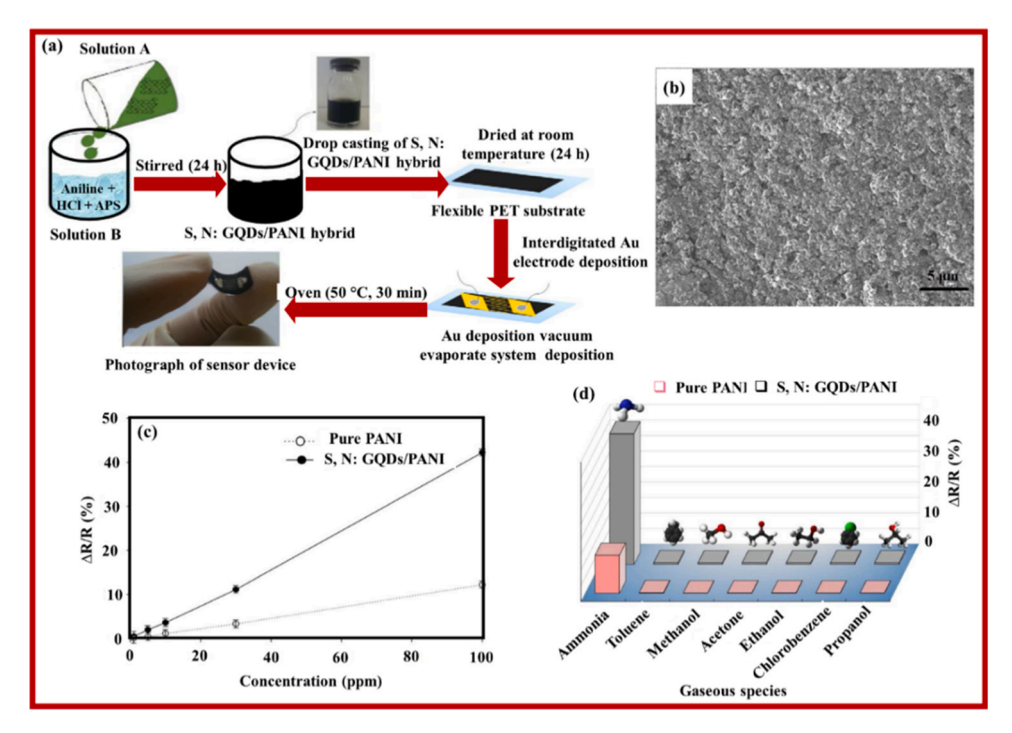


Fig. 7. (a) Schematic of gas sensor preparation pathway, (b) FESEM pattern of S, N: GQD/PANI sensing film, (c) gas response of flexible prepared samples, and (d) selectivity of the flexible prepared samples [53].

composite, synthesized via a microwave-assisted method for ethanol vapor detection at room temperature, which is well-characterized using TEM, XRD, and other techniques. The results show fast response (85 s) and recovery (62 s) times for 100 ppm ethanol at room temperature. However, the lack of information on sensitivity and baseline resistance values for each sensor (bare PANI vs. composite) hinders a complete performance comparison.

Punrat et al. [58] presented a robust strategy for detecting chromium (VI) at low concentrations using a PANI–GQD-modified screen-printed carbon electrode in a flow-based system. The sensor demonstrates significant potential for environmental monitoring, with a low LOD of 0.097 mg L $^{-1}$ within the linear range of 0.1–10 mg L $^{-1}$. Hong et al. [59] demonstrates a highly sensitive NH $_3$ gas sensor based on the PANI/N-GQD/hollow $\rm In_2O_3$ composite at room temperature. The composite sensor with 20 wt% N-GQD loading exhibits a significant response (15.2) to 1 ppm NH $_3$, over 4 times higher than the PANI sensor alone. This suggests improved sensitivity due to N-GQDs. The sensor operates at room temperature and detects NH $_3$ within a relevant range (0.6–2.0 ppm) for breath analysis of potential liver or kidney issues. Additionally, the sensor shows good selectivity and repeatability for 1.0 and 2.0 ppm NH $_3$, making it a promising candidate for practical breath diagnostic applications.

Further studies should focus on optimizing the synthesis of PANI/GQDs, exploring additional applications, and validating the method's performance across a wide range of sample matrices and conditions. Table 5 provides a comprehensive overview of research findings, outlining the advantages and disadvantages of PANI–GQD nanocomposites in sensor applications.

4.3.2. Biosensors

PANI–GQD nanocomposites have exhibited promising potential in healthcare applications, particularly in the development of biosensors [64–68,290]. Combined with the unique optical and electronic properties of GQDs, the biocompatibility of PANI facilitates the fabrication of sensitive and selective biosensors for the detection of biomolecules such as DNA, proteins, and enzymes. The integration of PANI–GQD nanocomposites into healthcare devices holds great promise for early disease

diagnosis and personalized medicine.

Ahmadi-Kashani et al. [64] explore a promising pH-sensitive nanocarrier based on the PANI/N-GQD/MO/LDH composite for targeted DOX delivery in cancer treatment. The results demonstrate exceptional DOX encapsulation (90 %) with minimal release (4 % over 72 hours) at neutral pH, suggesting controlled drug storage. At tumor-mimicking acidic pH, a high release (~80 %) indicates pH-triggered delivery to cancer cells. The carrier also exhibits good biocompatibility with minimal toxicity to healthy cells and significant cancer cell death (up to 40 %), suggesting a potential therapeutic benefit. Further investigation into in vivo efficacy and long-term toxicity is needed for clinical translation. Chang et al.[65] developed NGQD/PANI biosensors via an innovative approach for the detection of glucose from human sweat with high sensitivity (23.52 mM⁻¹). Further research should explore the optimization of biosensor performance, integration with wireless communication technologies for real-time data transmission, and validation in clinical settings to assess accuracy and reliability.

Ganganboina et al. [66] fabricated a label-free impedimetric immunosensor based on N,S-GQD-Au-PANI for the detection of carcinoembryonic antigen, demonstrating high sensitivity, selectivity, stability, and a low LOD of 0.01 ng/mL within the linear range of 0.5–1000 ng/mL, surpassing other amino acids (Fig. 8). Future research endeavors should prioritize the optimization of sensor parameters, exploration of multiplexed detection for multiple cancer markers, and initiation of clinical validation studies to facilitate broad clinical adoption.

Takemura et al. [67] presented a significant approach to white spot syndrome virus detection using a disposable sensing matrix based on N, S-GQDs/AuNP-PANI, reporting high sensitivity and stability. Further studies should focus on optimizing biosensor performance, validating its accuracy and reliability in real-world samples, and exploring its potential for integration into on-site diagnostic platforms for aquaculture settings. Liu et al. [68] report a highly sensitive ECL immunosensor based on the novel GO/PANI/CdSe nanocomposite for detecting interleukin-6 (IL-6). The sensor demonstrates excellent performance, with a low LOD of 0.17 pg/mL, a wide linear range, high specificity, and good stability. However, the use of cadmium in CdSe quantum dots

Journal of Environmental Chemical Engineering 12 (2024) 113460

 Table 5

 Relevant studies related to PANI–GQD composites for sensor applications.

Morphology	Method	Advantages	Disadvantages	Application	Finding	References
Uniform fibrous	Chemical oxidative polymerization	Excellent response, high sensitivity, selectivity, flexibility, low cost, and wearable	Complex fabrication synthesis, limited scalability, and potential cross-sensitivity	NH ₃ sensor	Sensitivity with 42 % and 385 % at 100 ppm and 1000 ppm, outstanding selectivity, and rapid room temperature recovery	[53]
Regular nanosolid tube	Chemical oxidative polymerization	Novel immunosensor, high conductivity, surface area, sensitivity, and low LOD	Complex electrode preparation; sample-specific optimization needed; and limited discussion on interference	Detecting a depression marker	Broad linearity (0.0976–100 ng/mL) with low 3σ LOD (0.05 ng/mL)	[54]
-	Chemical oxidative polymerization	Uniformly distributed NGQDs, room- temperature sensor, high sensitivity, and reproducibility	Limited discussion on selectivity, variable response to environment; and real-world optimization needed	Ethanol vapors	Efficient response to 50–150 ppm ethanol at room temperature, reproducible signal at 100 ppm, and relative humidity of 45 %	[55]
Porous nanostructure	Chemical oxidative polymerization	High sensitivity, selectivity, stable repeatability, and fast response and recovery time	Complex synthesis needs gas optimization, limited discussion on scalability for production	Acetone vapors	Low LOD (0.1 ppm) and higher response value (2 at 0.5 ppm) at room temperature	[56]
Oval	Chemical oxidative polymerization	High fluorescent stability and stable emission peak	Complex synthesis, limited discussion on specific sensing applications	Practical sensing	High and stable emission peak at 348 nm	[57]
Smooth surface	Electrochemical oxidative polymerization	Rapid determination of Cr(VI) and high sensitivity	Specificity only demonstrated for Cr(VI), potential for electrode fouling over time, and limited discussion on potential interference	Removal of Cr(VI)	Wide linear range (0.1–10 mg/L) and a LOD (0.097 mg/L)	[58]
Nanofiber	Chemical oxidative polymerization	Breath analysis for hepatic/kidney disease, high sensitivity, selectivity, and repeatability	Complex fabrication method, and limited discussion on potential interference with other gases	NH ₃ sensor	Superior 15.2 response to 1 ppm NH ₃ , high sensitivity (0.6–2.0 ppm), enhanced selectivity, and repeatability at room temperature	[59]
-	Chemical oxidative polymerization	Low toxicity toward investigated organisms and high sensitivity	Limited toxicity scope, broad assessment needed for various organisms, long-term effects	Removal of toxic hexavalent chromium (Cr(VI)) ions from water	Low acute toxicity in freshwater Ostracods and saltwater Artemia salina (-EC50 values: 157.6 \pm 6.4 mg/L, 476 \pm 25.1 mg/L)	[60]
Porous structure	Electrochemical oxidative polymerization	Simple, good selectivity, sensitivity, and repeatability	Real-world sample variability, interference, and matrix-specific optimization	Removal of imidacloprid.	Wide linear range from 0.03 to 12.0 $\mu mol \ L^{-1}$ with a LOD of 9 nmol L^{-1}	[61]
Spontaneous	Hydrothermal	Excellent sensitivity and selectivity in real environmental samples	Validation in diverse conditions and optimization for various samples needed	Removal of Cd(II)	Ultra-high sensitivity level of 1 \times 10 ppb	[62]
Crystalline	Hydrothermal	High sensitivity, selectivity, and stability	Validation in diverse environments, optimization, limited discussion on cross- activity	For 2, 4, 6-trinitrophenol (TNP)	Low LOD as 0.2 ppb (~200 ng/l or 1 nM)	[63]

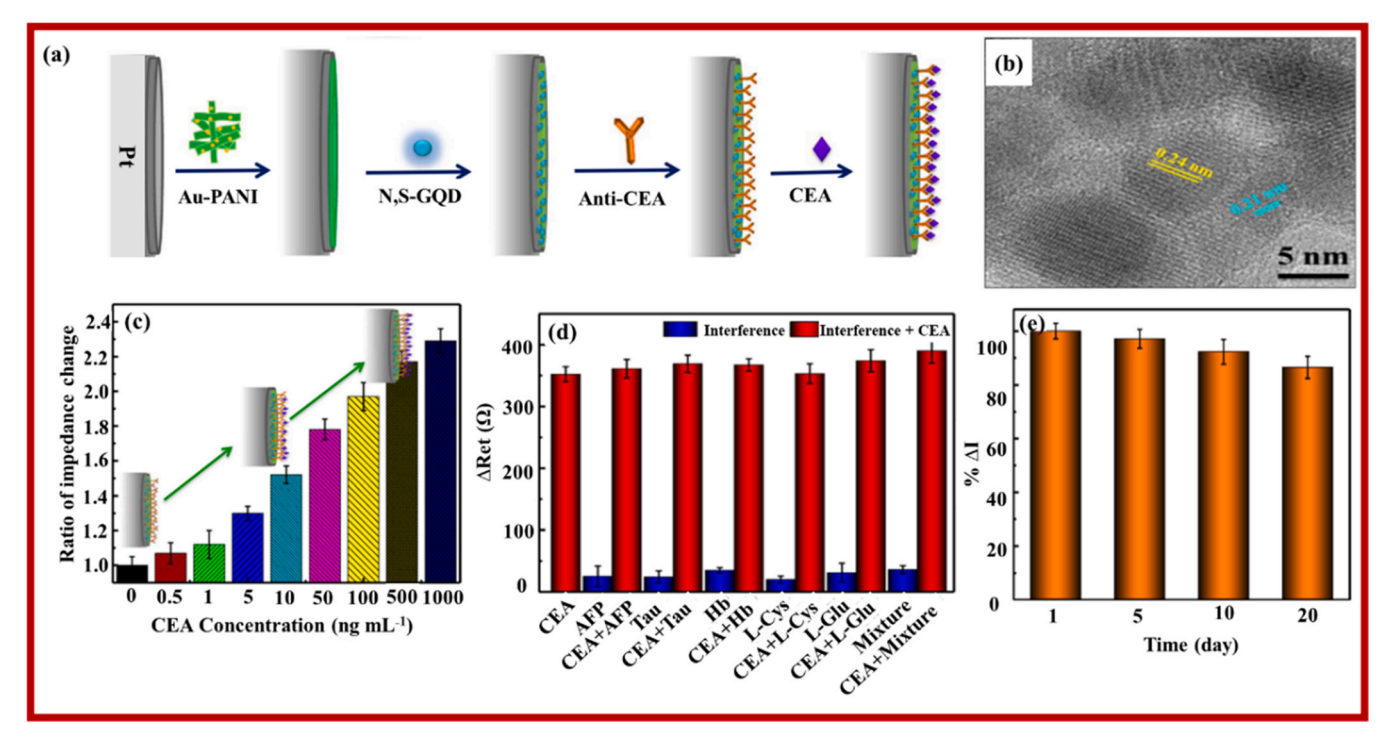


Fig. 8. Illustration of (a) construction of label-free CEA electrochemically impedimetric immunosensor, (b) HRTEM pattern of N, S-GQD@Au-PANI nanocomposites, (c) impedance change ratio (d) specificity and (d) stability of prepared samples [66].

raises concerns, as cadmium is a known toxic heavy metal. Its potential impact on human health, particularly for in vivo applications, requires further investigation. Table 6 presents a comprehensive overview of research findings, including the advantages and disadvantages of PANI–GQD nanocomposites in biosensor applications.

4.3.3. Supercapacitors

PANI–GQD nanocomposites have emerged as promising materials for application in supercapacitors, representing a synergistic integration of the unique properties of PANI and GQDs [69–78,80]. PANI, a conductive polymer, combines with GQDs, which have a high surface

area and conductivity, forming a nanocomposite with enhanced charge storage. This synergy addresses limitations in traditional supercapacitors, improving conductivity, energy storage, and structural stability. Ongoing research aims to optimize PANI–GQD compositions, showcasing their potential for high-performance, durable energy storage devices.

Liu et al. [70] present a promising asymmetric micro-supercapacitor design using GQDs/PANI nanofibers. The results demonstrate exceptional rate capability (up to $1000~V~s^{-1}$) and a fast power response (115.9 μ s relaxation time), exceeding those of previously reported electrode materials. The device exhibits good cycling stability after 1500 cycles in

Table 6Relevant studies related to PANI–GQD composites for biosensor applications.

Morphology	Method	Advantages	Disadvantages	Application	Finding	References
Closely and continuously aggregated	Chemical oxidative polymerization	pH-sensitive, biocompatible nanocarrier, with remarkable blood compatibility	Requires more on long-term effects, stability in biological environments, and off-target effects	Detection of doxorubicin (DOX)	90 % DOX encapsulation, gradual release (4 % in 72 h); pH-triggered release (80 %) in acidic environments	[64]
Corn	Electrochemical oxidative polymerization	Superior glucose detection, high sensitivity, and reliability	Needs validation in diverse physiological conditions and real-world scenarios. Long- term stability and scalability	Detection of non-invasive glucose	Sensitivity with 23.52 mM	[65]
-	Simple solution mixing	Highly sensitive, stable label-free immunosensor with excellent conductivity and selectivity	Optimization required for broader applications; validation needed in diverse clinical settings	Detection of CEA	Wide linear range (0.5– 1000 ng mL^{-1}) with a LOD of 0.01 ng mL^{-1}	[66]
Rough surface	Simple solution mixing	Highly sensitive, disposable electrodes ensure long-term stability	Further validation in real- world aquaculture settings needed. Challenges in mass production and scalability	Detection of white spot syndrome virus	Wide linear range from (1.45×102–1.45×105 DNA copies/mL), with a LOD of 48.4 DNA copies/mL	[67]
Homogenous	Simple solution mixing	High sensitivity, long-term stability, reproducibility, biocompatibility, dispersity, and solubility	Further validation needed in complex biological samples or clinical settings; selectivity	Detection of human interleukin-6 (IL-6)	Broad linear range (0.0005–10 ng/mL) and a LOD of 0.17 pg/mL	[68]
Nanosolid tube	Chemical oxidative polymerization	Good selectivity, sensitivity, acceptable reproducibility, and long-term stability	Further validation in complex traditional Chinese medicine samples and optimization for broad applicability.	Detection of calycosin	Broad detection range (1.1×10 ⁻⁵ to 3.52×10 ⁻⁴ mol/L) and a LOD of 9.8×10 ⁻⁶ mol/L (S/N = 3)	[290]

an aqueous electrolyte. An all-solid-state version using a gel electrolyte also shows promising performance. These findings highlight the potential of GQDs for high-performance supercapacitors. However, including specific capacitance values and comparing them to established materials would provide a stronger context for the device's overall performance. Oskueyan et al. [75] demonstrates improved supercapacitor performance based on the N,S-doped GQDs@CeO₂/PANI composites. The PANI/5 wt% N,S-GQDs@CeO₂ electrode achieves a high specific capacity (189 C g⁻¹) compared to PANI/CeO₂ electrodes. This suggests that incorporating GQDs increases the active surface area and improves performance. Notably, the capacity retention remains good (75 % after 1000 cycles), indicating good cycling stability. However, the lack of information on energy density and comparison with other composite materials limits a complete evaluation.

Xing et al.[76] developed NGQDs/PANI as a supercapacitor electrode via oxidative chemical polymerization. The electrochemical properties of the electrode were evaluated, and the results revealed a high specific capacitance of 506 F/g at 0.5 A/g and excellent cycling stability with 80.2 % of initial capacitance retained over 5000 cycles at a current density of 5 A/g. Their study concluded that NGOD/PANI materials hold promise for utilization in future supercapacitor applications, highlighting their potential use in energy storage devices. Kuzhandaivel et al. [77] established a high-performance supercapacitor electrode material based on S,N-GQDPANI2 with impressive properties. The results show an exceptional specific capacitance of 645 F g⁻¹ at 0.5 A g⁻¹, attributed to a combination of high surface area (154 m² g⁻¹) and the beneficial effects of sulfur and nitrogen doping. The material achieves a good energy density (17.25 Wh kg⁻¹) and an outstanding volumetric energy density (18.11 Wh L⁻¹) for practical applications. It also exhibits remarkable cycling stability, with 90 % capacitance retention after 1000 cycles, indicating excellent long-term performance. However, further investigation into its rate capability (performance at high current densities) is needed to provide a more complete picture, as this is crucial for practical applications requiring fast charging and discharging.

Arthisree et al.[78] investigated a novel and eco-friendly ternary polymer nanocomposite (PVB, PANI, PEDOT:PSS)/GQD for efficient supercapacitors. Despite the challenge of integrating the insulating PVB, the prepared composite showed enhanced conductivity, flexibility, and cost-effectiveness. Electrochemical analysis confirmed its promising performance, achieving a high capacitance value of 4998 Fg⁻¹ cm⁻² This work highlighted the composite's potential for practical supercapacitor applications, combining electrical properties, stability, and fabrication simplicity. Maity et al.[80] synthesized a PANI-GQD composite by oxidative chemical polymerization, demonstrating its enhanced thermal stability, increased conductivity, fluorescence quenching, and tremendous specific capacitance with a value of \sim 1044 F g⁻¹ at a present density of 1 A g⁻¹ and reasonable cyclic stability with a lifetime retention value of 80.1 % after 3000 cycles (Fig. 9). Their study provided insights into the structure-property relationships of PANI-GOD hybrids and their potential applications in photovoltaics. Table 7 presents a comprehensive overview of research findings, outlining the advantages and disadvantages of PANI-GQD nanocomposites in supercapacitor applications.

4.3.4. Solar cells

PANI–GQD nanocomposites have emerged as promising materials in solar cells, representing a synergistic integration of the unique properties of PANI and GQDs. Solar energy is clean and renewable energy that can be converted into electrical energy to support our daily life [70,79, 80]. However, solar energy is only available in the day but not at night. Therefore, energy storage is an important topic in energy applications and remains one of the major challenges in renewable energy.

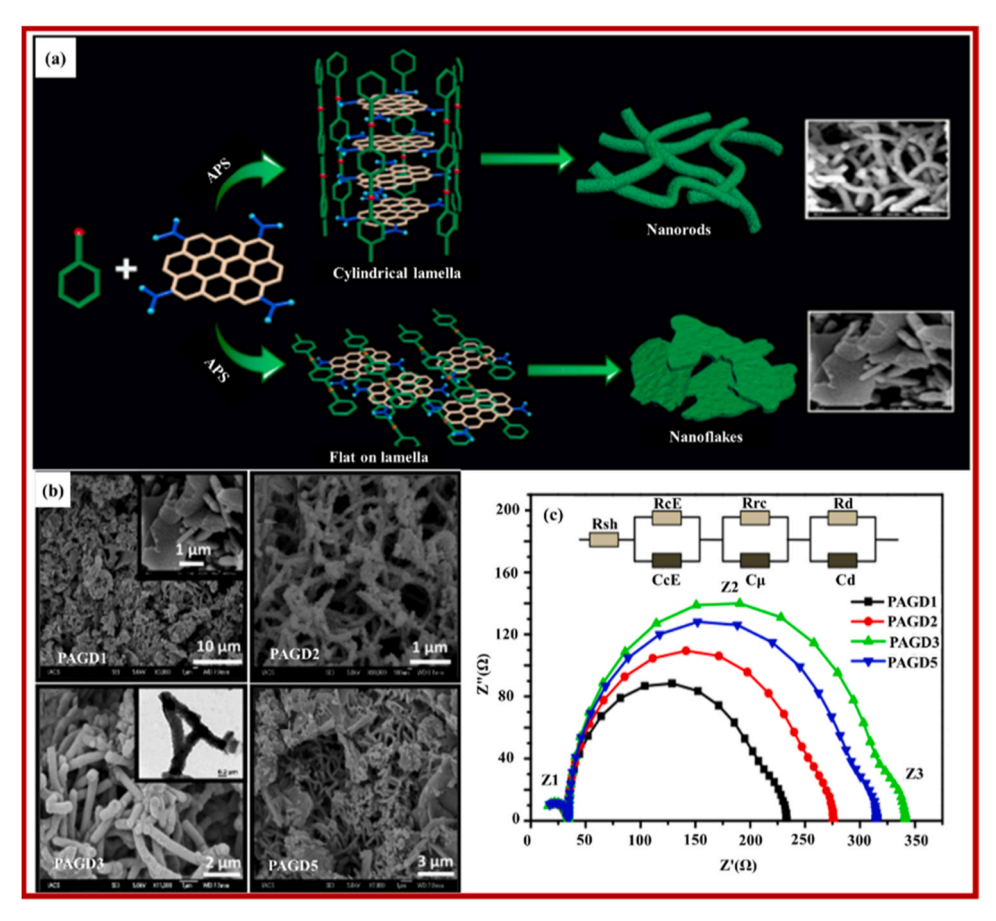


Fig. 9. (a) Diagram of PANI-GQD, (b) FESEM pattern, and (c) electrochemical impedance spectra of the prepared sample [80].

Table 7Relevant studies related to the application of PANI–GQD composites in supercapacitors.

Morphology	Method	Advantages	Disadvantages	Application	Finding	Reference
Uniform structure	Chemical oxidative polymerization	Good structural electrochemical performance, large BET- specific surface area, and high specific capacitance	Composite material stability, validation for supercapacitor use, optimization for scalability and cost- effectiveness	Energy storage/ Supercapacitors	Large BET specific surface area (44.5 m ² /g) and high specific capacitance (245 F/g)	[71]
Nanofiber	Chemical oxidative polymerization	Excellent specific capacitance, and moderate cyclic stability	Further discussion required for the synthesis, scalability, and cost-effectiveness; further characterization and optimization for broad applicability	Supercapacitors	Exceptional 1044 F/g capacitance at 1 A/g, 80.1 % retention after 3000 cycles	[74]
High-efficient	Chemical oxidative polymerization	Highly efficient hybrid electrode materials with high capacity and stability	Optimization of capacity, stability, scalability, and cost- effectiveness is crucial.	Supercapacitor	Max 189 C/g capacity at 1 A/g, 75 % retention after 1000 cycles	[75]
Rough morphology	Chemical oxidative polymerization	Facil synthesis method, high specific capacitance, and cycling stability	Optimization is vital for capacitance, stability, scalability, cost-effectiveness; durability, and performance	Supercapacitors	506 F/g capacitance at 0.5 A/g, 80.2 % retention after 5000 cycles at 5 A/g	[76]
Mace-like morphology	Electrochemical oxidative polymerization	High specific capacitance	Further PANI–GQD film optimization required; details on long-term stability and cycling are lacking. Scalability, cost-effectiveness	Supercapacitor	At a scan rate of 10 mV/s, tested in 0.5 M $\rm H_2SO_4~(-0.20~V~to~0.60~V)$	[69]
Nanofiber	Electrochemical oxidative polymerization	Novel approach with simple fabrication, excellent electrochemical performance, and rate capability	Lack of characterization and device parameters. Validation and optimization needed	Micro- supercapacitors	Superior rate capability (1000 V·s ⁻¹), faster power response, enhanced stability (1500 cycles)	[70]
Well dispersed without agglomeration	Simple solution mixing	High optical and electrical conductivity, selectivity, stability, and specific capacitance	Insufficient discussion on interferences, large sample size validation needed	Supercapacitor	Supercapacitor values range (105–587 F/g·cm²) at 670 mA/g,	[66]
Nanosized and denser	LbL assembly	Simple synthesis, excellent conductivity, capacitance, and catalytic activity	Challenges undisclosed; varied condition material characterization; real-world detection limit validation essential	Supercapacitors/ H ₂ O ₂	Remarkable 648 F/g capacitance, electrochemical activity, wide linear range of $(5.0\times10^{-7}-3.5\times10^{-5} \text{ M})$, and low detection $(1.1 \ \mu\text{M})$	[73]
Nanoflakes and agglomerate	LbL assembly	Good dispersion and homogenous morphology, and excellent electrochemical catalytic capacity	Validation of electrochemical catalytic activity with real- world samples necessary for practical use	Supercapacitors/ H ₂ O ₂	Excellent electrochemical catalytic activity from 10 to 150 mV s ⁻¹	[291]
Pine cone shape- like	Polycondensation	Enhanced electrical conductivity, and ion storage, high specific capacitance, and energy density	Optimization of composite performance for specific applications	Supercapacitors	Highest 645 F/g capacitance at 0.5 A/g, 90 % retention after 1000 cycles	[77]
Filler-like molecular arrangement	Solution-casting	Enhanced electrical conductivity, flexibility, and high specific capacitance	Further validation in diverse conditions for broad applicability, exploring performance variations	Supercapacitors	High capacitance value of 4998 ${\rm Fg}^{-1}~{\rm cm}^{-2}$	[78]
Mix rods and flakes	Chemical oxidative polymerization	Effective charge transfer, improved conductivity, enhanced thermal stability, high capacitance, and structural integrity	Validation in varied conditions for broad use. Exploration of performance variations	Supercapacitors	High capacitance (1044 F g ⁻¹), good stability (80.1 % after 3000 cycles)	[80]
Highly porous structure	Simple physical mixing	Simple synthesis, high capacity, energy density, power density, and remarkable redox activity	Insufficient details on structural analysis, limited insight into performance enhancement	Supercapacitors	High peak capacities of 295 mAh $\rm g^{-1}$, energy density of 62.1 Wh $\rm kg^{-1}$, and power density of 4140 W $\rm kg^{-1}$	[253]

Dinari et al. [79] prepared a PANI–GQD nanocomposite using electrochemical polymerization for dye-sensitized solar cells (DSSCs). The prepared composite demonstrated enhanced catalytic activity as confirmed by various characterization techniques. DSSCs employing this electrode achieved a 1.6 % efficiency, surpassing pristine PANI electrodes. This finding suggested PANI–GQD's potential as a cost-effective alternative for DSSCs (Fig. 10).

Mombru et al. [83] explore the potential of edge-modified GQDs in PANI for solar cells using a combined theoretical approach. The study suggests that hydroxyl groups on GQD edges enhance their interaction with PANI, leading to improved electronic properties. Notably, this

modification promotes efficient electron-hole separation, which is critical for solar cells upon light excitation. These findings are promising for the development of GQD-based solar cells. However, the lack of experimental data on actual power conversion efficiency hinders a complete assessment. Validating the theoretical findings with laboratory experiments would strengthen the case for practical applications. Gebreegziabher et al. [298] explore PANI-GQDs as a potential material for photovoltaic cells. The PANI-GQD hybrid shows improved light absorption and thermal stability compared to pristine PANI. The composite material exhibits some photovoltaic behavior with a power conversion efficiency of 0.857 % under simulated sunlight. However, this efficiency

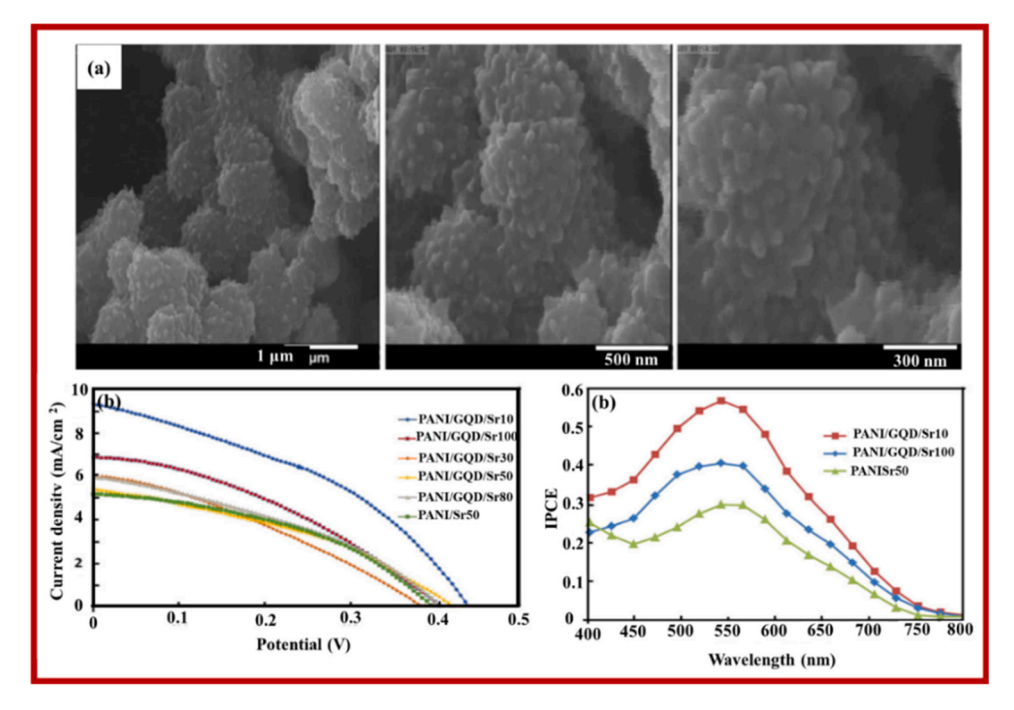


Fig. 10. (a) FESEM images of PANI–GQD with different magnification, (b) photocurrent density–photovoltage (J–V) curves, and (d) comparison of IPCE spectra of DSSCs using prepared samples [79].

is significantly lower than that of commercially available solar cell materials, which typically exceed 15 %. Further optimization and investigation into the reasons behind the decreased Raman peaks and XRD shift are necessary for practical applications. Table 8 presents a comprehensive overview of research findings, including the advantages and disadvantages of PANI–GQD nanocomposites in solar cell applications.

4.3.5. Optoelectronics

Researchers have sought to enhance the optoelectronic properties of PANI by incorporating GQDs into its structure, resulting in PANI–GQD nanocomposites. With their quantum confinement effects and tunable bandgap, GQDs offer distinct advantages in improving the photoresponsive characteristics of the nanocomposite. The synergistic combination of PANI and GQDs results in a material that exhibits improved charge carrier mobility, enhanced light absorption, and efficient charge separation. As a consequence, PANI–GQD nanocomposites have become particularly attractive for applications in optoelectronic devices [81–85, 291].

Luk et al. [81] synthesized an Au/PANI-GQD composite film via chemical oxidative polymerization and investigated the transport and optical properties by varying the mole concentration of PANI and the size of GQDs. Influenced by PANI content and GQD size, tunable properties are linked to the surface states of GQDs, offering potential for

photonic device applications due to adjustable luminescence and electrical behavior. Siddique et al. [82] developed a NGQD-PANI nanocomposite and found that varying NGQD doping levels and temperature led to distinct conduction regimes, with a 50-fold enhancement in conductivity. Their research offered insights into the interplay of extrinsic parameters such as temperature and voltage bias with intrinsic material properties including doping, which is crucial for understanding the electronic properties of NGQD-PANI composites and guiding their technological applications (Fig. 11). Jamdegni et al. [84] introduce a promising PANI-fGQD composite for stable electrochromic devices. The result shows improved electrochemical performance with well-defined redox peaks and higher current densities compared to PANI. It exhibits a wider color change (pale yellow to blue) with excellent contrast (62 % at 658 nm), surpassing pristine PANI. Remarkably fast response times (0.9 s for coloration and 1.4 s for bleaching) and outstanding stability (15,000 cycles) highlight its potential. However, the study lacks data on mechanical flexibility, a crucial aspect for practical flexible electrochromic applications. Mombru et al. [85] explore the impact of incorporating GOQDs on the electrical properties of PANI for electronic devices. The addition of GOQDs alters PANI's microstructure and reduces its polaron population (charge carriers), as observed through X-ray and Raman techniques. This results in a significant increase in resistivity compared to pure PANI. Interestingly, the electrical transport exhibits increased hopping dimensionality even with low GOQD

Table 8Relevant studies related to the application of PANI–GQD composites in solar cells.

Morphology	Method	Advantages	Disadvantages	Application	energy efficiency	References
3D porous network structure	Electrochemical oxidative polymerization	Excellent rate capability cyclic stability, and fast power response capability	Scalability and cost-effectiveness; long-term stability under various conditions	Plastic solar cells/ photovoltaic cells	0.857 %	[70]
Mace-like morphology	Electrochemical oxidative polymerization	Simple synthesis method, cost- effective, high electrochemical catalytic activity, and photovoltaic performance	Limited discussion on synergistic mechanism, lack of comprehensive long-term stability analysis	DSSCs	1.6 %	[79]
Nanorods	Chemical oxidative polymerization	Effective charge transfer, enhanced thermal stability, DC conductivity, good photovoltaic activity	Scalability and cost-effectiveness limitations, impedance data interpretation complexity	DSSCs	3.12 %	[80]

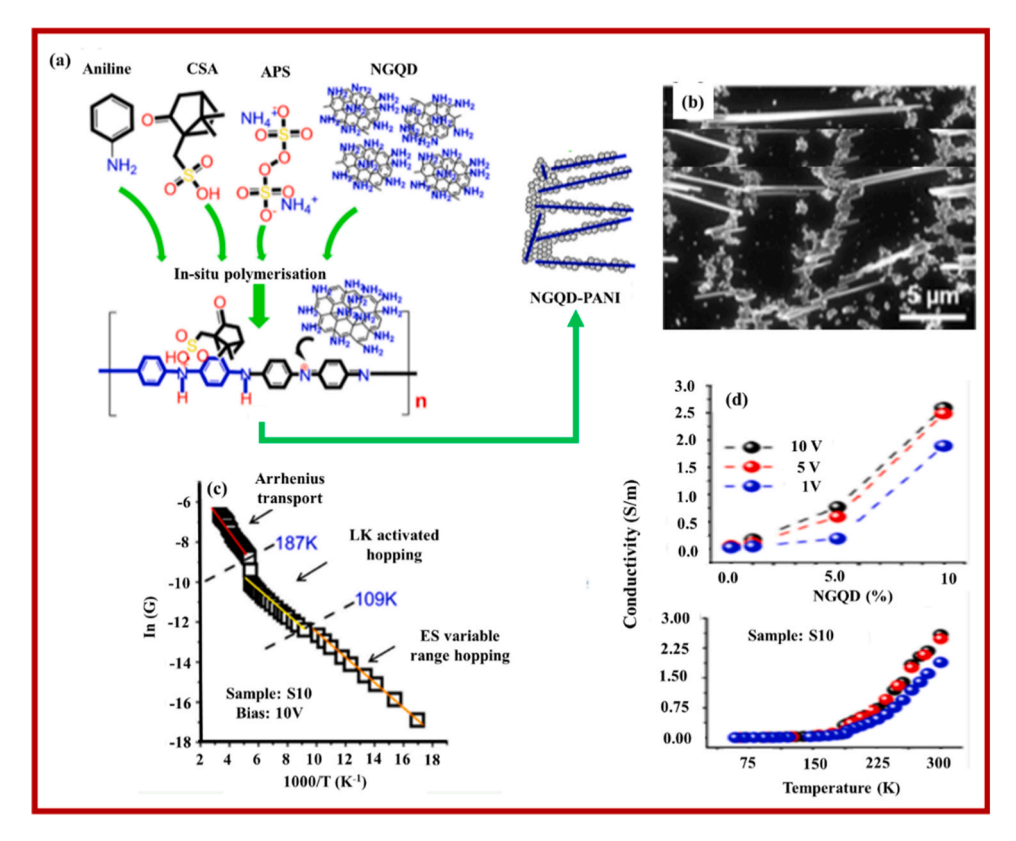


Fig. 11. (a) Diagram of the preparation of NGQD—PANI, (b) FESEM pattern, (c) variation of conductance, and (d) room-temperature and temperature-dependent I—V characteristics of PANI—GQD composite [82].

content. While the study reveals changes in dimensionality, it lacks data on the absolute conductivity values. Conductivity is a crucial parameter for electronic devices, and the lower conductivity due to increased resistivity might limit the applicability of PANI-GOQD composites. Table 9 presents a comprehensive overview of research findings, including the advantages and disadvantages of PANI-GQD nanocomposites for opto-electronic applications.

4.3.6. Coating

PANI–GQD nanocomposites demonstrate promise for coatings [86], featuring unique properties resulting from the synergy between PANI and GQDs. Incorporating GQDs enhances the electrical conductivity, mechanical strength, and thermal stability of the nanocomposite, making it ideal for applications requiring a blend of these qualities, such as

corrosion protection, antistatic coatings, and electromagnetic interference shielding. Optimizing the formulation, deposition techniques, and performance through further research is crucial for enhancing the practical utilization of PANI–GQD nanocomposite coatings in real-world scenarios. Ramezanzadeh et al. [86] successfully developed GOQD-PANI as an advanced and highly crystalline carbon-based luminescent nanomaterial for the fabrication of an effective anticorrosion epoxy system on mild steel through salt spray and EIS tests. They explored environmentally friendly alternatives to traditional anticorrosive pigments by employing GOQD-PANI in polymer composites. The synthesized GOQDs were characterized, and their effect on epoxy coatings was analyzed. the results revealed their enhanced barrier properties and inhibitive action, showcasing their potential for anticorrosive coatings. The findings also suggested that the fine dispersion of GOQD-PANI in the epoxy matrix

Table 9Relevant studies related to the application of PANI–GQD composites in optoelectronics.

Morphology	Method	Advantages	Disadvantages	Application	Finding	References
Irregular	Chemical oxidative polymerization	Facile, low cost, good optical, and electrical properties	Composite film stability unclear. Further characterization needed for mechanistic understanding.	Photonic devices	Tunable luminescence and electrical hysteresis	[81]
Nanorods	Chemical oxidative polymerization	Rich electrical conductivity, clear conduction mechanism understanding	Limited scalability, cost- effectiveness, doping optimization; challenges in integration	Charge Transport	Temperature-dependent conductivity regimes; 50- fold enhancement	[82]
-	Molecular dynamics	Novel approach, good structural, and electrical properties	Missing details on computational methods, scaling challenges from simulations to application	Optoelectronic	Enhanced interaction, and electronic	[83]
Randomly oriented nanorods	Electrochemical oxidative polymerization	Highly Stable, flexible electrochromic electrode	Limited characterization impedes the understanding of electrochromic behavior mechanism.	Electrochromic	Vivid color change, 62 % contrast, rapid response, 15000-cycle stability	[84]
Pellets surface	Simple solution mixing	High electrical transport performance	Insufficient focus on scalability, device applications, and underlying property changes	Potential electronic device	Structural changes impact resistivity and dimensionality	[85]

filled the pores and defects, blocking diffusion pathways and improving corrosion resistance. This research contributed to the development of effective and sustainable anticorrosive coatings using carbon-based nanomaterials (Fig. 12).

5. Challenges and limitations

Considering all the facts, we individually emphasized some of the opinions listed in Fig. 13 that are native yet crucial for the growth of PANI–GQD nanocomposites in several applications.

- 1) Structural optimization: PANI–GQD nanocomposites hold promise but need structural optimization for improved performance. Refining synthesis methods to control GQD characteristics and exploring alternative polymers or dopants for stability and conductivity enhancement are recommended. Morsy et al. [286] fabricated a novel humidity sensor based on PANI/GQDs/MnO2 via an in-situ polymerization reaction. The combination of MnO2 and GQDs prevents the stacking of graphene sheets due to van der Waals forces and aids in better dispersion. XRD data confirms the nanoscale structure (crystallite size < 30 nm), while SEM images reveal a PANI-dominant fibrous morphology. FTIR validates the composite's chemical composition. The sensor exhibits responsiveness across a wide humidity range (11–97 % RH) with moderate response and recovery times (120 s and 220 s, respectively). Further optimization could target faster response times for improved sensor performance.
- 2) Efficiency enhancement: Current PANI-GQD nanocomposites face efficiency limitations. Overcoming charge transport, interfacial resistance, and stability issues by employing strategies such as surface functionalization and heteroatom doping can enhance the



Fig. 13. Challenges and limitations of PANI–GQD nanocomposites in several applications.

nanocomposite's efficiency. Siddique et al. [82] established NGQD-PANI composites that exhibit tunable electronic properties due to controlled doping and microstructure. These composites demonstrate conductivity across a wide range of temperatures with varying NGQD doping levels. A significant transition in conduction mechanisms and a 50-fold enhancement in conductivity is observed for samples with 10 % NGQD doping. Notably, the tunability of the crossover temperature between different conduction regimes as a

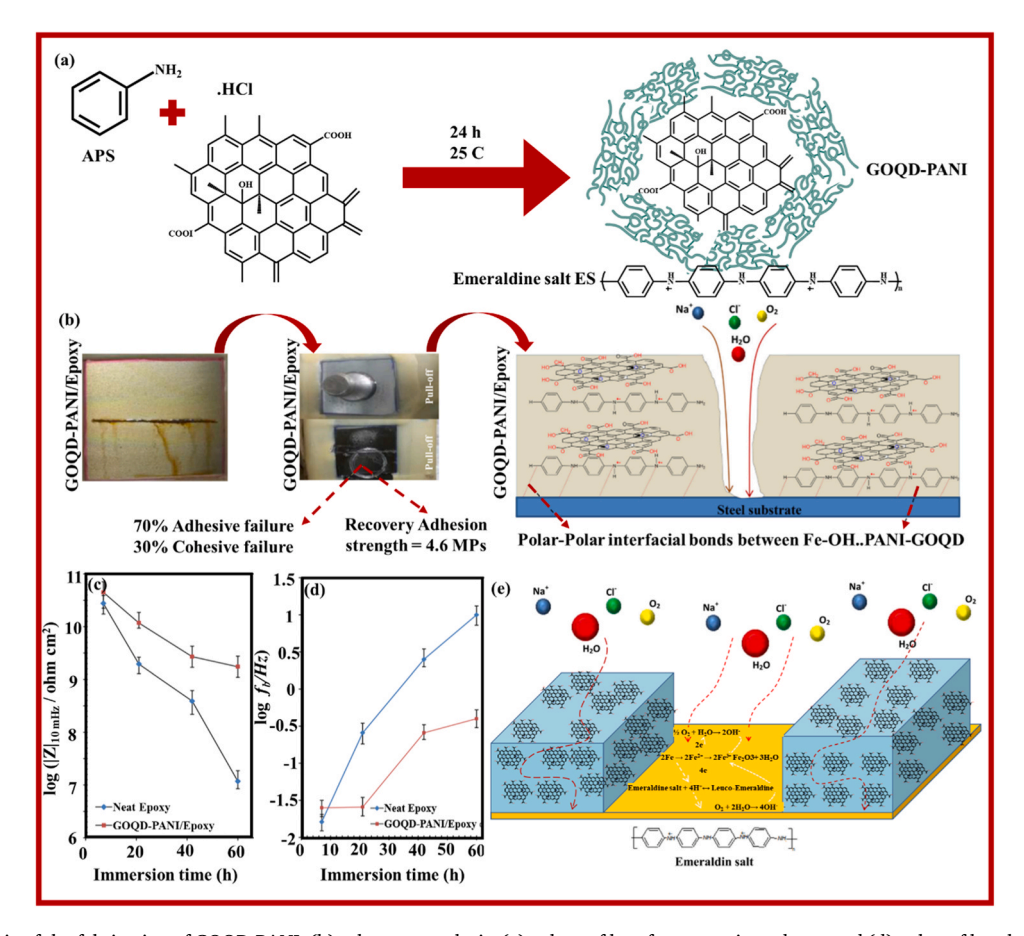


Fig. 12. (a). Schematic of the fabrication of GOQD-PANI, (b) salt spray analysis, (c) values of low-frequency impedance and (d) value of breakpoint frequency values for the prepared samples, (e) corrosion protection possible mechanism of GOQD-PANI.

- function of the applied voltage bias and doping is highlighted, demonstrating the interplay of material properties, voltage, and temperature. This work clarifies the conduction behavior in these promising materials for sensors and thermoelectrics.
- 3) Simulation calculations: Molecular dynamics and DFT provide atomic-level insights into PANI–GQD nanocomposites, aiding the understanding of interactions, predicting properties, and guiding experimental design. Mobru et al. [83] present a mixed method based on basic molecular dynamics combined with time-dependent density functional calculations to define the electrodynamic and optical properties of a PANI/GQDs composite. The analysis suggests that the interaction between PANI and GQDs, particularly with hydroxyl groups, leads to enhanced electronic properties, making it promising for optoelectronic applications like solar cells. However, the text lacks specific data on the magnitude of conductivity modification or the efficiency of electron-hole separation. Further experimental validation would strengthen these claims.
- 4) Integration with other materials: Integrating PANI–GQD with other materials can surpass limitations, yielding synergistic effects. Challenges include compatibility, dispersion, and interface engineering within composite systems. Researchers can overcome these issues by introducing novel materials and compatibilization methods to integrate PANI-GQD composites with other materials to improve adhesion and overall performance. Arthisree et al. [78] investigate a ternary polymer nanocomposite (made of PVB, PANI, PEDOT: PSS, and GQD) as a promising material for supercapacitors. The GQD size is significantly reduced in the composite (6 \pm 2 nm) compared to pristine GQD (50 \pm 5 nm), suggesting interaction with the polymer matrix. The researchers found that incorporating 1 wt% GQD into the nanocomposite leads to an optimal capacitance of 4998 Fg $^{-1}$ cm $^{-2}$, highlighting the potential of this material for supercapacitor applications.
- 5) Scale-up and manufacturing challenges: Scaling PANI–GQD nano-composite production to an industrial level is accompanied by increased cost, synthesis complexity, and processing hurdles. Prioritizing cost-effective synthesis, processing, and quality control strategies ensures manufacturing consistency. Shao et al. [278] present a promising, scalable method for high-performance, flexible supercapacitors based on PANI/GQDs/graphene co-coated compressed non-woven towel (PGG/CNWT). They address a key challenge by using a facile 'dyeing and drying' technique to coat a commercially available fabric (CNWT) with rGO for a flexible substrate. Further enhancement is achieved by incorporating OH-GQDs and electrodeposited PANI, leading to a high areal capacitance of 195 mF cm⁻² at 0.1 mA cm⁻² and excellent stability (96.5 % retention after 6000 cycles). This simple and scalable approach makes PGG/CNWT electrodes attractive for future flexible and wearable electronics.

6. Conclusion and future perspectives

In summary, we presented a state-of-the-art review encompassing the comprehensive synthesis strategies and properties of PANI-GQD nanocomposites across various applications. The absence of a literature review on PANI-GQD nanocomposites prompted our investigation into the differences and key factors determining their performance, including morphology, synthesis methods, and conditions, which were discussed in detail and tabulated in this work. We also reviewed recent studies on the synthesis, properties, and application methods of PANI-based and GQD-based nanocomposites. Research on PANI-GQD nanocomposites has demonstrated their significantly tailored and improved properties. The growing interest in PANI-GQD nanocomposites has brought to light their various practical applications, including in sensors, biosensors, supercapacitors, solar cells, optoelectronics, and coatings. The synthesis of PANI-GQD nanocomposites, particularly the processes responsible for their unique properties, has been studied in detail. GQD proves to be an excellent substitute for strong oxidizers, mitigating the harmful effects on the environment, and a helpful template for the formation of PANI-based QD nanocomposites. By selecting the right dopant and reducing the band gap, the synthesis and fabrication of PANI-GQD nanocomposites through chemical oxidative polymerization can enhance their electrical conductivity. Incorporating GQD into PANI can also improve the cycling stability and electrochemical capacity of the nanocomposite when applied in supercapacitors and energy storage. The compiled studies on PANI-GQD nanocomposites indicated their great potential for sensing applications. The PL mechanism of PANI-GQD still requires detailed investigation for upcoming sensing applications. Factors such as tunable PL emissions, low cost, and environmentally friendly properties should be considered.

Nevertheless, a significant gap remains in the literature regarding the sensing properties of PANI–GQD nanocomposites to detect other toxic chemicals, such as polycyclic aromatic hydrocarbons. So far, the developed PANI–GQD nanocomposites are vital for other potential applications, such as fuel cells and drug delivery. Therefore, further studies are needed to improve the fabrication strategies and properties of PANI–GQD nanocomposites for these specific applications. For the enhanced detection of toxic chemicals using PANI–GQD nanocomposites, specific methods can be explored as follows:

- Surface functionalization: Functionalizing PANI–GQD surfaces with receptors enhances the selectivity for target toxins, improving detection accuracy in complex samples.
- Advanced analytical techniques: Integrating PANI–GQD nanocomposites using advanced techniques such SERS or electrochemical sensors improves their sensitivity and detection limits for trace toxic chemicals.
- 3) New detection mechanisms: Novel detection mechanisms with PANI–GQD nanocomposites must be explored. For instance, leveraging GQDs' photoluminescent properties with PANI could enable fluorescence-based detection methods for toxins, advancing current sensitive and selective detection platforms.
- 4) Synthesis parameter optimization: Optimizing the synthesis parameters of PANI–GQD nanocomposites can significantly impact their detection performance. Parameters such as PANI to GQD ratio, dopant selection, reaction temperature, and time can influence the morphology and surface properties of the nanocomposites, ultimately affecting their sensing capabilities.
- 5) Nanocomposite arrays: Creating arrays of PANI-GQD nanocomposites with diverse compositions or surface modifications can expand their toxin detection range and enhance their analyte discrimination. Array sensors offer multiplexing and reliability for real-world applications.
- 6) Miniaturization for portability: Miniaturizing PANI–GQD sensors for integration into portable devices enables the on-site, real-time monitoring of toxins. Microfabrication and low-power electronics can advance signal processing for this purpose.

CRediT authorship contribution statement

Suraya Abdul Rashid: Writing – review & editing, Visualization, Supervision, Investigation. Siti Kartom Kamarudin: Writing – review & editing, Supervision, Software, Methodology, Conceptualization. Mahnoush Beygisangchin: Writing – review & editing, Writing – original draft, Software, Methodology, Investigation, Conceptualization.

Declaration of Competing Interest

The authors declare that they have no known competing financial interests or personal relationships that could have appeared to influence the work reported in this paper

Data availability

Data will be made available on request.

Acknowledgements

The authors would like to thank Ministry of Higher Education of Malaysia under HiCoE -2023-001 and Universiti Kebangsaan Malaysia for supporting this research project through RIA 2 (Modal Insan Penyelidikan) and the Universiti Putra Malaysia for its financial support via Geran Universiti Putra Malaysia Inisiatif Putra Berimpak 9674700.

References

- A. Saraswat, S. Kumar, A topical study of electrochemical response of functionalized conducting polyaniline: an overview, Eur. Polym. J. 182 (2023) 111714, https://doi.org/10.1016/j.eurpolymj.2022.111714.
- [2] S. Jadoun, J.P. Fuentes, B.F. Urbano, J. Yáñez, A review on adsorption of heavy metals from wastewater using conducting polymer-based materials, J. Environ. Chem. Eng. 11 (2023) 109226, https://doi.org/10.1016/j.jece.2022.109226.
- [3] S.A. Mazari, E. Ali, R. Abro, F.S.A. Khan, I. Ahmed, M. Ahmed, S. Nizamuddin, T. H. Siddiqui, N. Hossain, N.M. Mubarak, A. Shah, Nanomaterials: applications, waste-handling, environmental toxicities, and future challenges a review, J. Environ. Chem. Eng. 9 (2021) 105028, https://doi.org/10.1016/j.iece.2021.105028
- [4] H. Shirakawa, E.J. Louis, A.G. MacDiarmid, C.K. Chiang, A.J. Heeger, Synthesis of electrically conducting organic polymers: Halogen derivatives of polyacetylene, (CH)x, J. Chem. Soc. Chem. Commun. (1977) 578–580, https://doi.org/10.1039/ C39770000578.
- [5] N.N. Khalid, N.A.M. Radzuan, A.B. Sulong, F.M. Foudzi, Conductive polymer composites using 3D printing for electronic devices: A review, in: 2023: p. 040006. https://doi.org/10.1063/5.0116323.
- [6] A.L. Pang, A. Arsad, M.A. Ahmad Zaini, R. Garg, M. Saqlain Iqbal, U. Pal, M.A. S. Mohammad Haniff, A. Azlan Hamzah, S.-Y. Pung, M. Ahmadipour, A comprehensive review on photocatalytic removal of heavy metal ions by polyaniline-based nanocomposites, Chem. Eng. Commun. (2023) 1–25, https://doi.org/10.1080/00986445.2023.2227568.
- [7] M. Beygisangchin, S. Abdul Rashid, S. Shafie, A.R. Sadrolhosseini, H.N. Lim, Preparations, properties, and applications of polyaniline and polyaniline thin films—a review, Polymers 13 (2021) 2003, https://doi.org/10.3390/ polym13122003.
- [8] M. Beygisangchin, S. Abdul Rashid, S. Shafie, A.R. Sadrolhosseini, Polyaniline synthesized by different dopants for fluorene detection via photoluminescence spectroscopy, Materials 14 (2021) 7382, https://doi.org/10.3390/ma14237382.
- [9] M. Beygisangchin, S.A. Rashid, H.N. Lim, S. Shafie, A.R. Sadrolhosseini, Effect of toluene-4-sulfonic acid monohydrate concentrations on properties of polyaniline for pyrene detection via photoluminescence spectroscopy, Opt. Mater. (Amst.) 131 (2022) 112711, https://doi.org/10.1016/j.optmat.2022.112711.
- [10] M. Beygisangchin, S. Abdul Rashid, S. Shafie, H.N. Lim, Evaluation of N-methyl-2-pyrrolidone concentration on synthesis and characterization of 1% toluene-4-sulfonic acid monohydrate doped polyaniline film, J. Inorg. Organomet Polym. Mater. 33 (2023) 1246–1260, https://doi.org/10.1007/s10904-023-02574-3.
- [11] M. Beygisangchin, S.A. Rashid, S. Shafie, Investigation on polyaniline synthesised by camphor sulphonic acid; optical, thermal, structural, and electrical properties, Int J. Nanotechnol. 20 (2023) 998–1009, https://doi.org/10.1504/ JJNT.2023.135814.
- [12] X. Liu, W. Zheng, R. Kumar, M. Kumar, J. Zhang, Conducting polymer-based nanostructures for gas sensors, Coord. Chem. Rev. 462 (2022) 214517, https://doi.org/10.1016/j.ccr.2022.214517.
- [13] P. Zarrintaj, H. Vahabi, M.R. Saeb, M. MozafariApplication of polyaniline and its derivatives Elsevier, Fundamentals and Emerging Applications of Polyaniline, 2019, , 259–272, 10.1016/B978-0-12-817915-4.00014-2.
- [14] S. Ramanavicius, A. Ramanavicius, Conducting polymers in the design of biosensors and biofuel cells, Polymers 13 (2021) 1–19, https://doi.org/10.3390/ polym13010049.
- [15] F. Usman, J.O. Dennis, A.I. Aljameel, M.K.M. Ali, O. Aldaghri, K.H. Ibnaouf, Z. U. Zango, M. Beygisangchin, A. Alsadig, F. Meriaudeau, Plasmonic biosensors for the detection of lung cancer biomarkers: a review, Chemosensors 9 (2021) 326, https://doi.org/10.3390/chemosensors9110326.
- [16] J. Iqbal, M.O. Ansari, A. Numan, S. Wageh, A. Al-Ghamdi, M.G. Alam, P. Kumar, R. Jafer, S. Bashir, A.H. Rajpar, Hydrothermally assisted synthesis of porous polyaniline@carbon nanotubes—manganese dioxide ternary composite for potential application in supercapattery, Polymers 12 (2020) 2918, https://doi.org/10.3390/polym12122918.
- [17] F. Boorboor Ajdari, E. Kowsari, M. Niknam Shahrak, A. Ehsani, Z. Kiaei, H. Torkzaban, M. Ershadi, S. Kholghi Eshkalak, V. Haddadi-Asl, A. Chinnappan, S. Ramakrishna, A review on the field patents and recent developments over the application of metal organic frameworks (MOFs) in supercapacitors, Coord. Chem. Rev. 422 (2020) 213441, https://doi.org/10.1016/j.ccr.2020.213441.
- [18] H. Lyu, Triple layer tungsten trioxide, graphene, and polyaniline composite films for combined energy storage and electrochromic applications, Polymers 12 (2020), https://doi.org/10.3390/polym12010049.

- [19] Z. Li, L. Gong, Research progress on applications of polyaniline (PANI) for electrochemical energy storage and conversion, Materials 13 (2020) 548, https://doi.org/10/3390/ma13030548
- [20] H.R. Mohseni, M. Dehghanipour, N. Dehghan, F. Tamaddon, M. Ahmadi, M. Sabet, A. Behjat, Enhancement of the photovoltaic performance and the stability of perovskite solar cells via the modification of electron transport layers with reduced graphene oxide/polyaniline composite, Sol. Energy 213 (2021) 59-66, https://doi.org/10.1016/j.solener.2020.11.017.
- [21] S. Elakkiya, G. Arthanareeswaran, Evaluation of membrane tailored with biocompatible halloysite-polyaniline nanomaterial for efficient removal of carcinogenic disinfection by-products precursor from water, Environ. Res 204 (2022) 112408, https://doi.org/10.1016/j.envres.2021.112408.
- [22] E.B. Caldona, A.C.C. de Leon, B.B. Pajarito, R.C. Advincula, Novel anti-corrosion coatings from rubber-modified polybenzoxazine-based polyaniline composites, Appl. Surf. Sci. 422 (2017) 162–171, https://doi.org/10.1016/j. apsusc.2017.05.083.
- [23] F. Ghorbani, A. Zamanian, A. Aidun, Conductive electrospun polyurethanepolyaniline scaffolds coated with poly(vinyl alcohol)-GPTMS under oxygen plasma surface modification, Mater. Today Commun. 22 (2020) 100752, https:// doi.org/10.1016/j.mtcomm.2019.100752.
- [24] K. Pirnat, J. Bitenc, I. Jerman, R. Dominko, B. Genorio, Redox-active functionalized graphene nanoribbons As electrode material for Li-ion batteries, 351–351, ECS Meet. Abstr. MA2015-01 (2015), https://doi.org/10.1149/ MA2015-01/2/351.
- [25] F. Jia, L. Yang, L. Sun, D. Yu, Y. Song, Y. Wang, M.J. Kipper, J. Tang, L. Huang, Efficient separation of dyes using two-dimensional heterogeneous composite membranes, Water Res 247 (2023) 120693, https://doi.org/10.1016/j. watres.2023.120693.
- [26] D. Yu, L. Sun, Y. Zhang, Y. Song, C. Jia, Y. Wang, Y. Wang, M.J. Kipper, J. Tang, L. Huang, Two-dimensional graphene oxide/MXene lamellar membrane cross-linked by urea with adjustable interlayer spacing for efficient dye rejection and ion sieving, Chem. Eng. J. 480 (2024) 148009, https://doi.org/10.1016/j.cei.2023.148009.
- [27] D. Yu, X. Xiao, C. Shokoohi, Y. Wang, L. Sun, Z. Juan, M.J. Kipper, J. Tang, L. Huang, G.S. Han, H.S. Jung, J. Chen, Recent advances in stimuli-responsive smart membranes for nanofiltration, Adv. Funct. Mater. 33 (2023), https://doi. org/10.1002/adfm.202211983.
- [28] Z. Han, X. Xiao, H. Qu, M. Hu, C. Au, A. Nashalian, X. Xiao, Y. Wang, L. Yang, F. Jia, T. Wang, Z. Ye, P. Servati, L. Huang, Z. Zhu, J. Tang, J. Chen, Ultrafast and selective nanofiltration enabled by graphene oxide membranes with unzipped carbon nanotube networks, ACS Appl. Mater. Interfaces 14 (2022) 1850–1860, https://doi.org/10.1021/acsami.1c17201.
- [29] Z. Zhang, X. Xiao, Y. Zhou, L. Huang, Y. Wang, Q. Rong, Z. Han, H. Qu, Z. Zhu, S. Xu, J. Tang, J. Chen, Bioinspired graphene oxide membranes with pH-responsive nanochannels for high-performance nanofiltration, ACS Nano 15 (2021) 13178–13187. https://doi.org/10.1021/acsnano.1c02719.
- [30] S. Wang, D. Hu, Y. Liu, H. Xiong, Synthesis of ferrihydrite/polyaniline composite using waste Fe(III)/EPS-cultures with polyaniline and its application for tetracycline photo-Fenton degradation, J. Environ. Chem. Eng. 12 (2024) 112180, https://doi.org/10.1016/j.jece.2024.112180.
- [31] A.A. Wani, N. Shaari, A.A. Ansari, S. Mohd, P. Tiwari, S.K. Kamarudin, R. K. Gupta, Polyaniline-based functional nanohybrid materials towards environmental remediation; current progress, challenges, and future perspectives, J. Environ. Chem. Eng. 11 (2023) 111254, https://doi.org/10.1016/j.iece.2023.111254
- [32] R.N. Kasavo, M. Bhaumik, H.G. Brink, Removal of chromium from aqueous solution using a nanocomposite of nickel ferrite and polyaniline doped with 2naphthalene sulfonic acid, J. Environ. Chem. Eng. 11 (2023) 111229, https://doi. org/10.1016/j.jece.2023.111229.
- [33] C. Li, B. Liu, D. Fang, P. Zhang, F. Li, X. Qiu, X. Mo, K. Li, Polyaniline-derived mesoporous carbon electrode for selective and efficient ammonium removal with in a flow-electrode capacitive deionization system, J. Environ. Chem. Eng. 11 (2023) 110857, https://doi.org/10.1016/j.jece.2023.110857.
- [34] T. ul Haq Zia, S.F. Shah, A. ul Haq, B. Ara, K. Gul, Fabricating ternary α-Fe2O3 nanoparticles-polyaniline-graphite nanoplatelets nanocomposite with enhanced photoelectrochemical activity for potential use as peroxidase mimic as well as photocatalyst, J. Environ. Chem. Eng. 11 (2023) 110410, https://doi.org/10.1016/j.jece.2023.110410.
- [35] P. Tian, L. Tang, K.S. Teng, S.P. Lau, Graphene quantum dots from chemistry to applications, Mater. Today Chem. 10 (2018) 221–258, https://doi.org/10.1016/j. mtchem.2018.09.007.
- [36] G. Li, Z. Liu, W. Gao, B. Tang, Recent advancement in graphene quantum dots based fluorescent sensor: design, construction and bio-medical applications, Coord. Chem. Rev. 478 (2023) 214966, https://doi.org/10.1016/j. ccr.2022.214966.
- [37] Y.F. Zhu, Q. Jiang, Edge or interface effect on bandgap openings in graphene nanostructures: a thermodynamic approach, Coord. Chem. Rev. 326 (2016) 1–33, https://doi.org/10.1016/j.ccr.2016.06.012.
- [38] A. Ghaffarkhah, E. Hosseini, M. Kamkar, A.A. Sehat, S. Dordanihaghighi, A. Allahbakhsh, C. van der Kuur, M. Arjmand, Synthesis, applications, and prospects of graphene quantum dots: a comprehensive review, Small 18 (2022), https://doi.org/10.1002/smll.202102683.
- [39] P.V. Ravi, V. Subramaniyam, N. Saravanakumar, A. Pattabiraman, M. Pichumani, What works and what doesn't when graphene quantum dots are functionalized for contemporary applications, Coord. Chem. Rev. 493 (2023) 215270, https://doi.org/10.1016/j.ccr.2023.215270.

- [40] Y. Lei, Y. Wang, P. Du, Y. Wu, C. Li, B. Du, L. Luo, Z. Sun, B. Zou, Preparation and photoelectric properties of nitrogen-doped graphene quantum dots modified SnO2 composites, Mater. Sci. Semicond. Process 141 (2022) 106416, https://doi. org/10.1016/j.mssp.2021.106416.
- [41] P.-C. Wu, J.-Y. Wang, W.-L. Wang, C.-Y. Chang, C.-H. Huang, K.-L. Yang, J.-C. Chang, C.-L.L. Hsu, S.-Y. Chen, T.-M. Chou, Efficient two-photon luminescence for cellular imaging using biocompatible nitrogen-doped graphene quantum dots conjugated with polymers, Nanoscale 10 (2018) 109–117.
- [42] F. Gao, C.L. Yang, G. Jiang, Effects of the coupling between electrode and GQD-anthoxanthin nanocomposites for dye-sensitized solar cell: DFT and TD-DFT investigations, J. Photochem. Photobio. A Chem. 407 (2021) 113080, https://doi.org/10.1016/j.jphotochem.2020.113080.
- [43] N.S. Mohamed Mustakim, C.A. Ubani, S. Sepeai, N. Ahmad Ludin, M.A. Mat Teridi, M.A. Ibrahim, Quantum dots processed by SILAR for solar cell applications, Sol. Energy 163 (2018) 256–270, https://doi.org/10.1016/j. solener.2018.02.003.
- [44] M. Mehrzad-Samarin, F. Faridbod, A.S. Dezfuli, M.R. Ganjali, A novel metronidazole fluorescent nanosensor based on graphene quantum dots embedded silica molecularly imprinted polymer, Biosens. Bioelectron. 92 (2017) 618-622
- [45] T. Balakrishnan, W.L. Ang, E. Mahmoudi, A.W. Mohammad, N.S. Sambudi, Formation mechanism and application potential of carbon dots synthesized from palm kernel shell via microwave assisted method, Carbon Resour. Convers. 5 (2022) 150–166, https://doi.org/10.1016/j.crcon.2022.01.003.
- [46] L. Yin, D. Zhang, W. Li, Y. Hu, L. Wang, J. Zhang, White light emitting diodes based on green graphene quantum dots and red graphene quantum dots, Mol. Cryst. Liq. Cryst. 6 (1) (2022), https://doi.org/10.1080/ 15/41466 (2021) 107(1976)
- [47] Z. Zeng, S. Chen, T.T.Y. Tan, F.X. Xiao, Graphene quantum dots (GQDs) and its derivatives for multifarious photocatalysis and photoelectrocatalysis, Catal. Today 315 (2018) 171–183, https://doi.org/10.1016/j.cattod.2018.01.005.
- [48] A. Salleh, M.B. Fauzi, The in vivo, in vitro and in ovo evaluation of quantum dots in wound healing: a review, Polymers 13 (2021) 191, https://doi.org/10.3390/ polym13020191.
- [49] M. Hassan, K. Dave, R. Chandrawati, F. Dehghani, V.G. Gomes, 3D printing of biopolymer nanocomposites for tissue engineering: nanomaterials, processing and structure-function relation, Eur. Polym. J. 121 (2019) 109340, https://doi. org/10.1016/j.eurpolymi.2019.109340.
- [50] N.F. Raduwan, N. Shaari, S.K. Kamarudin, M.S. Masdar, R.M. Yunus, An overview of nanomaterials in fuel cells: synthesis method and application, Int J. Hydrog. Energy 47 (2022) 18468–18495, https://doi.org/10.1016/j. iihydene.2022.03.035.
- [51] N. Shaari, S.K. Kamarudin, R. Bahru, Carbon and graphene quantum dots in fuel cell application: an overview, Int J. Energy Res 45 (2021) 1396–1424, https://doi.org/10.1002/er.5889.
- [52] S.H. Osman, S.K. Kamarudin, N.A. Karim, S. Basri, Application of graphene in <scp>low-temperature</scp> fuel cell technology: an overview, Int J. Energy Res 45 (2021) 18318–18336, https://doi.org/10.1002/er.6969.
- [53] J.N. Gavgani, A. Hasani, M. Nouri, M. Mahyari, A. Salehi, Highly sensitive and flexible ammonia sensor based on S and N co-doped graphene quantum dots/ polyaniline hybrid at room temperature, Sens Actuators B Chem. 229 (2016) 239–248, https://doi.org/10.1016/j.snb.2016.01.086.
- [54] B. Sun, Y. Wang, D. Li, W. Li, X. Gou, Y. Gou, F. Hu, Development of a sensitive electrochemical immunosensor using polyaniline functionalized graphene quantum dots for detecting a depression marker, Mater. Sci. Eng.: C. 111 (2020) 110797, https://doi.org/10.1016/j.msec.2020.110797.
- [55] C.M. Masemola, N. Moloto, Z.N. Tetana, S.S. Gqoba, P.K. Mubiayi, E.C. Linganiso, N-doped graphene quantum dot-modified polyaniline for room-temperature sensing of alcohol vapors, Mater. Chem. Phys. 287 (2022) 126229, https://doi. org/10.1016/j.matchemphys.2022.126229.
- [56] D. Zhang, Z. Wu, X. Zong, Metal-organic frameworks-derived zinc oxide nanopolyhedra/S, N: graphene quantum dots/polyaniline ternary nanohybrid for high-performance acetone sensing, Sens Actuators B Chem. 288 (2019) 232–242, https://doi.org/10.1016/j.snb.2019.02.093.
- [57] A. Shokry, M.M.A. Khalil, H. Ibrahim, M. Soliman, S. Ebrahim, Highly luminescent ternary nanocomposite of polyaniline, silver nanoparticles and graphene oxide quantum dots, Sci. Rep. 9 (2019) 16984, https://doi.org/ 10.1038/s41598-019-53584-6.
- [58] E. Punrat, C. Maksuk, S. Chuanuwatanakul, W. Wonsawat, O. Chailapakul, Polyaniline/graphene quantum dot-modified screen-printed carbon electrode for the rapid determination of Cr(VI) using stopped-flow analysis coupled with voltammetric technique, Talanta 150 (2016) 198–205, https://doi.org/10.1016/ j.talanta.2015.12.016.
- [59] S.-Z. Hong, Q.-Y. Huang, T.-M. Wu, The room temperature highly sensitive ammonia gas sensor based on polyaniline and nitrogen-doped graphene quantum dot-coated hollow indium oxide nanofiber composite, Polymers 13 (2021) 3676, https://doi.org/10.3390/polym13213676.
- [60] A. Shokry, M. Khalil, H. Ibrahim, M. Soliman, S. Ebrahim, Acute toxicity assessment of polyaniline/Ag nanoparticles/graphene oxide quantum dots on Cypridopsis vidua and Artemia salina, Sci. Rep. 11 (2021) 5336, https://doi.org. 10.1038/s41598-021-84903-5.
- [61] P. Nasr-Esfahani, A.A. Ensafi, B. Rezaei, Fabrication of a highly sensitive and selective modified electrode for imidacloprid determination based on designed nanocomposite graphene quantum dots/ionic liquid/multiwall carbon nanotubes/polyaniline, Sens Actuators B Chem. 296 (2019) 126682, https://doi. org/10.1016/j.snb.2019.126682.

- [62] S. Saisree, R. Aswathi, J.S. Arya Nair, K.Y. Sandhya, Radical sensitivity and selectivity in the electrochemical sensing of cadmium ions in water by polyaniline-derived nitrogen-doped graphene quantum dots, N. J. Chem. 45 (2021) 110–122, https://doi.org/10.1039/D0NJ03988H.
- [63] A. Ramachandran, A.N. J S, S. Karunakaran Yesodha, Polyaniline-derived nitrogen-doped graphene quantum dots for the ultratrace level electrochemical detection of trinitrophenol and the effective differentiation of nitroaromatics: structure matters, ACS Sustain Chem. Eng. 7 (2019) 6732–6743, https://doi.org/ 10.1021/acssuschemeng.8b05996.
- [64] M. Ahmadi-Kashani, H. Dehghani, A. Zarrabi, A biocompatible nanoplatform formed by MgAl-layered double hydroxide modified Mn3O4/N-graphene quantum dot conjugated-polyaniline for pH-triggered release of doxorubicin, Mater. Sci. Eng.: C. 114 (2020) 111055, https://doi.org/10.1016/j. msec.2020.111055.
- [65] Y.-H. Chang, C.-C. Chang, L.-Y. Chang, P.-C. Wang, P. Kanokpaka, M.-H. Yeh, Self-powered triboelectric sensor with N-doped graphene quantum dots decorated polyaniline layer for non-invasive glucose monitoring in human sweat, Nano Energy 112 (2023) 108505, https://doi.org/10.1016/j.nanoen.2023.108505.
- [66] A.B. Ganganboina, R.-A. Doong, Graphene quantum dots decorated gold-polyaniline nanowire for impedimetric detection of carcinoembryonic antigen, Sci. Rep. 9 (2019) 7214, https://doi.org/10.1038/s41598-019-43740-3.
- [67] K. Takemura, J. Satoh, J. Boonyakida, S. Park, A.D. Chowdhury, E.Y. Park, Electrochemical detection of white spot syndrome virus with a silicone rubber disposable electrode composed of graphene quantum dots and gold nanoparticleembedded polyaniline nanowires, J. Nanobiotechnol. 18 (2020) 152, https://doi. org/10.1186/s12951-020-00712-4.
- [68] P.-Z. Liu, X.-W. Hu, C.-J. Mao, H.-L. Niu, J.-M. Song, B.-K. Jin, S.-Y. Zhang, Electrochemiluminescence immunosensor based on graphene oxide nanosheets/ polyaniline nanowires/CdSe quantum dots nanocomposites for ultrasensitive determination of human interleukin-6, Electro Acta 113 (2013) 176–180, https:// doi.org/10.1016/j.electacta.2013.09.074.
- [69] M. Dinari, M.M. Momeni, M. Goudarzirad, Nanocomposite films of polyaniline/ graphene quantum dots and its supercapacitor properties, Surf. Eng. 32 (2016) 535–540, https://doi.org/10.1080/02670844.2015.1108047.
- [70] W. Liu, X. Yan, J. Chen, Y. Feng, Q. Xue, Novel and high-performance asymmetric micro-supercapacitors based on graphene quantum dots and polyaniline nanofibers, Nanoscale 5 (2013) 6053, https://doi.org/10.1039/c3nr01139a.
- [71] J. Breczko, B. Grzeskiewicz, E. Gradzka, D.M. Bobrowska, A. Basa, J. Goclon, K. Winkler, Synthesis of polyaniline nanotubes decorated with graphene quantum dots: structural & electrochemical studies, Electro Acta 388 (2021) 138614, https://doi.org/10.1016/j.electacta.2021.138614.
- [72] D. Arthisree, W. Madhuri, Optically active polymer nanocomposite composed of polyaniline, polyacrylonitrile and green-synthesized graphene quantum dot for supercapacitor application, Int J. Hydrog. Energy 45 (2020) 9317–9327, https:// doi.org/10.1016/j.ijhydene.2020.01.179.
- [73] S. Wang, K. Zhang, Q. Wang, Y. Fan, J. Shen, L. Li, L. Yang, W. Zhang, Graphene quantum dot-assisted preparation of water-borne reduced graphene oxide/polyaniline: from composite powder to layer-by-layer self-assembly film and performance enhancement, Electro Acta 295 (2019) 29–38, https://doi.org/10.1016/j.electra.018.10.135
- [74] S. Mondal, U. Rana, S. Malik, Graphene quantum dot-doped polyaniline nanofiber as high performance supercapacitor electrode materials, Chem. Commun. 51 (2015) 12365–12368, https://doi.org/10.1039/C5CC03981A.
- [75] G. Oskueyan, M.M. Lakouraj, M. Mahyari, Nitrogen and sulfur Co-doped graphene quantum dots decorated CeO2 nanoparticles/ polyaniline: as high efficient hybrid supercapacitor electrode materials, Electro Acta 299 (2019) 125–131, https://doi.org/10.1016/j.electacta.2018.12.179.
 [76] R. Xing, X. Gong, X. Zhuang, Y. Li, C. Bulin, X. Ge, B. Zhang, Synthesis and
- [76] R. Xing, X. Gong, X. Zhuang, Y. Li, C. Bulin, X. Ge, B. Zhang, Synthesis and improved electrochemical properties of nitrogen-doped graphene quantum dot–modified polyaniline, J. Nanopart. Res. 24 (2022) 32, https://doi.org/ 10.1007/s11051-022-05418-2.
- [77] H. Kuzhandaivel, S. Manickam, S.K. Balasingam, M.C. Franklin, H.-J. Kim, K. S. Nallathambi, Sulfur and nitrogen-doped graphene quantum dots/PANI nanocomposites for supercapacitors, N. J. Chem. 45 (2021) 4101–4110, https://doi.org/10.1039/D1N.100038A.
- [78] D. Arthisree, W. Madhuri, N. Saravanan, B. Dinesh, S. Saikrithika, A.S. Kumar, A ternary polymer nanocomposite film composed of green-synthesized graphene quantum dots, polyaniline, polyvinyl butyral and poly(3,4ethylenedioxythiophene) polystyrene sulfonate for supercapacitor application, J. Energy Storage 35 (2021) 102333, https://doi.org/10.1016/j. est.2021.102333.
- [79] M. Dinari, M.M. Momeni, M. Goudarzirad, Dye-sensitized solar cells based on nanocomposite of polyaniline/graphene quantum dots, J. Mater. Sci. 51 (2016) 2964–2971, https://doi.org/10.1007/s10853-015-9605-9.
- [80] N. Maity, A. Kuila, S. Das, D. Mandal, A. Shit, A.K. Nandi, Optoelectronic and photovoltaic properties of graphene quantum dot–polyaniline nanostructures, J. Mater. Chem. A Mater. 3 (2015) 20736–20748, https://doi.org/10.1039/ CETA-06-576C
- [81] C.M. Luk, B.L. Chen, K.S. Teng, L.B. Tang, S.P. Lau, Optically and electrically tunable graphene quantum dot–polyaniline composite films, J. Mater. Chem. C. 2 (2014) 4526–4532, https://doi.org/10.1039/C4TC00498A.
- [82] A.B. Siddique, K. Morrison, G. Venkat, A.K. Pramanick, N. Banerjee, M. Ray, Charge transport through functionalized graphene quantum dots embedded in a polyaniline matrix, ACS Appl. Electron Mater. 3 (2021) 1437–1446, https://doi. org/10.1021/acsaelm.1c00057.

- [83] D. Mombrú, M. Romero, R. Faccio, Á.W. Mombrú, Electronic structure of edgemodified graphene quantum dots interacting with polyaniline: vibrational and optical properties, J. Phys. Chem. C. 121 (2017) 16576–16583, https://doi.org/ 10.1021/acs.incc.7b03604
- [84] M. Jamdegni, A. Kaur, Electrochromic behavior of highly stable, flexible electrochromic electrode based on covalently bonded polyaniline-graphene quantum dot composite, J. Electrochem Soc. 166 (2019) H502–H509, https://doi. org/10.1149/2.0281912jes.
- [85] D. Mombrú, M. Romero, R. Faccio, Á.W. Mombrú, Tuning electrical transport mechanism of polyaniline–graphene oxide quantum dots nanocomposites for potential electronic device applications, J. Phys. Chem. C. 120 (2016) 25117–25123, https://doi.org/10.1021/acs.jpcc.6b08954.
- [86] B. Ramezanzadeh, B. Karimi, M. Ramezanzadeh, M. Rostami, Synthesis and characterization of polyaniline tailored graphene oxide quantum dot as an advance and highly crystalline carbon-based luminescent nanomaterial for fabrication of an effective anti-corrosion epoxy system on mild steel, J. Taiwan Inst. Chem. Eng. 95 (2019) 369–382, https://doi.org/10.1016/j. jtice.2018.07.041.
- [87] H.Y. Mohammed, M.A. Farea, P.W. Sayyad, N.N. Ingle, T. Al-Gahouari, M. M. Mahadik, G.A. Bodkhe, S.M. Shirsat, M.D. Shirsat, Selective and sensitive chemiresistive sensors based on polyaniline/graphene oxide nanocomposite: a cost-effective approach, J. Sci.: Adv. Mater. Devices 7 (2022) 100391, https://doi.org/10.1016/j.isamd.2021.08.004.
- [88] S. Hosseini, M. Norouzi, J. Xu, A sensitive strain sensor based on multi-walled carbon nanotubes/polyaniline/silicone rubber nanocomposite for human motion detection, Sci 5 (2023) 36, https://doi.org/10.3390/sci5030036.
- [89] K.S.M. Kumara, P. Shivakumar, V. Ganesh, S. Budagumpi, S.K. Bose, K. Hareesh, D.H. Nagaraju, Hydrogels of PANI doped with Fe3O4 and GO for highly stable sensor for sensitive and selective determination of heavy metal ions, Inorg. Chem. Commun. 158 (2023) 111553, https://doi.org/10.1016/j.inoche.2023.111553.
- [90] G. Sasikanth, B.V.R.S. Subramanyam, D. Maity, T.N. Narayanan, T. P. Radhakrishnan, Low conductivity polyaniline-gold nanocomposite via interfacial polymerization: efficient humidity sensing by thin films and mechanistic insights through in situ experiments, J. Phys. Chem. C. 127 (2023) 18107–18116, https://doi.org/10.1021/acs.jpcc.3c03866.
- [91] P. Adhav, D. Pawar, B. Diwate, M. Bora, S. Jagtap, A. Chourasia, S. Dallavalle, V. Chabukswar, Room temperature operable ultra-sensitive ammonia sensor based on polyaniline-silver (PANI-Ag) nanocomposites synthesized by ultrasonication, Synth. Met 293 (2023) 117237, https://doi.org/10.1016/j. synthmet.2022.117237.
- [92] N.M. Naim, H. Abdullah, A.A. Hamid, Influence of Ag and Pd contents on the properties of PANI–Ag–Pd nanocomposite thin films and its performance as electrochemical sensor for E. coli detection, Electron. Mater. Lett. 15 (2019) 70–79. https://doi.org/10.1007/s13391-018-0087-1.
- [93] Z. Xie, J. Wang, J.T.W. Yeow, Doped polyaniline/graphene composites for photothermoelectric detectors, ACS Appl. Nano Mater. 5 (2022) 7967–7973, https://doi.org/10.1021/acsanm.2c01039.
- [94] X. Li, X. Li, H. Li, Y. Zhao, J. Wu, S. Yan, Z. Yu, Reshapable MXene/graphene oxide/polyaniline plastic hybrids with patternable surfaces for highly efficient solar-driven water purification, Adv. Funct. Mater. 32 (2022), https://doi.org/ 10.1002/adfm.202110636
- [95] J. Wang, J. Feng, C. Wei, Molecularly imprinted polyaniline immobilized on Fe3O4/ZnO composite for selective degradation of amoxycillin under visible light irradiation, Appl. Surf. Sci. 609 (2023) 155324, https://doi.org/10.1016/j. appus 2023 155324
- [96] T.-H. Wang, C.-Y. Lin, Y.-C. Huang, C.-Y. Li, Facile electrosynthesis of polyaniline gold nanoparticle core-shell nanofiber for efficient electrocatalytic CO2 reduction, Electro Acta 437 (2023) 141500, https://doi.org/10.1016/j. electacta.2022.141500.
- [97] E.F. Aboelfetoh, E.A. Bakr, Synthesis of ternary nanocomposite of carbon nanotubes/silver ferrite/polyaniline for oxidative elimination of azo dyes, J. Mol. Struct. 1294 (2023) 136558, https://doi.org/10.1016/j.molstruc.2023.136558.
- [98] L. Ouyang, B. Qiu, Positive effects of magnetic Fe3O4@polyaniline on aerobic granular sludge: aerobic granulation, granule stability and pollutants removal performance, Bioresour. Technol. 368 (2023) 128296, https://doi.org/10.1016/j. biortech.2022.128296.
- [99] H. Zhang, L. Du, J. Xing, G. Wei, X. Quan, Electro-conductive crosslinked polyaniline/carbon nanotube nanofiltration membrane for electro-enhanced removal of bisphenol A, Front Environ. Sci. Eng. 17 (2023) 59, https://doi.org/ 10.1007/s11783.093.1659.3
- [100] J. Iqbal, M.O. Ansari, A. Numan, S. Wageh, A. Al-Ghamdi, M.G. Alam, P. Kumar, R. Jafer, S. Bashir, A.H. Rajpar, Hydrothermally assisted synthesis of porous polyaniline@carbon nanotubes—manganese dioxide ternary composite for potential application in supercapattery, Polymers 12 (2020) 2918, https://doi.org/10.3390/polym12122918.
- [101] J. Upadhyay, R. Borah, T.M. Das, J.M. Das, Flexible solid-state supercapacitor based on ternary nanocomposites of reduced graphene oxide and ruthenium oxide nanoparticles bridged by polyaniline nanofibers, J. Energy Storage 72 (2023) 108600, https://doi.org/10.1016/j.est.2023.108600.
- [102] G. Singh, Y. Kumar, S. Husain, Fabrication of high energy density symmetric polyaniline/functionalized multiwalled carbon nanotubes supercapacitor device with swift charge transport in different electrolytic mediums, J. Energy Storage 65 (2023) 107328, https://doi.org/10.1016/j.est.2023.107328.
- [103] V.S. Patil, S.S. Thoravat, S.S. Kundale, T.D. Dongale, P.S. Patil, S.A. Jadhav, Synthesis and testing of polyaniline grafted functional magnetite (Fe3O4) nanoparticles and rGO based nanocomposites for supercapacitor application,

- Chem. Phys. Lett. 814 (2023) 140334, https://doi.org/10.1016/j.cnlett 2023 140334
- [104] Y. Zhang, C.-G. Zhou, X. Yan, H.-L. Gao, K.-Z. Gao, Y. Cao, Synthesis of Nafion-reduced graphene oxide/polyaniline as novel positive electrode additives for high performance lead-acid batteries, Electro Acta 466 (2023) 143045, https://doi.org/10.1016/j.electacta.2023.143045.
- [105] X. Wang, J. Qin, Q. Hu, P. Das, P. Wen, S. Zheng, F. Zhou, L. Feng, Z. Wu, Multifunctional mesoporous polyaniline/graphene nanosheets for flexible planar integrated microsystem of zinc ion microbattery and gas sensor, Small 18 (2022), https://doi.org/10.1002/smll.202200678.
- [106] D. Guo, K. Jiang, H. Gan, Y. Ren, J. Long, Y. Li, B. Yin, Template-oriented polyaniline-supported palladium nanoclusters for reductive homocoupling of furfural derivatives, Angew. Chem. 135 (2023), https://doi.org/10.1002/ ange.202304662.
- [107] S. Dutt, R. Kumar, P.F. Siril, Green synthesis of a palladium-polyaniline nanocomposite for green Suzuki-Miyaura coupling reactions, RSC Adv. 5 (2015) 33786-33791, https://doi.org/10.1039/C5RA05007C.
- [108] B. Gu, S. He, W. Zhou, J. Kang, K. Cheng, Q. Zhang, Y. Wang, Polyaniline-supported iron catalyst for selective synthesis of lower olefins from syngas, J. Energy Chem. 26 (2017) 608–615, https://doi.org/10.1016/j.iechem.2017.04.009
- [109] Z. Li, S. Yang, Y. Song, H. Xu, Z. Wang, W. Wang, Z. Dang, Y. Zhao, In-situ modified titanium suboxides with polyaniline/graphene as anode to enhance biovoltage production of microbial fuel cell, Int J. Hydrog. Energy 44 (2019) 6862–6870, https://doi.org/10.1016/j.ijhydene.2018.12.106.
- [110] A.A. Yaqoob, A. Serrà, S.A. Bhawani, M.N.M. Ibrahim, A. Khan, H.S. Alorfi, A. M. Asiri, M.A. Hussein, I. Khan, K. Umar, Utilizing biomass-based graphene oxide-polyaniline-Ag electrodes in microbial fuel cells to boost energy generation and heavy metal removal, Polymers 14 (2022) 845, https://doi.org/10.3390/polym14040845.
- [111] X. Du, P. Li, Z. Guan, Y. Wen, Polyaniline/carbon nanotube-modified carbon felt for accelerating underwater microbial gas production to enhance power generation, ChemNanoMat 9 (2023), https://doi.org/10.1002/cnma.202200488.
- [112] N. Shakeel, R. Perveen, M. Imran Ahamed, A. Ahmad, Inamuddin, Cherry-like Pt@Fe3O4 decorated MWCNT/PANI nanohybrid based bioanode for glucose biofuel cell application, Fuel 341 (2023) 127579, https://doi.org/10.1016/j. fuel.2023.127579.
- [113] M. Waqas, L. Campbell, P. T. Polyaniline-coated surface-modified Ag/PANI nanostructures for antibacterial and colorimetric melamine sensing in milk samples, ACS Omega 8 (2023) 24010–24015, https://doi.org/10.1021/ programme 20/2077
- [114] H. Abdullah, S.M. Mustaza, S.K. Bejo, I. Yahya, N. Kamal, M.H.D. Othman, Identification of *Leptospira* in water by Fe-Pd-doped polyaniline nanocomposite thin film, 184798042110113, Nanomater. Nanotechnol. 11 (2021), https://doi. org/10.1177/18479804211011389.
- [115] S.M. Sheta, S.M. El-Sheikh, D.I. Osman, A.M. Salem, O.I. Ali, F.A. Harraz, W. G. Shousha, M.A. Shoeib, S.M. Shawky, D.D. Dionysiou, A novel HCV electrochemical biosensor based on a polyaniline@Ni-MOF nanocomposite, Dalton Trans. 49 (2020) 8918–8926, https://doi.org/10.1039/D0DT01408G.
- [116] A.S. Najibzad, R. Amini, M. Rostami, P. Kardar, M. Fedel, Active corrosion performance of magnesium by silane coatings reinforced with polyaniline/ praseodymium, Prog. Org. Coat. 140 (2020) 105504, https://doi.org/10.1016/j. porgroat 2019 105504
- [117] Y. Cai, T. Liu, L. Cheng, S. Guo, S. Huang, Z. Hu, Y. Wang, H. Yu, D. Chen, Mechanical and electrochemical properties of carbon nanotubule-polyaniline nanowire/polyaniline nanoparticle high-strength ultra-flexible aerogel buckypaper, Colloids Surf. A Physicochem Eng. Asp. 682 (2024) 132868, https:// doi.org/10.1016/i.colsurfa.2023.132868.
- [118] M. Mohammadi, S.A. Kahani, Conductive nano-Al/polyaniline composites prepared via mechanical milling, Mater. Chem. Phys. 316 (2024) 129086, https://doi.org/10.1016/j.matchemphys.2024.129086
- https://doi.org/10.1016/j.matchemphys.2024.129086.

 [119] A.-H.A. Shah, M. Kamran, S. Bilal, R. Ullah, Cost effective chemical oxidative synthesis of soluble and electroactive polyaniline salt and its application as anticorrosive agent for steel, Materials 12 (2019) 1527, https://doi.org/10.3390/mai.2091527
- [120] D. Lan, Y. Wang, Y. Wang, X. Zhu, H. Li, X. Guo, J. Ren, Z. Guo, G. Wu, Impact mechanisms of aggregation state regulation strategies on the microwave absorption properties of flexible polyaniline, J. Colloid Interface Sci. 651 (2023) 494–503, https://doi.org/10.1016/ji.jcis.2023.08.019.
- [121] Z.M. Ali, M.N. Murshed, M.E. El Sayed, A. Samir, R.M. Alsharabi, M.O. Farea, A new fabrication strategy of Ag2O doped PANI as a highly stable and room temperature operable carbon monoxide gas sensor, Opt. Mater. 144 (2023) 114324, https://doi.org/10.1016/j.optmat.2023.114324.
- [122] Y. Xu, X. Liang, X. Shen, W. Yu, X. Yang, Q. Li, X. Ge, L. Wu, T. Xu, In situ construction of ultra-thin PANI/CeOx layer on proton exchange membrane for enhanced oxidation resistance in PEMFC, J. Memb. Sci. 689 (2024) 122167, https://doi.org/10.1016/j.memsci.2023.122167.
- [123] M. Yang, J. Liu, C. Hu, W. Zhang, J. Jiao, N. Cui, L. Gu, Highly sensitive self-powered ammonia gas detection enabled by a rationally designed PANI/commercial cellulosic paper based triboelectric nanogenerator, J. Mater. Chem. A Mater. 11 (2023) 21937–21947, https://doi.org/10.1039/D3TA04974D.
- [124] B. Sun, J. Zhang, W. Ge, F. Tian, C. Zhao, H. Suo, D. Liu, High performance self-supported nickel oxalate/polyaniline electrode: a novel high sensitivity electrochemical ammonia sensor, J. Mater. Sci.: Mater. Electron. 34 (2023) 202, https://doi.org/10.1007/s10854-022-09527-5.

- [125] F.F.F. Garrudo, L.F.V. Ferreira, A.M. Ferraria, A.M.B. do Rego, A. Charas, V. André, M.T. Duarte, R.J. Linhardt, F.C. Ferreira, J. Morgado, Pseudo-doping effect on structural and electrical properties of polyaniline-camphorsulfonic acid, Synth. Met 301 (2024) 117523, https://doi.org/10.1016/j. synthmet.2023.117523.
- [126] C. Wang, Y. Liao, H.-Y. Yu, Y. Dong, J. Yao, Homogeneous wet-spinning construction of skin-core structured PANI/cellulose conductive fibers for gas sensing and e-textile applications, Carbohydr. Polym. 319 (2023) 121175, https://doi.org/10.1016/j.carbpol.2023.121175.
- [127] A. Samadi, Z. Wang, S. Wang, S.K. Nataraj, L. Kong, S. Zhao, Polyaniline-based adsorbents for water treatment: roles of low-cost materials and 2D materials, Chem. Eng. J. 478 (2023) 147506, https://doi.org/10.1016/j.cej.2023.147506.
- [128] A. Khattari, J. Bensalah, A. Habsaoui, Z. Safi, N. Wazzan, A. Berisha, A. Hsini, M. Tahaikt, A. Elmidaoui, Use of a novel low-cost adsorbent PANI@Clay composite to effectively remove OG dye from wastewater: insights from isotherm kinetic and thermodynamic modeling, investigation using density functional theory DFT/MC/MID, Mater. Sci. Eng.: B 302 (2024) 117201, https://doi.org/10.1016/j.mseb.2024.117201.
- [129] M. Beygisangchin, A. Hossein Baghdadi, S. Kartom Kamarudin, S. Abdul Rashid, J. Jakmunee, N. Shaari, Recent progress in polyaniline and its composites; synthesis, properties, and applications, Eur. Polym. J. (2024) 112948, https://doi. org/10.1016/j.eurpolymj.2024.112948.
- [130] A.G. MacDiarmid, Polyaniline and polypyrrole: where are we headed, Synth. Met 84 (1997) 27–34, https://doi.org/10.1016/S0379-6779(97)80658-3.
- [131] H. Wang, H. Wen, B. Hu, G. Fei, Y. Shen, L. Sun, D. Yang, Facile approach to fabricate waterborne polyaniline nanocomposites with environmental benignity and high physical properties, Sci. Rep. 7 (2017) 43694, https://doi.org/10.1038/ srep43694.
- [132] S. Sinha, S. Bhadra, D. Khastgir, Effect of dopant type on the properties of polyaniline, J. Appl. Polym. Sci. 112 (2009) 3135–3140, https://doi.org/ 10.1002/app.29708.
- [133] M.V. Kulkarni, A.K. Viswanath, R. Marimuthu, T. Seth, Synthesis and characterization of polyaniline doped with organic acids, J. Polym. Sci. A Polym. Chem. 42 (2004) 2043–2049, https://doi.org/10.1002/pola.11030.
- [134] D.W. Hatchett, M. Josowicz, J. Janata, Acid doping of polyaniline: spectroscopic and electrochemical studies, J. Phys. Chem. B 103 (1999) 10992–10998, https:// doi.org/10.1021/jp991110z.
- [135] M. Fayzan, A. Nawaz, R. Khan, S. Javed, A. Tariq, M. Azeem, A. Riaz, A. Shafqat, H.M. Cheema, M. Afrab, I. Ahmad, R. Jan, Results in physics EMI shielding properties of polymer blends with inclusion of graphene nano platelets, Results Phys. 14 (2019) 102365, https://doi.org/10.1016/j.rinp.2019.102365.
- [136] N. Gospodinova, L. Terlemezyan, Conducting polymers prepared by oxidative polymerization: polyaniline, Prog. Polym. Sci. 23 (1998) 1443–1484, https://doi. org/10.1016/S0079-6700(98)00008-2.
- [137] N.Y. Elamin, A. Modwi, W. Abd El-Fattah, A. Rajeh, Synthesis and structural of Fe3O4 magnetic nanoparticles and its effect on the structural optical, and magnetic properties of novel Poly(methyl methacrylate)/ Polyaniline composite for electromagnetic and optical applications, Opt. Mater. 135 (2023) 113323, https://doi.org/10.1016/j.optmat.2022.113323.
 [138] W. Hai, C. Chen, Q. Yu, M. Li, Z. Jiang, H. Shao, G. Shao, J. Jiang, N. Chen, S. Bi,
- [138] W. Hai, C. Chen, Q. Yu, M. Li, Z. Jiang, H. Shao, G. Shao, J. Jiang, N. Chen, S. Bi, Sandwich structure electromagnetic interference shielding composites based on Fe3O4 nanoparticles/PANI/laser-induced graphene with near-zero electromagnetic waves transmission, Appl. Surf. Sci. 637 (2023) 157975, https:// doi.org/10.1016/j.apsusc.2023.157975.
- [139] M.Z. Khan, I.H. Gul, M.M. Baig, M.A. Akram, Facile synthesis of a multifunctional ternary SnO2/MWCNTs/PANI nanocomposite: detailed analysis of dielectric, electrochemical, and water splitting applications, Electro Acta 441 (2023) 141816. https://doi.org/10.1016/j.electacta.2023.141816.
- [140] L.F. Calheiros Souto, B.G. Soares, Electromagnetic wave absorption, EMI shielding effectiveness and electrical properties of ethylene vinyl Acetate (EVA)/ Polyaniline (PAni) blends prepared by in situ polymerization, Synth. Met 298 (2023) 117441, https://doi.org/10.1016/j.synthmet.2023.117441.
- [141] A.M. El-naggar, A. Alsaggaf, Z.K. Heiba, A.M. Kamal, A.M. Aldhafiri, A. Fatehmulla, M.B. Mohamed, Exploring the structural, optical and electrical characteristics of PVA/PANi blends, Opt. Mater. 139 (2023) 113771, https://doi. org/10.1016/j.optmat.2023.113771.
- [142] N. Kumari Jangid, S. Jadoun, N. Kaur, RETRACTED: a review on high-throughput synthesis, deposition of thin films and properties of polyaniline, Eur. Polym. J. 125 (2020) 109485, https://doi.org/10.1016/j.eurpolymj.2020.109485.
- [143] N. Ahmad, D. Bano, S. Jabeen, N. Ahmad, A. Iqbal, Waris, A.H. Anwer, C. Jeong, Insight into the adsorption thermodynamics, kinetics, and photocatalytic studies of polyaniline/SnS2 nanocomposite for dye removal, J. Hazard. Mater. Adv. 10 (2023) 100321, https://doi.org/10.1016/j.hazadv.2023.100321.
- [144] Y. Rong, W. Yan, Z. Wang, X. Hao, G. Guan, Rapid and selective removal of Pb ions by electroactive titanium Dioxide/Polyaniline ion exchange film, Sep Purif. Technol. 312 (2023) 123386, https://doi.org/10.1016/j.seppur.2023.123386.
- [145] Y. Ren, B. Yan, C. Lin, P. Wang, M. Zhou, L. Cui, Y. Yu, Q. Wang, Multifunctional textile constructed via polyaniline-mediated copper sulfide nanoparticle growth for rapid photothermal antibacterial and antioxidation applications, ACS Appl. Nano Mater. 6 (2023) 1212–1223, https://doi.org/10.1021/acsanm.2c04797.
- [146] C. Chen, B. Wang, G. Xiao, F. Zhong, J. Zhou, M. Cao, Z. Yang, C. Chen, R. Zou, Flower-like Ni-Al/LDH synergistic polyaniline anchored to the carbon sphere surface to improve the fire performance of waterborne epoxy coatings, Prog. Org. Coat. 186 (2024) 108068, https://doi.org/10.1016/j.porgcoat.2023.108068.

- [147] H. Fu, B. Gao, Y. Qiao, W. Zhu, Z. Liu, G. Wei, Z. Feng, A.R. Kamali, Graphene nanonetwork embedded with polyaniline nanoparticles as anode of Li-ion battery, Chem. Eng. J. 477 (2023) 146936, https://doi.org/10.1016/j.cej.2023.146936.
- [148] J. Liang, A. Rawal, M. Yu, K. Xiao, H. Liu, Y. Jiang, A. Lennon, D.-W. Wang, Low-potential solid-solid interfacial charging on layered polyaniline anode for high voltage pseudocapacitive intercalation Li-ion supercapacitors, Nano Energy 105 (2023) 108010, https://doi.org/10.1016/j.nanoen.2022.108010.
- [149] P. Kulshrestha, B. Kyoung Shin, S. Falak, D. Sung Huh, Bio-inspired hierarchical structure of polyaniline in the pore surface of polymer film through interfacial polymerization as a smart material sensitive to pH, Eur. Polym. J. 187 (2023) 111893, https://doi.org/10.1016/j.eurpolymj.2023.111893.
- [150] B. Hazmi, M. Beygisangchin, U. Rashid, W.N.A.W. Mokhtar, T. Tsubota, A. Alsalme, C. Ngamcharussrivichai, Glycerol-based retrievable heterogeneous catalysts for single-pot esterification of palm fatty acid distillate to biodiesel, Molecules 27 (2022) 7142, https://doi.org/10.3390/molecules27207142.
- [151] F. Fenniche, Y. Khane, A. Henni, D. Aouf, D. Elhak Djafri, Synthesis and characterization of PANI nanofibers high-performance thin films via electrochemical methods, Results Chem. 4 (2022) 100596, https://doi.org/ 10.1016/i.rechem.2022.100596.
- [152] H.A. Al-Aoh, N. Badi, A.S. Roy, A.M. Alsharari, S. Abd El Wanees, A. Albaqami, A. Ignatiev, Preparation of anionic surfactant-based one-dimensional nanostructured polyaniline fibers for hydrogen storage applications, Polymers 15 (2023) 1658, https://doi.org/10.3390/polym15071658.
- [153] Z.S. Ali, A.M. Shano, The influence of solvents on polyaniline nanofibers synthesized by a hydrothermal method and their application in gas sensors, J. Electron Mater. 49 (2020) 5528–5533, https://doi.org/10.1007/s11664-020-08277-6.
- [154] N.A. Miraqyan, R.S. Durgaryan, N.A. Durgaryan, Synthesis and investigation of methyl and methoxy groups containing polyaniline derivatives in organic medium, Polym. Bull. (2024), https://doi.org/10.1007/s00289-023-05100-0.
- [155] L. Li, G. Wu, G. Yang, J. Peng, J. Zhao, J.-J. Zhu, Focusing on luminescent graphene quantum dots: current status and future perspectives, Nanoscale 5 (2013) 4015–4039, https://doi.org/10.1039/C3NR33849E.
- [156] H. Sun, L. Wu, W. Wei, X. Qu, Recent advances in graphene quantum dots for sensing, Mater. Today 16 (2013) 433–442, https://doi.org/10.1016/j. mattod.2013.10.020.
- [157] C.M. Luk, L.B. Tang, W.F. Zhang, S.F. Yu, K.S. Teng, S.P. Lau, An efficient and stable fluorescent graphene quantum dot-agar composite as a converting material in white light emitting diodes, J. Mater. Chem. 22 (2012) 22378–22381, https:// doi.org/10.1039/c2jm35305a.
- [158] A.R. Sadrolhosseini, M. Beygisangchin, S. Shafie, S.A. Rashid, H. Nezakati, Laser ablated titanium oxide nanoparticles in carbon quantum dots solution for detection of sugar using fluorescence spectroscopy, Mater. Res Express 8 (2021) 105003, https://doi.org/10.1088/2053-1591/abdf0f.
- [159] A.R. Sadrolhosseini, G. Krishnan, S. Safie, M. Beygisangchin, S.A. Rashid, S. W. Harun, Enhancement of the fluorescence property of carbon quantum dots based on laser ablated gold nanoparticles to evaluate pyrene, Opt. Mater. Express 10 (2020) 2227, https://doi.org/10.1364/OME.396914.
- [160] S.H. Song, M.H. Jang, J. Chung, S.H. Jin, B.H. Kim, S.H. Hur, S. Yoo, Y.H. Cho, S. Jeon, Highly efficient light-emitting diode of graphene quantum dots fabricated from graphite intercalation compounds, Adv. Opt. Mater. 2 (2014) 1016–1023, https://doi.org/10.1002/adom.201400184.
- [161] Y. Ji, J. Hu, J. Biskupek, U. Kaiser, Y. Song, C. Streb, Polyoxometalate-based bottom-up fabrication of graphene quantum dot/manganese vanadate composites as lithium ion battery anodes, Chem. –A Eur. J. 23 (2017) 16637–16643.
- [162] J. Dong, K. Wang, L. Sun, B. Sun, M. Yang, H. Chen, Y. Wang, J. Sun, L. Dong, Application of graphene quantum dots for simultaneous fluorescence imaging and tumor-targeted drug delivery, Sens Actuators B Chem. 256 (2018) 616–623, https://doi.org/10.1016/j.snb.2017.09.200.
- [163] C. Shen, S. Ge, Y. Pang, F. Xi, J. Liu, X. Dong, P. Chen, Facile and scalable preparation of highly luminescent N,S co-doped graphene quantum dots and their application for parallel detection of multiple metal ions, J. Mater. Chem. B 5 (2017) 6593–6600, https://doi.org/10.1039/C7TB00506G.
- [164] R. Suryawanshi, R. Kurrey, S. Sahu, K.K. Ghosh, Facile and scalable synthesis of un-doped, doped and co-doped graphene quantum dots: a comparative study on their impact for environmental applications, RSC Adv. 13 (2023) 701–719, https://doi.org/10.1039/D2RA05275J.
- [165] V. Dananjaya, S. Marimuthu, R. (Chunhui Yang, A.N. Grace, C. Abeykoon, Synthesis, properties, applications, 3D printing and machine learning of graphene quantum dots in polymer nanocomposites, Prog. Mater. Sci. 144 (2024) 101282, https://doi.org/10.1016/j.pmatsci.2024.101282.
- [166] F. Yan, Y. Jiang, X. Sun, Z. Bai, Y. Zhang, X. Zhou, Surface modification and chemical functionalization of carbon dots: a review, Microchim. Acta 185 (2018) 424. https://doi.org/10.1007/s00604-018-2953-9.
- [167] B. Geng, F. Fang, P. Li, S. Xu, D. Pan, Y. Zhang, L. Shen, Surface charge-dependent osteogenic behaviors of edge-functionalized graphene quantum dots, Chem. Eng. J. 417 (2021) 128125, https://doi.org/10.1016/j.cej.2020.128125.
- [168] S. Yang, J. Sun, P. He, X. Deng, Z. Wang, C. Hu, G. Ding, X. Xie, Selenium doped graphene quantum dots as an ultrasensitive redox fluorescent switch, Chem. Mater. 27 (2015) 2004–2011, https://doi.org/10.1021/acs.chemmater.5b00112.
- [169] T. Gao, X. Wang, J. Zhao, P. Jiang, F.-L. Jiang, Y. Liu, Bridge between temperature and light: bottom-up synthetic route to structure-defined graphene quantum dots as a temperature probe in vitro and in cells, ACS Appl. Mater. Interfaces 12 (2020) 22002–22011, https://doi.org/10.1021/acsami.0c02500.
- [170] T. Gao, X. Wang, L.-Y. Yang, H. He, X.-X. Ba, J. Zhao, F.-L. Jiang, Y. Liu, Red, Yellow, and blue luminescence by graphene quantum dots: syntheses,

- mechanism, and cellular imaging, ACS Appl. Mater. Interfaces 9 (2017) 24846–24856, https://doi.org/10.1021/acsami.7b05569.
- [171] N.A.A. Anas, Y.W. Fen, N.A.S. Omar, W.M.E.M.M. Daniyal, N.S.M. Ramdzan, S. Saleviter, Development of graphene quantum dots-based optical sensor for toxic metal ion detection, Sensors 19 (2019) 3850, https://doi.org/10.3390/ s19183850
- [172] F. Anjila P.K, G.R. Tharani, A. Sundaramoorthy, V. Kumar Shanmugam, K. Subramani, S. Chinnathambi, G.N. Pandian, V. Raghavan, A.N. Grace, S. Ganesan, M. Rajendiran, An ultra-sensitive detection of melamine in milk using rare-earth doped graphene quantum dots- synthesis and optical spectroscopic approach, Microchem. J. 196 (2024) 109670, https://doi.org/10.1016/j. microc.2023.109670.
- [173] T. Balakrishnan, W.L. Ang, E. Mahmoudi, Highly sensitive fluorescent nitrobenzene gas sensing by nitrogen-doped graphene quantum dots embedded in ZIF-8 nanocomposite, Mater. Sci. Eng.: B 304 (2024) 117377, https://doi.org/ 10.1016/j.mseb.2024.117377.
- [174] A. Abbas, Q. Liang, S. Abbas, M. Liaqat, S. Rubab, T.A. Tabish, Eco-Friendly Sustainable Synthesis of Graphene Quantum Dots from Biowaste as a Highly Selective Sensor, Nanomaterials 12 (2022) 3696, https://doi.org/10.3390/ page 12/203696
- [175] A. Halder, M. Godoy-Gallardo, J. Ashley, X. Feng, T. Zhou, L. Hosta-Rigau, Y. Sun, One-pot green synthesis of biocompatible graphene quantum dots and their cell uptake studies, ACS Appl. Bio Mater. 1 (2018) 452–461, https://doi.org/ 10.1021/acsahm.8b00170.
- [176] A. Abbas, T.A. Tabish, S.J. Bull, T.M. Lim, A.N. Phan, High yield synthesis of graphene quantum dots from biomass waste as a highly selective probe for Fe3+ sensing, Sci. Rep. 10 (2020) 21262, https://doi.org/10.1038/s41598-020-78070-
- [177] A. Abbas, S. Rubab, A. Rehman, S. Irfan, H.M.A. Sharif, Q. Liang, T.A. Tabish, One-step green synthesis of biomass-derived graphene quantum dots as a highly selective optical sensing probe, Mater. Today Chem. 30 (2023) 101555, https:// doi.org/10.1016/j.mtchem.2023.101555.
- [178] A. Lakshmi-Narayana, N. Attarzadeh, V. Shutthanandan, C.V. Ramana, High-performance NiCo 2 O 4 /graphene quantum dots for asymmetric and symmetric supercapacitors with enhanced energy efficiency, Adv. Funct. Mater. (2024), https://doi.org/10.1002/adfm.202316379.
- [179] J. Zhang, J. Yu, H. Yin, Z. Jia, C. Shi, Y. Yue, An ammonia-sensitive fluorescence sensor based on polyvinyl alcohol-graphene quantum dots/halloysite nanotubes hybrid film for monitoring fish freshness, Food Chem. 454 (2024) 139734, https://doi.org/10.1016/j.foodchem.2024.139734.
- [180] R. Carbajal-Valdez, J.L. Jiménez-Pérez, A. Cruz-Orea, J.F. Sánchez-Ramírez, M. A. Algatti, Thermo-optic characterization of graphene oxide quantum dot semiconductors for the determination of quantum efficiency, J. Mater. Sci.: Mater. Electron. 35 (2024) 848, https://doi.org/10.1007/s10854-024-12594-5.
- [181] X.-J. Jin, L. Tan, Z.-Q. Zhao, M.-C. Li, Q.-Y. Zhou, J.-J. Zhang, T.-B. Lv, Q. Deng, J. Wang, Z. Zeng, S. Deng, G.-P. Dai, Facile synthesis of graphene quantum dots with red emission and high quantum yield, N. J. Chem. 47 (2023) 2221–2229, https://doi.org/10.1039/D2NJ04491A.
- [182] D.S. Bajwa, S. Chanda, C. Ryan, S.G. Bajwa, N. Stark, K. Matteson, Graphene quantum dots/cellulose nanocrystal inclusion complex for enhancing the physical and thermal properties of HDPE polymer matrix, Carbohydr. Polym. Technol. Appl. 7 (2024) 100450, https://doi.org/10.1016/j.carpta.2024.100450.
- [183] T. Das, S. Das, B.C. A, Fabrication of a label-free immunosensor using surface-engineered AuPt@GQD core-shell nanocomposite for the selective detection of trace levels of *Escherichia coli* from contaminated food samples, ACS Biomater. Sci. Eng. (2024). https://doi.org/10.1021/acsbiomaterials.4c00297.
- Sci. Eng. (2024), https://doi.org/10.1021/acsbiomaterials.4c00297.
 [184] J. Feng, Q. Guo, H. Liu, D. Chen, Z. Tian, F. Xia, S. Ma, L. Yu, L. Dong, Theoretical insights into tunable optical and electronic properties of graphene quantum dots through phosphorization, Carbon N. Y 155 (2019) 491–498, https://doi.org/10.1016/j.carbon.2019.09.009
- [185] F. Ullah, R. Bashiri, N. Muti Mohamed, A. Zaleska-Medynska, C.F. Kait, U. Ghani, M.U. Shahid, M.S.M. Saheed, Exploring graphene quantum dots@TiO2 rutile (0 1 1) interface for visible-driven hydrogen production in photoelectrochemical cell: density functional theory and experimental study, Appl. Surf. Sci. 576 (2022) 151871, https://doi.org/10.1016/j.apsusc.2021.151871
- [186] V. Sharma, B. Roondhe, S. Saxena, A. Shukla, Role of functionalized graphene quantum dots in hydrogen evolution reaction: a density functional theory study, Int J. Hydrog. Energy 47 (2022) 41748–41758, https://doi.org/10.1016/j. iihydene.2022.02.161.
- [187] X. Yan, X. Cui, B. Li, L.S. Li, Large, solution-processable graphene quantum dots as light absorbers for photovoltaics, Nano Lett. 10 (2010) 1869–1873, https://doi. org/10.1021/nl101060h.
- [188] C. Hu, T.-R. Su, T.-J. Lin, C.-W. Chang, K.-L. Tung, Yellowish and blue luminescent graphene oxide quantum dots prepared via a microwave-assisted hydrothermal route using H 2 O 2 and KMnO 4 as oxidizing agents, N. J. Chem. 42 (2018) 3999–4007, https://doi.org/10.1039/C7NJ03337K.
- [189] J. Lu, P.S.E. Yeo, C.K. Gan, P. Wu, K.P. Loh, Transforming C 60 molecules into graphene quantum dots, Nat. Nanotechnol. 6 (2011) 247–252, https://doi.org/ 10.1038/nnano.2011.30.
- [190] A. Allahbakhsh, A.R. Bahramian, Self-assembly of graphene quantum dots into hydrogels and cryogels: dynamic light scattering, UV–Vis spectroscopy and structural investigations, J. Mol. Liq. 265 (2018) 172–180.
- [191] S. Kim, S.W. Hwang, M.K. Kim, D.Y. Shin, D.H. Shin, C.O. Kim, S.B. Yang, J. H. Park, E. Hwang, S.H. Choi, G. Ko, S. Sim, C. Sone, H.J. Choi, S. Bae, B.H. Hong, Anomalous behaviors of visible luminescence from graphene quantum dots:

- interplay between size and shape, ACS Nano 6 (2012) 8203–8208, https://doi.org/10.1021/mp302978r
- [192] L.A. Ponomarenko, F. Schedin, M.I. Katsnelson, R. Yang, E.W. Hill, K. S. Novoselov, A.K. Geim, Chaotic dirac billiard in graphene quantum dots, Science 320 (1979) (2008) 356–358, https://doi.org/10.1126/science.1154663.
- J. Peng, W. Gao, B.K. Gupta, Z. Liu, R. Romero-Aburto, L. Ge, L. Song, L.
 B. Alemany, X. Zhan, G. Gao, S.A. Vithayathil, B.A. Kaipparettu, A.A. Marti,
 T. Hayashi, J.J. Zhu, P.M. Ajayan, Graphene quantum dots derived from carbon fibers, Nano Lett. 12 (2012) 844–849, https://doi.org/10.1021/nl2038979.
- [194] X. Zhou, Y. Zhang, C. Wang, X. Wu, Y. Yang, B. Zheng, H. Wu, S. Guo, J. Zhang, https://doi.org/10.1021/nn301629v, ACS Nano 6 (2012) 6592–6599, https://doi.org/10.1021/nn301629v.
- [195] T. Gokus, R.R. Nair, A. Bonetti, M. Böhmler, A. Lombardo, K.S. Novoselov, A. K. Geim, A.C. Ferrari, A. Hartschuh, Making graphene luminescent by oxygen plasma treatment, ACS Nano 3 (2009) 3963–3968, https://doi.org/10.1021/pn9012753
- [196] N. Li, F. Zhang, H. Wang, S. Hou, Catalytic degradation of 4-nitrophenol in polluted water by three-dimensional gold nanoparticles/reduced graphene oxide microspheres, Eng. Sci. (2019), https://doi.org/10.30919/es8d509.
- [197] J.-S. Yang, D.Z. Pai, W.-H. Chiang, Microplasma-enhanced synthesis of colloidal graphene quantum dots at ambient conditions, Carbon N. Y 153 (2019) 315–319.
- [198] F. Liu, M.-H. Jang, H.D. Ha, J.-H. Kim, Y.-H. Cho, T.S. Seo, Graphene quantum dots: facile synthetic method for pristine graphene quantum dots and graphene oxide quantum dots: origin of blue and green luminescence (Adv. Mater. 27/ 2013), 3748–3748, Adv. Mater. 25 (2013), https://doi.org/10.1002/ adma.201370175.
- [199] J. He, Z. Li, R. Zhao, Y. Lu, L. Shi, J. Liu, X. Dong, F. Xi, Aqueous synthesis of amphiphilic graphene quantum dots and their application as surfactants for preparing of fluorescent polymer microspheres, Colloids Surf. A Physicochem Eng. Asp. 563 (2019) 77–83.
- [200] A. Shukla, P. Dhanasekaran, N. Nagaraju, S.D. Bhat, V.K. Pillai, A facile synthesis of graphene nanoribbon-quantum dot hybrids and their application for composite electrolyte membrane in direct methanol fuel cells, Electro Acta 297 (2019) 267–280.
- [201] H. Kalita, V.S. Palaparthy, M.S. Baghini, M. Aslam, Electrochemical synthesis of graphene quantum dots from graphene oxide at room temperature and its soil moisture sensing properties, Carbon N. Y 165 (2020) 9–17.
- [202] M.J. Deka, D. Chowdhury, CVD assisted hydrophobic graphene quantum dots: fluorescence sensor for aromatic amino acids, ChemistrySelect 2 (2017) 1999–2005, https://doi.org/10.1002/slct.201601737.
- [203] R.L. Calabro, D.-S. Yang, D.Y. Kim, Liquid-phase laser ablation synthesis of graphene quantum dots from carbon nano-onions: comparison with chemical oxidation, J. Colloid Interface Sci. 527 (2018) 132–140.
- [204] S. Zhuo, M. Shao, S. Lee, upconversion GQD_tio2_ACSnano 2012.pdf, (2012) 1059–1064.
- [205] P. Rani, R. Dalal, S. Srivastava, Effect of surface modification on optical and electronic properties of graphene quantum dots, Appl. Surf. Sci. 609 (2023) 155379, https://doi.org/10.1016/j.apsusc.2022.155379.
- [206] F. Barati, M. Avatefi, N.B. Moghadam, S. Asghari, E. Ekrami, M. Mahmoudifard, A review of graphene quantum dots and their potential biomedical applications, J. Biomater. Appl. 37 (2023) 1137–1158, https://doi.org/10.1177/ 2025/2020/2011/57811
- [207] K. Niveria, P. Singh, M. Yadav, A.K. VermaQuantum Dot (QD)-Induced Toxicity and Biocompatibility Cham, Springer International Publishing, Handbook of II-VI Semiconductor-Based Sensors and Radiation Detectors, 2023, , 181–211, 10.1007/978-3-031-19531-0_8.
- [208] M.H. Karami, M. Abdouss, A. Rahdar, S. Pandey, Graphene quantum dots: Background, synthesis methods, and applications as nanocarrier in drug delivery and cancer treatment: an updated review, Inorg. Chem. Commun. 161 (2024) 112032, https://doi.org/10.1016/j.inoche.2024.112032.
- [209] S. Setianto, C. Panatarani, D. Singh, I.M. Joni, Semi-empirical infrared spectra simulation of pyrene-like molecules insight for simple analysis of functionalization graphene quantum dots, Sci. Rep. 13 (2023) 2282, https://doi. org/10.1038/s41598-023-29486-z.
- [210] H. Cho, G. Bae, B.H. Hong, Engineering functionalization and properties of graphene quantum dots (GQDs) with controllable synthesis for energy and display applications, Nanoscale (2024), https://doi.org/10.1039/D3NR05842E.
- [211] Q. Wang, P. Xu, D. Lv, Y. Xu, J. Zhang, T. Liu, W. Yang, P. Ma, A novel strategy for the preparation of multifunctional and robust polyhydroxyalkanoates/GQDs nanocomposites with UV-resistance, pH-responsive and antibacterial properties, Chem. Eng. J. 477 (2023) 147106, https://doi.org/10.1016/j.cej.2023.147106.
- [212] H. Shabbir, M. Wojnicki, Recent progress of non-cadmium and organic quantum dots for optoelectronic applications with a focus on photodetector devices, Electronics 12 (2023) 1327, https://doi.org/10.3390/electronics12061327.
- [213] N. Nesakumar, S. Srinivasan, S. Alwarappan, Graphene quantum dots: synthesis, properties, and applications to the development of optical and electrochemical sensors for chemical sensing, Microchim. Acta 189 (2022) 258, https://doi.org/10.1007/c00604.022.05253.
- [214] R. Rabeya, S. Mahalingam, A. Manap, M. Satgunam, Md Akhtaruzzaman, C. H. Chia, Structural defects in graphene quantum dots: a review, Int J. Quantum Chem. 122 (2022), https://doi.org/10.1002/qua.26900.
- [215] S.S. Durodola, A.S. Adekunle, L.O. Olasunkanmi, J.A.O. Oyekunle, O.T. Ore, S. O. Oluwafemi, A review on graphene quantum dots for electrochemical detection of emerging pollutants, J. Fluor. 32 (2022) 2223–2236, https://doi.org/10.1007/s10895-022-03018-w.

- [216] S. Sengupta, S. Pal, A. Pal, S. Maity, K. Sarkar, M. Das, A review on synthesis, toxicity profile and biomedical applications of graphene quantum dots (GQDs), Inorg. Chim. Acta 557 (2023) 121677, https://doi.org/10.1016/j.ica.2023.121677.
- [217] M. Handayani, Hendrik, A. Abbas, I. Anshori, R. Mulyawan, A. Satriawan, W. Shalannanda, C. Setianingsih, C.T.R. Pingak, Q. Zahro, A.C.S. Rurisa, I. Setiawan, K. Khotimah, G.K. Sunnardianto, Y.D. Rahmayanti, Development of graphene and graphene quantum dots toward biomedical engineering applications: a review, Nanotechnol. Rev. 12 (2023), https://doi.org/10.1515/ntrev-2023-0168.
- [218] H. Yan, Q. Wang, J. Wang, W. Shang, Z. Xiong, L. Zhao, X. Sun, J. Tian, F. Kang, S. Yun, Planted GRaphene Quantum Dots for Targeted, Enhanced Tumor Imaging and Long-term Visualization of Local Pharmacokinetics, Adv. Mater. 35 (2023), https://doi.org/10.1002/adma.202210809.
- [219] Z. Li, G. Qi, G. Shi, M. Zhang, H. Hu, L. Hao, Engineered graphene quantum dots as a magnetic resonance signal amplifier for biomedical imaging, Molecules 28 (2023) 2363, https://doi.org/10.3390/molecules28052363.
- [220] A. Bhaloo, S. Nguyen, B.H. Lee, A. Valimukhametova, R. Gonzalez-Rodriguez, O. Sottile, A. Dorsky, A.V. Naumov, Doped graphene quantum dots as biocompatible radical scavenging agents, Antioxidants 12 (2023) 1536, https://doi.org/10.3390/antiox12081536.
- [221] E. Seyyedi Zadeh, N. Ghanbari, Z. Salehi, S. Derakhti, G. Amoabediny, M. Akbari, M. Asadi Tokmedash, Smart pH-responsive magnetic graphene quantum dots nanocarriers for anticancer drug delivery of curcumin, Mater. Chem. Phys. 297 (2023) 127336, https://doi.org/10.1016/j.matchemphys.2023.127336.
- [222] H.K. Mohammed-Ahmed, M. Nakipoglu, A. Tezcaner, D. Keskin, Z. Evis, Functionalization of graphene oxide quantum dots for anticancer drug delivery, J. Drug Deliv. Sci. Technol. 80 (2023) 104199, https://doi.org/10.1016/j. jddst.2023.104199.
- [223] D. Kurniawan, J. Mathew, M.R. Rahardja, H. Pham, P. Wong, N.V. Rao, K. (Ken Ostrikov, W. Chiang, Plasma-enabled graphene quantum dot hydrogels as smart anticancer drug nanocarriers, Small 19 (2023), https://doi.org/10.1002/ smll.202206813.
- [224] S. Ostovar, M. Pourmadadi, M.A. Zaker, Co-biopolymer of chitosan/ carboxymethyl cellulose hydrogel improved by zinc oxide and graphene quantum dots nanoparticles as pH-sensitive nanocomposite for quercetin delivery to brain cancer treatment, Int J. Biol. Macromol. 253 (2023) 127091, https://doi.org/ 10.1016/i.iibiomac.2023.127091.
- [225] A. Soleimany, S. Khoee, D. Dastan, Z. Shi, S. Yu, B. Sarmento, Two-photon photodynamic therapy based on FRET using tumor-cell targeted riboflavin conjugated graphene quantum dot, J. Photochem. Photobio. B 238 (2023) 112602, https://doi.org/10.1016/j.jphotobiol.2022.112602.
- [226] Y. Yang, B. Wang, X. Zhang, H. Li, S. Yue, Y. Zhang, Y. Yang, M. Liu, C. Ye, P. Huang, X. Zhou, Activatable graphene quantum-dot-based nanotransformers for long-period tumor imaging and repeated photodynamic therapy, Adv. Mater. 35 (2023). https://doi.org/10.1002/adma.202211337.
- [227] A.J. Anjusha, S. Thirunavukkarasu, A.N. Resmi, R.S. Jayasree, S. Dhanapandian, N. Krishnakumar, Multifunctional amino functionalized graphene quantum dots wrapped upconversion nanoparticles for photodynamic therapy and X-ray CT imaging, Inorg. Chem. Commun. 149 (2023) 110428, https://doi.org/10.1016/j.inoche.2023.110428.
- [228] W.-S. Kuo, C.-Y. Chang, H.-Y. Chuang, P.-L. Su, J.-Y. Wang, P.-C. Wu, H.-F. Kao, S.-W. Tseng, S.-H. Lin, Y.-S. Lin, C.-C. Chang, Single-sized N-functionality graphene quantum dot in tunable dual-modality near infrared-I/II illumination detection and photodynamic therapy under multiphoton nonlinear excitation, Biosens. Bioelectron. 241 (2023) 115648, https://doi.org/10.1016/j. bios. 2023.115648
- [229] S.H. Kang, J.-Y. Lee, S.K. Kim, S.-H. Byun, I. Choi, S.J. Hong, Graphene quantum dots-loaded macrophages as a biomimetic delivery system for bioimaging and photodynamic therapy, J. Drug Deliv. Sci. Technol. 85 (2023) 104620, https:// doi.org/10.1016/j.jddst.2023.104620.
- [230] J. Zhang, P. Fan, Y. Shi, X. Huang, C. Shi, W. Ye, H. Tong, F. Shan, Z. Zhang, Near-Infrared-mediated self-assembly of graphene quantum dot-based nanoprobes to silence heat shock protein expression for mild photothermal therapy in liposarcoma, ACS Appl. Nano Mater. 6 (2023) 16276–16285, https://doi.org/10.1021/acsapm.3c02387
- [231] B. Lee, G.A. Stokes, A. Valimukhametova, S. Nguyen, R. Gonzalez-Rodriguez, A. Bhaloo, J. Coffer, A.V. Naumov, Automated approach to in vitro image-guided photothermal therapy with top-down and bottom-up-synthesized graphene quantum dots, Nanomaterials 13 (2023) 805, https://doi.org/10.3390/ panel 3050805
- [232] T.C. Lebepe, S. Parani, R. Maluleke, V. Ncapayi, O.A. Aladesuyi, A. Komiya, T. Kodama, O.S. Oluwafemi, NIR-II window absorbing graphene oxide-coated gold nanorods and graphene quantum dot-coupled gold nanorods for photothermal cancer therapy, Nanotechnol. Rev. 12 (2023), https://doi.org/ 10.1515/ntrev-2022-0541.
- [233] A. Soleimany, S. Khoee, S. Dias, B. Sarmento, Exploring low-power single-pulsed laser-triggered two-photon photodynamic/photothermal combination therapy using a gold nanostar/graphene quantum dot nanohybrid, ACS Appl. Mater. Interfaces 15 (2023) 20811–20821, https://doi.org/10.1021/acsami.3c03578.
- [234] X. ZHANG, S. LU, D. HE, M. CHAI, Z. WU, X. YAO, Y. YANG, Antibacterial property of graphene quantum dots-modified TiO2 nanorods on titanium dental implant, Trans. Nonferrous Met. Soc. China 33 (2023) 2395–2405, https://doi. org/10.1016/S1003-6326(23)66267-3.
- [235] R.M. Yusuf, S.R. Amelia, Y. Rohmatulloh, Sanusi, P. Listiani, Y. Ichikawa, M. Honda, T. Sudiarti, A.L. Ivansyah, The effect of the graphene oxide quantum

- dot (GOQD) synthesis method on the photocatalytic and antibacterial activities of GOQD/ZnO, Diam. Relat. Mater. 140 (2023) 110495, https://doi.org/10.1016/j.diamond.2023.110495.
- [236] O. Kahraman, E. Turunc, A. Dogen, R. Binzet, Synthesis of graphene quantum dot magnesium hydroxide nanocomposites and investigation of their antioxidant and antimicrobial activities, Curr. Microbiol 80 (2023) 181, https://doi.org/10.1007/ c00284.033.03296.0
- [237] S. Jana, T. Dey, B.N. Shivakiran Bhaktha, S.K. Ray, Probing the tunable optical properties of highly luminescent functionalized graphene quantum dots as downconverters for superior detection of ultraviolet radiation, Mater. Today Nano 24 (2023) 100400, https://doi.org/10.1016/j.mtnano.2023.100400.
- [238] M. Li, J. Liu, T. Zhang, N. Liang, L. Yan, F. Lv, W. Kong, F. Liu, L. Long, Enhanced performance of self-powered ZnO-based PEC type UV photodetectors by loading GQDs to construct heterojunctions, Mater. Res Bull. 172 (2024) 112657, https:// doi.org/10.1016/j.materresbull.2023.112657.
- [239] E. Orhan, A. Anter, M. Ulusoy, B. Polat, C. Okuyucu, M. Yıldız, Ş. Altındal, Effect of gadolinium on electrical properties of polyethyleneimine functionalized and nitrogen-doped graphene quantum dot nanocomposite based diode, Adv. Electron Mater. 9 (2023), https://doi.org/10.1002/aelm.202300261.
- [240] T. Gao, S. Guo, J. Zhang, J. Chen, S. Yin, N. Peng, Q. Cai, H. Xu, Y. Liu, Red, yellow, green, and blue light-emitting highly crystallized graphene quantum dots derived from lignin: controllable syntheses and light-emitting diode applications, Green. Chem. 25 (2023) 8869–8884, https://doi.org/10.1039/D3GC02702C.
- [241] C.-C. Hsu, L. Laysandra, Y.-C. Chiu, W.-R. Liu, Pivotal role of Boron-doped graphene quantum dots in stretchable and Self-Healable red emission nanocomposite film: one step advance for white light emitting diodes application, Chem. Eng. J. 473 (2023) 145469, https://doi.org/10.1016/j.cej.2023.145469.
- [242] Y. Zhao, B. Gu, G. Guo, Y. Li, T. Li, Y. Zhu, X. Wang, D. Chen, Bright tunable multicolor graphene quantum dots for light-emitting devices and anticounterfeiting applications, ACS Appl. Nano Mater. 6 (2023) 3245–3253, https://doi.org/10.1021/acsanm.2c04928.
- [243] A. Sarwar, A. Razzaq, M. Zafar, I. Idrees, F. Rehman, W.Y. Kim, Copper tungstate (CuWO4)/graphene quantum dots (GQDs) composite photocatalyst for enhanced degradation of phenol under visible light irradiation, Results Phys. 45 (2023) 106253, https://doi.org/10.1016/j.rinp.2023.106253.
- [244] B. Rabeie, N.M. Mahmoodi, Hierarchical ternary titanium dioxide decorated with graphene quantum dot/ZIF-8 nanocomposite for the photocatalytic degradation of doxycycline and dye using visible light, J. Water Process Eng. 54 (2023) 103976, https://doi.org/10.1016/j.jwpe.2023.103976.
- [245] H.-A.S. Tohamy, N.A. Fathy, M. El-Sakhawy, S. Kamel, Boosting the adsorption capacity and photocatalytic activity of activated carbon by graphene quantum dots and titanium dioxide, Diam. Relat. Mater. 132 (2023) 109640, https://doi. org/10.1016/j.diamond.2022.109640.
- [246] M. Tang, K. Tang, D. Wang, J. Yu, W. Kong, H. Shao, F. Li, X. Zhang, J. Lei, N. Liu, Photocatalytic reduction of CO2 in aqueous phase using amino-functionalized MOFs loaded with hydroxy-functionalized graphene quantum dots, Sep Purif. Technol. 329 (2024) 125245, https://doi.org/10.1016/j.seppur.2023.125245.
- [247] T. Li, R. Li, L. Yang, R. Wang, R. Liu, Y. Chen, S. Yan, S. Ramakrishna, Y. Long, Flexible PTh/GQDs/TiO 2 composite with superior visible-light photocatalytic properties for rapid degradation pollutants, RSC Adv. 13 (2023) 1765–1778, https://doi.org/10.1039/D2RA07084G.
- [248] F. Khan, V. Ahmad, T. Alshahrani, M. Al-Rasheidi, A.M. Alanazi, K. Irshad, M. H. Zahir, J.H. Kim, Influence of synthesis parameters of N-doped graphene quantum dots and polymer composite layer on the performance of CIGS solar cells, Opt. Mater. (Amst.) 135 (2023) 113251, https://doi.org/10.1016/j.optmat.2022.113251.
- [249] V. Gayathri, E. Praveen, K. Jayakumar, S. Karazhanov, C.R. Mohan, Graphene quantum dots assisted CuCo2S4/MWCNT nanoflakes as superior bifunctional electrocatalysts for dye-sensitized solar cell and supercapacitor applications, Colloids Surf. A Physicochem Eng. Asp. 662 (2023) 130948, https://doi.org/ 10.1016/j.colsurfa.2023.130948.
- [250] Y. Areerob, W.-C. Oh, C. Hamontree, T. Nachaithong, S. Nijpanich, K. Pattarith, A novel of WS2–MoCuO3 supported with graphene quantum dot as counter electrode for dye-sensitized solar cells application, Sci. Rep. 13 (2023) 7762, https://doi.org/10.1038/s41598-023-34637-3.
- [251] M. Esteves, D. Mombrú, M. Romero, L. Fernández-Werner, R. Faccio, A. W. Mombrú, The structural, optical and electrical properties of sodium titanate nanotubes sensitized with nitrogen/sulfur co-doped graphene quantum dots as potential materials for quantum dots sensitized solar cells, Mater. Today Electron. 3 (2023) 100029, https://doi.org/10.1016/j.mtelec.2023.100029.
- [252] E. Payami, R. Teimuri-Mofrad, Development of ternary nanocomposite based on ferrocenyl-modified graphene quantum dots for high-performance energy storage applications, J. Energy Storage 72 (2023) 108346, https://doi.org/10.1016/j. est 2023 108346
- [253] E. Payami, R. Teimuri-Mofrad, Ternary nanocomposite of GQDs-polyFc/Fe3O4/ PANI: design, synthesis, and applied for electrochemical energy storage, Electro Acta 439 (2023) 141706, https://doi.org/10.1016/j.electacta.2022.141706.
- [254] Y. Yan, Y. Hou, Z. Yu, L. Tu, S. Qin, D. Lan, S. Chen, J. Sun, S. Wang, B-doped graphene quantum dots implanted into bimetallic organic framework as a highly active and robust cathodic catalyst in the microbial fuel cell, Chemosphere 286 (2022) 131908, https://doi.org/10.1016/j.chemosphere.2021.131908.
- [255] J. Su, X. Zhang, X. Tong, X. Wang, P. Yang, F. Yao, R. Guo, C. Yuan, Preparation of graphene quantum dots with high quantum yield by a facile one-step method and applications for cell imaging, Mater. Lett. 271 (2020) 127806, https://doi.org/ 10.1016/j.matlet.2020.127806.

- [256] K.M. Mohamed, A.J.P. Paul Winston, K. Akash, P. Sagayaraj, S. Rajeshkumar, R. Ravindhran, S.A. Jayanthi, J.J. Vijaya, Novel green synthesis of Value-Added graphene quantum dots from bagasse and pith for biological applications, Biocatal. Agric. Biotechnol. 58 (2024) 103219, https://doi.org/10.1016/j. bcab.2024.103219.
- [257] H. Poursadegh, M. Barzegarzadeh, M.S. Amini-Fazl, Preparation of pH-sensitive chitosan-magnetic graphene quantum dot bionanocomposite hydrogel beads for drug delivery application: emphasis on effects nanoparticles, Polyhedron 247 (2024) 116705, https://doi.org/10.1016/j.poly.2023.116705.
- [258] M. Najafi, Z. Khoddam, M. Masnavi, M. Pourmadadi, M. Abdouss, Physicochemical and in vitro characterization of Agarose based nanocarriers incorporated with Graphene Quantum Dots/α-Fe2O3 for targeted drug delivery of Quercetin to liver cancer treatment, Mater. Chem. Phys. 320 (2024) 129333, https://doi.org/10.1016/j.matchemphys.2024.129333.
- [259] R. Mojgan, S. Ehsan, Z. Mostafa, High photoluminescence and afterglow emission of nitrogen-doped graphene quantum dots/TiO2 nanocomposite for use as a photodynamic therapy photosensitizer, Appl. Phys. A 130 (2024) 144, https:// doi.org/10.1007/s00339-024-07305-0.
- [260] B.S. Dash, Y.-J. Lu, J.-P. Chen, Enhancing photothermal/photodynamic therapy for glioblastoma by tumor hypoxia alleviation and heat shock protein inhibition using IR820-conjugated reduced graphene oxide quantum dots, ACS Appl. Mater. Interfaces 16 (2024) 13543–13562, https://doi.org/10.1021/acsami.3c19152.
- [261] F. Kazeminava, S. Javanbakht, M. Zabihi, M. Abbaszadeh, V. Fakhrzadeh, H. S. Kafil, Z. Ahmadian, M. Joulaei, Z. Zahed, A. Motavalizadehkakhky, Z. Latifi, H. Eslami, Crosslinking chitosan with silver-sulfur doped graphene quantum dots: an efficient antibacterial nanocomposite hydrogel films, J. Polym. Environ. 32 (2024) 213–224, https://doi.org/10.1007/s10924-023-02929-4.
- [262] H. Mondal, T. Dey, R. Basori, Silicon nanowire arrays with nitrogen-doped graphene quantum dots for photodetectors, ACS Appl. Nano Mater. 4 (2021) 11938–11948, https://doi.org/10.1021/acsanm.1c02505.
- [263] X. Li, X. Chen, Y. Guo, B. Chen, C. Zhang, J. Yang, H. Lu, Enhancing the efficiency and stability of perovskite solar cells through gradient energy band tin oxide electron transport layer design with graphene quantum dot incorporation, ACS Appl. Energy Mater. 7 (2024) 2698–2706, https://doi.org/10.1021/ acsem/3c03121
- [264] S. Perveen, Sonadia, S. Hafeez, M.Z. Khan, A. Ul-Hamid, F. Azad, Electrochemical and dielectric analysis of multifunctional GQDs@PEG@Mg-ZnFe2O4 ternary nanohybrid for low-frequency electronics, water splitting, and sustainable energy storage applications, J. Alloy. Compd. 995 (2024) 174746, https://doi.org/ 10.1016/j.jallcom.2024.174746.
- [265] K.-C. Liu, P. Kumar Panda, B. Chandra Mallick, P.-C. Yang, W.-R. Liu, C.-T. Hsieh, Solid-phase microwave synthesis of high-entropy graphene quantum dots as metal-free electrochemical catalysts, Appl. Surf. Sci. 648 (2024) 159061, https://doi.org/10.1016/j.apsusc.2023.159061.
- [266] T. Nakashima, K. Shigekawa, S. Katao, F. Asanoma, T. Kawai, Solvation of quantum dots in 1-alkyl-1-methylpyrrolidinium ionic liquids: toward stably luminescent composites, Sci. Technol. Adv. Mater. 21 (2020) 187–194, https://doi.org/10.1080/14686996.2020.1735923
- [267] A. Mohammadi, M. Rahmandoust, F. Mirzajani, A. Azadkhah Shalmani, M. Raoufi, Optimization of the interaction of graphene quantum dots with lipase for biological applications, J. Biomed. Mater. Res B Appl. Biomater. 108 (2020) 2471–2483.
- [268] Y. Wang, A. Liu, Y. Han, T. Li, Sensors based on conductive polymers and their composites: a review, Polym. Int 69 (2020) 7–17, https://doi.org/10.1002/ pi.1007
- [269] A. Roy, A. Ray, S. Saha, M. Ghosh, T. Das, B. Satpati, M. Nandi, S. Das, NiO-CNT composite for high performance supercapacitor electrode and oxygen evolution reaction, Electro Acta 283 (2018) 327–337, https://doi.org/10.1016/j.electacta.2018.06.154.
- [270] Y. Xie, C. Xia, H. Du, W. Wang, Enhanced electrochemical performance of polyaniline/carbon/titanium nitride nanowire array for flexible supercapacitor, J. Power Sources 286 (2015) 561–570, https://doi.org/10.1016/j. ipowsour.2015.04.025.
- [271] N. Ruecha, N. Rodthongkum, D.M. Cate, J. Volckens, O. Chailapakul, C.S. Henry, Sensitive electrochemical sensor using a graphene–polyaniline nanocomposite for simultaneous detection of Zn(II), Cd(II), and Pb(II), Anal. Chim. Acta 874 (2015) 40–48, https://doi.org/10.1016/j.aca.2015.02.064.
- [272] D. Zhang, Z. Wu, X. Zong, Flexible and highly sensitive H2S gas sensor based on in-situ polymerized SnO2/rGO/PANI ternary nanocomposite with application in halitosis diagnosis, Sens Actuators B Chem. 289 (2019) 32–41, https://doi.org/ 10.1016/j.snb.2019.03.055.
- [273] L. Tang, X. Xie, Y. Zhou, G. Zeng, J. Tang, Y. Wu, B. Long, B. Peng, J. Zhu, A reusable electrochemical biosensor for highly sensitive detection of mercury ions with an anionic intercalator supported on ordered mesoporous carbon/selfdoped polyaniline nanofibers platform, Biochem Eng. J. 117 (2017) 7–14, https://doi.org/10.1016/j.bej.2016.09.011.
- [274] C. Ratlam, S. Phanichphant, S. Sriwichai, Development of dopamine biosensor based on polyaniline/carbon quantum dots composite, J. Polym. Res. 27 (2020) 183, https://doi.org/10.1007/s10965-020-02158-6.
- [275] A. Valizadeh, H. Mikaeili, M. Samiei, S.M. Farkhani, N. Zarghami, M. Kouhi, A. Akbarzadeh, S. Davaran, Quantum dots: synthesis, bioapplications, and toxicity, Nanoscale Res Lett. 7 (2012) 480, https://doi.org/10.1186/1556-276X-7-480

- [276] J.-P. Schwitzguébel, H. Wang, Environmental impact of aquaculture and countermeasures to aquaculture pollution in China, Environ. Sci. Pollut. Res Int 14 (2007) 452–462, https://doi.org/10.1065/espr2007.05.426.
- [277] J. Jin, Y. Zhou, Z. Xiong, G. Guo, Y. Sun, D. Li, Y. Liu, Stable GQD@PANi nanocomposites based on benzenoid structure for enhanced specific capacitance, Int J. Hydrog. Energy 43 (2018) 8426–8439, https://doi.org/10.1016/j. iibydene 2018 03 133
- [278] F. Shao, N. Hu, Y. Su, H. Li, B. Li, C. Zou, G. Li, Z. Yang, Y. Zhang, PANI/Graphene quantum dots/graphene co-coated compressed non-woven towel for wearable energy storage, Synth. Met 270 (2020) 116571, https://doi.org/10.1016/j. synthmet.2020.116571.
- [279] K. An, J. He, L. Yang, L. Shen, Y. Sun, Facile synthesis of loosely assembled <scp>α-MnO 2 </scp> nanofiber coated with <scp>GQD</scp> / <scp>PANI</scp> for enhancing capacity, Int J. Energy Res 44 (2020) 12180–12187, https://doi.org/10.1002/er.5860.
- [280] W.-F. Hsu, T.-M. Wu, Electrochemical sensor based on conductive polyaniline coated hollow tin oxide nanoparticles and nitrogen doped graphene quantum dots for sensitively detecting dopamine, J. Mater. Sci.: Mater. Electron. 30 (2019) 8449–8456, https://doi.org/10.1007/s10854-019-01165-8.
- [281] B. Getiren, H. Altınışık, Z. Çıplak, F. Soysal, N. Yıldız, Nitrogen-doped graphene quantum dots/co-doped PANI binary nanocomposites as high-performance supercapacitor electrode materials, Synth. Met 298 (2023) 117451, https://doi. org/10.1016/j.synthmet.2023.117451.
- [282] S. Wang, J. Shen, Q. Wang, Y. Fan, L. Li, K. Zhang, L. Yang, W. Zhang, X. Wang, High-performance layer-by-layer self-assembly PANI/GQD-rGO/CFC electrodes for a flexible solid-state supercapacitor by a facile spraying technique, ACS Appl. Energy Mater. 2 (2019) 1077–1085, https://doi.org/10.1021/acsaem.8b01631.
- [283] H. Qiu, X. Qu, Y. Zhang, S. Chen, Y. Shen, Robust PANI@MXene/GQDs-based fiber fabric electrodes via microfluidic wet-fusing spinning chemistry, Adv. Mater. 35 (2023), https://doi.org/10.1002/adma.202302326.
- [284] A. Kausar, Polyaniline and quantum dot-based nanostructures: developments and perspectives, J. Plast. Film. Sheet 36 (2020) 430–447, https://doi.org/10.1177/ 8756087920926649.
- [285] S.K. Lai, C.M. Luk, L. Tang, K.S. Teng, S.P. Lau, Photoresponse of polyaniline-functionalized graphene quantum dots, Nanoscale 7 (2015) 5338–5343, https://doi.org/10.1039/c4nr07565j.
- [286] M. Morsy, I. Gomaa, A.E.M. Abd Elhamid, H. Shawkey, M.A.S. Aly, A. Elzwawy, Ternary nanocomposite comprising MnO2, GQDs, and PANI as a potential structure for humidity sensing applications, Sci. Rep. 13 (2023) 21742, https://doi.org/10.1038/s41598-023-48928-2.
- [287] D. Kumar, E. Vashishth, S. Rani, A. Kumar, B. Nandan, S.S. Bahga, R.K. Srivastava, GQD-PAN-based high-performance supercapacitor: an approach towards wealth from waste, RSC Sustain. 2 (2024) 1515–1527, https://doi.org/10.1039/ D4SU00153B.
- [288] Y.-C. Lin, M. Rinawati, L.-Y. Chang, Y.-X. Wang, Y.-T. Wu, Y.-H. Yen, K.-J. Chen, K.-C. Ho, M.-H. Yeh, A non-invasive wearable sweat biosensor with a flexible N-GQDs/PANI nanocomposite layer for glucose monitoring, Sens Actuators B Chem. 383 (2023) 133617, https://doi.org/10.1016/j.snb.2023.133617.
- [289] G.G. Gebreegziabher, A.S. Asemahegne, D.W. Ayele, D. Mani, R. Narzary, P. P. Sahu, A. Kumar, Polyaniline–graphene quantum dots (PANI–GQDs) hybrid for plastic solar cell, Carbon Lett. 30 (2020) 1–11, https://doi.org/10.1007/s42823-019-00064-6.
- [290] J. Cai, B. Sun, X. Gou, Y. Gou, W. Li, F. Hu, A novel way for analysis of calycosin via polyaniline functionalized graphene quantum dots fabricated electrochemical sensor, J. Electroanal. Chem. 816 (2018) 123–131, https://doi.org/10.1016/j. ielechem.2018.03.035.
- [291] R. Guo, Y. Jiang, Q. Jia, H. Pei, Z. Mo, N. Liu, X. Niu, Z. Liu, Improved electrocatalytic performance from graphene quantum dots/three-dimensional graphene/polyaniline doped powder to layer-by-layer self-assembled membrane materials, Mater. Today Commun. 25 (2020) 101426, https://doi.org/10.1016/j. mtcomm.2020.101426.
- [292] I.J. Gómez, M. Vázquez Sulleiro, D. Mantione, N. Alegret, Carbon Nanomaterials embedded in conductive polymers: a state of the art, Polymers 13 (2021) 745, https://doi.org/10.3390/polym13050745.
- [293] A. Kausar, Polymer/carbon-based quantum dot nanocomposite: forthcoming materials for technical application, J. Macromol. Sci., Part A 56 (2019) 341–356, https://doi.org/10.1080/10601325.2019.1578614.
- [294] H.T. Das, P. Barai, S. Dutta, N. Das, P. Das, M. Roy, Md Alauddin, H.R. Barai, Polymer composites with quantum dots as potential electrode materials for supercapacitors application: a review, Polymers 14 (2022) 1053, https://doi.org/ 10.3390/polym14051053.
- [295] E. Roy, A. Nagar, A. Sharma, S. Roy, S. Pal, Graphene quantum dots and its modified application for energy storage and conversion, J. Energy Storage 39 (2021) 102606, https://doi.org/10.1016/j.est.2021.102606.
- 296] M. Văduva, M. Baibarac, O. Cramariuc, Functionalization of graphene derivatives with conducting polymers and their applications in uric acid detection, Molecules 28 (2022) 135, https://doi.org/10.3390/molecules28010135.
- [297] D. Mohanadas, Y. Sulaiman, Recent advances in development of electroactive composite materials for electrochromic and supercapacitor applications, J. Power Sources 523 (2022) 231029, https://doi.org/10.1016/j.jpowsour.2022.231029.
- [298] G.G. Gebreegziabher, A.S. Asemahegne, D.W. Ayele, D. Mani, R. Narzary, P. P. Sahu, A. Kumar, Polyaniline–graphene quantum dots (PANI–GQDs) hybrid for plastic solar cell, Carbon Lett. 30 (2020) 1–11, https://doi.org/10.1007/s42823-019-00064-6.